ACTA UNIVERSITATIS SZEGEDIENSIS

# ACTA MINERALOGICA-PETROGRAPHICA

TOMUS XXVI. Fasc. 2.

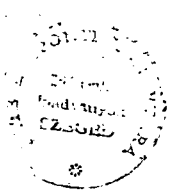

SZEGED, HUNGARIA
1984

## NOTE TO CONTRIBUTORS

### General

The Acta Mineralogica—Petrographica publishes original studies on the field of geochemistr mineralogy and petrology, first of all studies of Hungarian researchers, papers resulted in by co-op ration of Hungarian researchers and those of other countries and, in a limited volume, papers fro abroad on topics of global interest.

Manuscripts should be written in English and submitted to the Editor-in-chief, Institute Mineralogy, Geochemistry and Petrography, Attila József University, H-6701 Szeged, Pf. 65 Hungary.

The authors are responsibe for the accuracy of their data, references and quotations fro other sources.

### Manuscript

Manuscript should be typewritten with double spacing, 25 lines on a page and space for 50 lette in a line. Each new paragraph should begin with an indented line. Underline only words that shou be typed in italics.

Manuscripts should generally be organized in the following order:

Title
Name(s) of author(s) and their affiliations, in foot-note the address of the author to whon the correspondence should be sent.
Abstract
Introduction
Methods, techniques, material studied, description of the area investigated, etc.
Results
Discussion or conclusions
Acknowledgement
Explanation of plates (if any)
Tables
Captions of figures (drawings, photomicrographs, etc.)

### Abstract

The abstract cannot be longer than 500 words.

### Tables

The tables should typewritten on separate sheets and numbered according to their sequence in th text, which refers to all tables.

The title of the table as well as the column headings must be brief, but sufficiently explanatory

The tables generally should not exceed the type-area of the journal, i.e. 12.5×18.5 cm. Fold-outs can only exceptionally be accepted.

ACTA UNIVERSITATIS SZEGEDIENSIS

# ACTA MINERALOGICA-PETROGRAPHICA

TOMUS XXVI, Fasc. 2.

SZEGED, HUNGARIA
1984

HU ISSN 0365—8066

Adjuvantibus

BÉLA MOLNÁR et TIBOR SZEDERKÉNYI

Redigit

GYULA GRASSELLY

Edit

Institutum Mineralogicum, Geochimicum et Petrographicum
Universitatis Szegediensis de Attila József nominatae

Nota

Acta Miner. Petr., Szeged

Szerkeszti

GRASSELLY GYULA

a szerkesztőbizottság tagjai

MOLNÁR BÉLA és SZEDERKÉNYI TIBOR

Kiadja

a József Attila Tudományegyetem Ásványtani, Geokémiai és Kőzettani Tanszéke
H-6722 Szeged, Egyetem u. 2—6.

Kiadványunk címének rövidítése
Acta Miner. Petr., Szeged

CONTENTS

*Acta Mineralogica-Petrographica, Szeged, XXVI/2, 129 — 153, 1984*

# POLYMETAMORPHISM OF THE CRYSTALLINE BASEMENT OF THE SOMOGY—DRAVA BASIN (SOUTHWESTERN TRANSDANUBIA, HUNGARY)

P. ÁRKAI


## ABSTRACT

The crystalline basement of the Neogene depression of the Somogy—Drava Basin (SW-Transdanubia, Hungary) consists of medium-grade (almandine-amphibolite facies) polymetamorphic formations overprinted by a very low- and low-grade (anchi-, epizonal) retrograde, partly cataclastic metamorphism: gneiss, mica schist, amphibolite, as well as mylonite and blastomylonite.

Having applied the petrological and geochemical methods of lithofacies reconstruction the gneiss — mica schist and the mylonite — blastomylonite groups developed from them proved to be of sedimentary (para) origin: they were formed from carbonate-free or carbonate-poor pelitic-psammitic sediments. The amphibolite originated from basic igneous rock.

On the basis of the mineral-paragenetic, petrotextural and structural as well as geothermometric and geobarometric characteristics the following relative chronological succession of metamorphic events was determined:

*A)* The oldest one is a medium-grade (almandine-amphibolite facies), medium pressure (Barrovian) regional metamorphism with a geothermal gradient of 17 to 27 °C/km. Its temperature and pressure were 510 to 600 °C and 5.9 to 8.9 kbar, respectively. It was locally followed by

*B)* an andalusite-type (low pressure range) medium-grade (amphibolite facies) metamorphism with a gradient >34 °C/km and by

*C)* a low temperature (<450 °C), predominantly low pressure anchi-, epizonal retrograde, locally cataclastic metamorphism.

As to our recent knowledge — based on Alpine and Carpathian analogies — different hypothetic geochronological modells can be established, e. g.

— *A)* Caledonian, *B)* Hercynian, *C)* Hercynian and/or Alpine:

— *A)* older Hercynian, *B)* younger Hercynian and *C)* younger Hercynian and/or Alpine:

— *A)* Dalslandian (Early Baikalian), *B)* Hercynian, *C)* Hercynian and/or Alpine.

The mineral assemblages formed by weathering and by low temperature retrograde metamorphism were distinguished by means of the clay mineral associations and by the illite crystallinity.


## INTRODUCTION

Considering its geographic position, the Somogy—Dráva Basin links the Pannonian Basin with the Southern Alps and Internal Dinarides. This depression filled with a maximally 5.000 m thick sedimentary pile belongs to the Transdanubian Neogene Basin System. The aims of the present petrological and geochemical examinations of its crystalline basement are: the determination of the origin of these much debated polymetamorphic formations, the distinction and characterization of their metamorphic events and weathering processes. The investigations intend to contribute to the hydrocarbon prognostics of the basin on the one hand, and to the correlation of the metamorphic events of the afore-mentioned great geographic-geological units, on the other. The metamorphic-petrogenetic research of the core

samples deriving from hydrocarbon exploratory wells was initiated and supported by the National Oil and Gas Industrial Trust and by its affiliated firm, the Oil and Gas Mining Enterprise.

## GEOLOGY, PREVIOUS DATA

The geological and tectonic situation of the basement of the Somogy—Drava Basin is shown in *Fig. 1a.* The northern part of the basin belongs to the so called Igal—Bükk Alpine mobile belt extending between the Balaton and Zagreb—Hernád lineaments. As to the former ideas this belt might from the southwestern paleogeo-

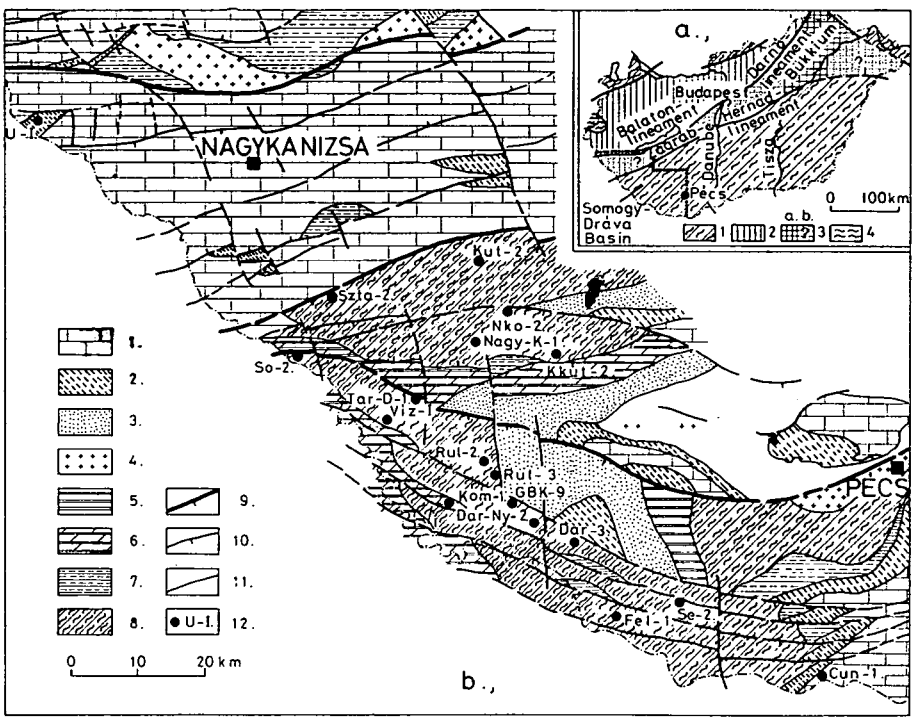


*Fig. 1. a:* Geological-tectonic position of the Somogy—Drava Basin.
Legend: 1) medium-grade polymetamorphic crystalline basement (pre-Hercynian?-Hercynian-Alpine?) locally with synkinematic Hercynian granitoid formations 2) Hercynian very low and low-grade metamorphic Early Paleozoic with post-kinematic Hercynian granitoid intrusions with non-metamorphic Late Paleozoic and Mesozoic (Transdanubian Central Mountains and the Little Plain) 3) Alpine very low- and low-grade metamorphic Paleozoic and Mesozoic (Bükkium, Igal—Bükk mobile belt): *a)* evidenced by investigations *b)* presumed *4)* Alpine low-grade metamorphic Mesozoic (Kőszeg Mountains, Penninic unit).

*b:* Geological and tectonic sketch of the pre-Tertiary basement of the Somogy—Drava Basin after BARDÓCZ (1973—1982). Simplified with sampling localities of metamorphic rocks. Legend: *1)* Mesozoic *2)* Permian partly Permo-Triassic *3)* Carboniferous *4)* granitoid rocks *5)* Early Paleozoic in general *6)* Devonian (?) *7)* Silurian (?) *8)* polymetamorphic crystalline basement (pre-Hercynian?-Hercynian-Alpine?) *9)* main compressive tectonic surfaces *10)* subordinate compression surfaces *11)* fault *12)* studied boreholes.

graphic ocnnection of the Bükkium characterized by South-Alpine, Dinaric affinity ("eugeosyncline", WEIN, 1969). However, the existence of this belt as a paleogeographic unit has not been proved [BALOGH, 1981, personal communication, KOVÁCS, 1982], and recently the present position of the Bükkium is explained by horizontal micro-plate movements along the Zagreb—Hernád lineament [KOVÁCS, 1982]. The stratigraphic, paleontological and lithofacies correlations of the Paleozoic and Mesozoic formations of the Bükkium and that of the southwestern part of the Igal—Bükk Belt are lacking. Traces of the Alpine (Cretaceous) regional metamorphism demonstrated in the Paleozoic and Mesozoic formations of the Bükkium [ÁRKAI, 1973, 1983, ÁRKAI, HORVÁTH and TÓTH, 1981] are unknown in the southwestern part of the belt belonging to the Somogy—Dráva Basin.

South of the Zagreb—Hernád lineament the crystalline basement is built up by pre-Hercynian (?) — Hercynian — Alpine (?) polymetamorphic formations of unclear evolution, locally accompanied by most likely Hercynian granitization (Mecsek Mountains, Danube—Tisza Interfluve).

The simplified variant of the map of the pre-Tertiary basement of the Somogy—Drava Basin constructed by BARDÓCZ (1973—1982) is shown in *Fig. 1b*. The basement units are bordered by compressive faults (overthrusts?) with strikes changing from NE—SW to NW—SE. The younger faults mostly perpendicular to the compressive ones are disjunctive.

According to the first petrographic description of the metamorphic basement of the Drava Basin [SZEPESHÁZY, 1958, 1959] most of the rocks having granite-like composition are "unequilibrated" metamorphites: tectonites, with different mylonite and phyllonite types depending on the intensity of the cataclastic metamorphism.

In the first petrogenetic synthesis of the SW-Transdanubian crystalline basement [BALÁZS, 1968] these polymetamorphites were believed to be ortho-rocks. The primary granitoid rocks were metamorphized in the Precambrian (Late Baikalian?) tectonocycle (meso- or occasionally kata-zonal gneiss formation). The epizonal mylonitization is presumably of Variscan age.

Essentially this synthesis can be found in the explanatory text of the map of metamorphites of the Carpatho—Balkan—Dinaride area [SZÁDECZKY-KARDOSS, JUHÁSZ, BALÁZS *et al.*, 1969] as well as in the map itself [SZÁDECZKY-KARDOSS, ÁRKAI *et al.*, 1976], with some modifications: the premetamorphic rocks are of Proterozoic age, an uncertain Early Baikalian metamorphism was followed by a Variscan epidote-amphibolite facies metamorphism and by an Alpine retrograde greenschist facies metamorphism. The anatexis (synkinematic granitization) observed in the polymetamorphic formations of the Mecsek Mountains and of the Danube—Tisza Interfluve seems to be also of Variscan age.

NAGY and SZEPESHÁZY [1971] pointed out the spatial variation of the grade and intensity of the Hercynian metamorphism in the basement rocks. In certain part of the Precambrian meso-zonal gneiss, mica schist, amphibolite sequence the weaker retrogressive effect resulted in mylonitization and phyllonite formation. Elsewhere these rocks were more strongly recrystallized (blastomylonites), and locally, in the high temperature zones anatexis, granitization took place without any signs of katazonal assemblages. The common greenschist facies retrograde event often called diaphtoresis can be bound partly to the Alpine cycle, as well.

Based on feldspar studies as well as on Rb—Sr isotope geochronological data BUDA [1972] established a model for the granitoid rocks of the Mecsek Mountains and of the Danube—Tisza Interfluve presuming Precambrian (?) sedimentation, Caledonian synkinematic anatexis and Variscan late-kinematic potash metasomatism.

In the region of the Görcsöny Ridge adjoining the Drava Basin, SZEDERKÉNYI [1975] demonstrated a Barrovian metamorphic sequence with increasing metamorphic grade from SW to NE from the chlorite zone up to the sillimanite zone. He determined the main tectonic directions of the basement and distinguished a two-phase (Precambrian and Variscan) granizitation in the Mecsek Mountains.

According to the lithostratigraphic correlation of JANTSKY [1976, 1979] the almandine-amphibolite facies ultrametamorphic (granitized) sequence of the Mecsek Mountains originated from Lower Proterozoic eugeosyncline pelitic-psammitic sediments and ophiolitic magmatites by pre-Baikalian (Gothian) amphibolite facies regional metamorphism and pre-Baikalian (Dalslandian) amphibolite facies ultrametamorphism. The diaphtoresis of the sequence is Baikalian (Riphean), the younger tectonocycles were not accompanied by regional metamorphic effects. The metamorphic evolution in the basement of the Drava Basin is similar to that of the Mecsek Mountains, except the ultrametamorphism (granitization).

The critical review of LELKES-FELVÁRI, SASSI *et al.*, [1981] based mainly on the studies of SZEDERKÉNYI considers the metamorphism of the crystalline basement of the Drava Basin and Görcsöny Ridge to be pre-Upper Carboniferous. As to the generally accepted view it is partly pre-Hercynian, though the sporadic age data refer to Hercynian thermal event only. The Barrovian, medium temperature gradient metamorphism (kyanite+staurolite) was overprinted by an andalusite-cordierite type, high thermal gradient recrystallization. This latter was locally accompanied by anatectic migmatizitation. At present the ages of the two metamorphic episodes are not known exactly.

It is obvious from this short review that our knowledge on the lithofacies of the premetamorphic rocks and on the polymetamorphic events and their chronology is full of contradictions and has not cleared up so far. The new petrological and geochemical data of this paper might contribute to solve the questions above.

## METHODS

Out of 15 boreholes *(Fig. 1b)* reaching the crystalline basement the complex investigation of 30 samples was carried out. In addition to the macroscopic and transmission microscopic studies X-ray diffractometric, electron microprobe, silicate-analytical and emission spectrographic methods were used.

The *X-ray diffractometric investigations* aimed:

— the determination of the qualitative and semiquantitative mineral composition, in the latter case using the direct method of NÁRAY-SZABÓ and PÉTER [1967] and also the data of BÁRDOSSY [1966, 1970], RISCHÁK and VICZIÁN [1974] as well as VICZIÁN and GHONEIM [1977]. The semiquantitative phase analysis was done by TÓTH, N. M. The results were corrected by the microscopic observations, by the solution residue data obtained by treatment with 3% HCl, and by the mineralogical recalculation of whole rock chemical analyses using also the chemical compositions of minerals determined by electron microprobe.

— The *measurement of illite crystallinity indices* referring to the structural ordering of the illite-muscovite group. The measurements were carried out in whole rock samples and in the fractions of less than 2 microns according to the methods of KÜBLER [1968, 1975] and WEAVER [1960]. The Kübler-index (=illite crystallinity= =IC=largeur de Scherrer=LS) denotes the width of the first (10 Å) basal reflection of the illite-muscovite at half height of the peak in $2\Theta$ degrees, under standardized circumstances (this value is abbreviated as half-width). The Weaver-index (sharpness

ratio) is the ratio of the peak-heights (intensities) measured on the basal reflection of the illite-muscovite at 10 and 10.5 Å (Weaver-index = $I_{10}$ Å/$I_{10.5}$ Å).

— The *determination of the metamorphic pressure* indicating $d_{060}$ or $6 \times d_{060} = b_0$ and the $d_{002}$ lattice parameters of the illite-muscovite group according to SASSI [1972] and GUIDOTTI and SASSI [1976], with corrections using the (211) and (100) reflections of the quartz in the rocks as "internal standards".

The X-ray analyses listed above were made by a Philips PW—1730 type diffractometer, with the following recording conditions: $CuK_\alpha$ radiation, 45 kV accelerating voltage, 35 mA, proportional counter, graphite monochromator, divergency and detector slits of 1°, goniometer speeds of 2°/min and 1/2°/min, respectively, time constant of 2 sec, and paper speed of 2 cm/min.

In silicate analyses made by LEFLER, J. and HANGYÁS, GY. a Carl Zeiss AASIM type atomic absorption spectrophotometer was used, in addition to the traditional gravimetric, photometric and chromatometric methods.

Trace elements were determined by TOMSCHEY, O. by means of a Carl Zeiss PGS—2 type plane grating spectrograph. In the quantitave evaluation the combined analytical and adjusting method was used. Recording conditions were: BIG—100 AC generator, Al 9999 electrodes, 1 mm electrode distance, 15 μm split, 50/1 spark, blende: 2, amperage: 7 A, exposition time: 164 sec, collimator: 10.6, plate quality: 23D56, developing in AGFA—1 at 20 °C for 5 min.

The chemical composition of rock forming and accessory minerals were analysed by NAGY, G. and DOBOSI, G. by means of a JEOL Superprobe—733. In correction calculations the ZAF program of the JEOL firm was used. In the qualitative chemical analyses an EDAX-system was applied.

## RESULTS

In Table 1 the location, number, depth interval and rock type of the investigated samples are listed. In Table 2 the semi-quantitative mineral compositions, in Table 3 the lattice parameters and the different indices characteristic of the structural ordering of the illite-muscovite group, in Table 4 the main element compositions and in Table 5 the trace element compositions are found. Table 6 contains the chemical compositions of the rock forming and accessory minerals analyzed by microprobe as well as the cation numbers per unit cells.

## DISCUSSION AND CONCLUSIONS

### *Rock types, mineral composition*

The rocks of the *gneiss group* are the most widespread (samples So—3.3, Viz—I.2,3, Tar—D—1.5,6, GBK—9.15, Dar—3.11, Fel—I.15, Se—2.16, Cun—1.14, Szta—2.20, Kut—2.16, Nagy—K—1.11, 12). These are composed of quartz, plagioclase (oligoclase), muscovite and biotite. Considerable amount of potash feldspar was found only in the sample Cun—1.14. The gneiss type containing only biotite out of the phyllosilicates is also rare (Dar—3.11). The samples So—3.3, Viz—I. 2, Dar—3.11, Se—2.16, Szta—2.21, Kut—2.16 and Nagy—K—1.11, 12 contain garnet, those of So—3.3, Dar—3.11, Kut—2.16 and Nagy—K—1.11 contain staurolite. The occurrences of kyanite (Nagy—K—1.11), sillimanite (So—3.3) and andalusite (Kut—2.16) are sporadic.

*Mica schists and feldspar bearing mica schists* being in close genetic and spatial relationship with the gneisses are less frequent (Viz—I. 5, 6, GB—29.2, Nagy—K—

TABLE 1

*List of the investigated rock samples from the crystalline basement of the Somogy—Drava Basin*

| Village | Borehole | Core | Depth (m) | Rock type |
|---|---|---|---|---|
| Somogyudvarhely | So—3. | 3 | 3001.0—3010.0 | gneiss |
| Vízvár | Víz—1 | 2 | 3287.0—3291.5 | gneiss |
| Vízvár | Víz—I | 3 | 3291.5—3295.0 | gneiss |
| Vízvár | Víz—I | 5 | 3465.0—3468.0 | mica schist |
| Vízvár | Víz—I | 6 | 3565.0—3566.5 | mica schist |
| Tarany | Tar—D—1 | 5 | 3011.0—3012.0 | gneiss |
| Tarany | Tar—D—1 | 6 | 3299.0—3300.0 | gneiss |
| Rinyaújlak | Rúl—2 | 2 | 2720.0—2723.5 | blastomylonite |
| Rinyaújlak | Rúl-3 | 2 | 2719.0—2723.0 | phyllonitic blastomylonite |
| Görgeteg-Babócsa | GB—29 | 2 | 1908.0—1911.0 | mica schist |
| Görgeteg-Babócsa | GB—29 | 4 | 2150.0—2151.0 | mica schist |
| Görgeteg-Babócsa | GBK—9 | 15 | 2702.0—2705.0 | gneiss |
| Darány | Dar—Ny—2 | 4 | 2697.0—2700.0 | amphibolite |
| Darány | Dar—3 | 11 | 2976.0—2980.0 | gneiss |
| Felsőszentmárton | Fel—I | 15 | 3991.2—3993.2 | gneiss |
| Sellye | Se—2 | 16 | 1798.0—1801.0 | gneiss |
| Sellye | Se—2 | 18 | 1950.0—1952.0 | gneiss |
| Cun | Cun—1 | 14 | 1969.5—1971.5 | gneiss |
| Szenta | Szta—2 | 20 | 2682.0—2684.0 | gneiss |
| Kutas | Kut—2 | 16 | 1947.0—1949.0 | gneiss |
| Nagyatád | Nagy—K—1 | 10 | 3071.0—3073.5 | mica schist |
| Nagyatád | Nagy—K—1 | 11 | 3220.0—3222.0 | gneiss |
| Nagyatád | Nagy—K—1 | 12 | 3299.0—3300.0 | gneiss |
| Nagykorpád | Nko—2 | 11 | 2065.0—2067.0 | mica schist |
| Kadarkut | Kkút—2 | 4 | 1219.0—1222.0 | mylonite |
| Kadarkút | Kkút—2 | 5 | 1222.0—1223.0 | blastomylonite |
| Kadarkút | Kkút—2 | 8 | 1415.0—1417.0 | blastomylonite |
| Kadarkút | Kkút—2 | 9 | 1531.0—1533.0 | blastomylonite |

1.10, Nko—2.11). Their rock forming minerals are similar to that of the gneiss group, the only difference being the lower (less than 20 weight percent) feldspar content. Their quartz/phyllosilicate ratios are rather changing. The accessory minerals are garnet (GB—29.2 and Viz—I.5) as well as straurolite (GB—29.2).

*Amphibolite* is subordinate in the basement (Dar—Ny—2.4). Its minerals are hornblende, plagioclase (oligoclase), quartz and small amounts of biotite, garnet and epidote.

The *mylonite* (GB—29.4, Se—2.18, Kkut—2.4) and *blastomylonite* varieties (Rul—2.2, Kkut—2.5, 8,9) were generated from the gneisses and mica schists by cataclastic (dynamic) metamorphism accompanied by a weak retrograde recrystallization which did not exceed the chlorite zone of the greenschist facies. These rock types are characterized by smaller feldspar content and by high sericite, chlorite and carbonate mineral contents as compared to the gneisses.

*Pre-metamorphic lithofacies*

The overwhelming majority of the gneisses, mica schists and mylonites, blastomylonites generated from them proved to be of *sedimentary* (para-) origin. They were formed presumably from carbonate-free or carbonate-poor pelitic-psammitic

TABLE 2

*Semiquantitative mineral composition of the rock samples (weight percent)*
(Analysed by P. ÁRKAI and M. N. TÓTH)

| Sample | Quartz | Plagioclase | K-feldspar | Hornblende | Biotite | Muscovite (+illite-sericite) | Chlorite | Kaolinite | Mixed layer clay min. | Calcite | Dolomite-ankerite | Siderite | Pyrite | Hematite | Goethite | Garnet | Staurolite | Kyanite | Sillimanite | Andalusite | Epidote |
|---|---|---|---|---|---|---|---|---|---|---|---|---|---|---|---|---|---|---|---|---|---|
| So—3.3 | 34 | 32 | — | — | 6 | 17 | 3 | 2 | — | — | — | 5 | — | 1 | — | tr | tr | — | tr | — | — |
| Víz—I.2 | 41 | 26 | — | — | — | 20 | 12 | — | — | 1 | — | — | — | tr | — | tr | — | — | — | — | — |
| Víz—I.3 | 18 | 56 | — | — | — | tr | 22 | — | — | 4 | — | tr | — | — | — | tr | — | — | — | — | — |
| Víz—I.5 | 14 | 11 | — | — | 15 | 45 | 14 | — | — | — | tr | — | — | — | — | tr | — | — | — | — | — |
| Víz—I.6 | 64 | 18 | — | — | — | 8 | 10 | tr | — | — | — | — | — | — | — | tr | — | — | — | — | — |
| Tar—D—1.5 | 33 | 18 | — | — | tr | 12 | 4 | 6 | — | 1 | 12 | 14 | — | tr | — | — | — | — | — | — | — |
| Tar—D—1.6 | 39 | 20 | — | — | tr | 16 | 19 | — | — | 6 | — | — | — | tr | — | tr | — | — | — | — | — |
| Rul—2.2 | 36 | 20 | — | — | — | 25 | 2 | 4 | — | — | — | 13 | — | tr | — | — | — | — | — | — | — |
| Rul—3.2 | 49 | 12 | 1 | — | — | 21 | — | 6 | — | — | — | 11 | — | tr | — | tr | — | — | — | — | — |
| GB—29.2 | 57 | 8 | — | — | 16 | 15 | — | 2 | — | — | — | 2 | — | tr | — | tr | tr | — | — | — | — |
| GB—29.4 | 68 | 8 | — | — | — | 10 | 14 | — | — | — | — | — | — | — | — | tr | — | — | — | — | — |
| GBK—9.15 | 46 | 38 | — | — | — | 10 | 3 | — | — | 3 | — | tr | — | — | — | — | — | — | — | — | — |
| Dar—Ny—2.4 | 3 | 30 | — | 57 | tr | — | 10 | — | — | — | — | — | — | — | — | tr | — | — | — | — | tr |
| Dar—3.11 | 46 | 31 | — | — | 15 | — | 6 | — | — | 1 | 1 | — | — | — | — | tr | tr | — | — | — | — |
| Fel—I.15 | 39 | 55 | — | — | tr | 3 | 3 | — | — | — | tr | — | — | tr | — | — | — | — | — | — | — |
| Se—2.16 | 45 | 15 | — | — | 21 | 2 | 2 | 15 | — | — | — | — | — | — | — | tr | — | — | — | — | — |
| Se—2.18 | 44 | 2 | — | — | — | 22 | tr | 8 | — | — | — | 24 | — | — | — | — | — | — | — | — | — |
| Cun—1.14 | 47 | — | 30 | — | 13 | 8 | — | — | — | — | 1 | tr | — | — | 1 | — | — | — | — | — | — |
| Szta—2.20 | 14 | 33 | — | — | — | 19 | 29 | — | — | 5 | — | — | — | tr | — | tr | — | — | — | — | — |
| Kut—2.16 | 21 | 21 | — | — | 9 | 26 | — | 8 | — | — | 13 | — | 2 | — | — | tr | tr | — | — | tr | — |
| Nagy—K—1.10 | 33 | — | 1 | — | — | 49 | — | 5 | — | — | — | 11 | — | 1 | — | — | — | — | — | — | — |
| Nagy—K—1.11 | 24 | 51 | — | — | 9 | 7 | 1 | 3 | — | — | 2 | 2 | — | 1 | — | tr | tr | tr | — | — | — |
| Nagy—K—1.12 | 49 | 16 | — | — | — | 20 | 1 | 1 | — | — | 6 | 7 | — | — | — | tr | — | — | — | — | — |
| Nko—2.11 | 38 | 11 | — | — | 8 | 30 | — | 5 | — | — | — | — | — | 8 | — | — | — | — | — | — | — |
| Kkút—2.4 | 3 | 48 | 37 | — | — | 5 | — | — | — | — | — | 7 | — | — | — | — | — | — | — | — | — |
| Kkút—2.5 | 27 | 40 | — | — | — | 12 | 18 | — | — | — | — | 3 | — | — | — | — | — | — | — | — | — |
| Kkút—2.8 | 30 | 33 | 25 | — | — | 6 | tr | 2 | — | — | — | 4 | — | tr | — | — | — | — | — | — | — |
| Kkút—2.9 | 38 | 35 | 16 | — | — | 6 | 3 | — | — | — | — | 2 | — | — | — | — | — | — | — | — | — |

tr = traces

TABLE 3

*X-ray diffractometric structural parameters of the illite-sericite-muscovite group*
(biotite-free samples)

| Sample | Whole rock samples (desoriented preparates) | | | | | | 2 μm ⌀ fractions (oriented prep.) | | | |
|---|---|---|---|---|---|---|---|---|---|---|
| | IC°2Θ (Kübler-index) | | Weaver-index | | $b_0$ (Å) | $d_{002}$ (Å) | IC° 2Θ (Kübler-index) | | Weaver-index | |
| | 2°/min | 1/2°/min | 2°/min | 1/2°/min | | | 2°/min | 1/2°/min | 2°/min | 1/2°/min |
| Víz—I.2 | 0.220 | 0.150 | 6.60 | 7.30 | 9.012 | 9.964 | n. d. | n. d. | n. d. | n. d. |
| Víz—I.6 | 0.172 | 0.097 | 8.14 | 9.75 | 9.055 | 9.952 | n. d. | n. d. | n. d. | n. d. |
| Rul—2.2 | 0.274 | 0.175 | 3.84 | 5.25 | 8.995 | 9.952 | n. d. | n. d. | n. d. | n. d. |
| Rul—3.2 | 0.209 | 0.136 | 5.07 | 5,77 | 9.003 | 9.946 | 0.568 | 0.446 | 1.98 | 2.35 |
| GB—29.4 | 0.230 | 0.158 | 8.25 | 11.56 | n. d. | 9.958 | 0.274 | 0.127 | 4.96 | 8.93 |
| Se—2.10 | 0.350 | 0.308 | 3.00 | 3.13 | 8.991 | 9.997 | 0.551 | 0.527 | 3.34 | 2.23 |
| Szta—2.20 | 0.296 | 0.207 | 3.79 | 4.20 | 9.003 | 9.964 | n. d. | n. d. | n. d. | n. d. |
| Nagy—K—1.10 | 0.203 | 0.126 | 6.52 | 8.20 | 8.996 | 9.958 | 0.481 | 0.420 | 3.25 | 2.86 |
| Nagy—K—1.12 | 0.221 | 0.158 | 5.39 | 5.08 | 8.998 | 9.958 | n. d. | n. d. | n. d. | n. d. |
| Kkút—2.5 | 0.209 | 0.124 | 9.50 | 10.88 | 9.906 | 9.952 | 0.208 | 0.140 | 6.25 | 2.69 |
| Kkút—2.8 | 0.170 | 0.109 | 9.82 | 7.30 | 9.001 | 9.913 | n. d. | n. d. | n. d. | n. d. |
| Kkút—2.9 | 0.132 | n. d. | 9.33 | n. d. | 9.008 | 10.048 | n. d. | n. d. | n. d. | n. d. |

n. d. = not determined

clastic sediments mixed in varying ratios. The observations evidenced the para-origin are as follows:

— detrital, rounded zircons in the samples Viz—I.2, 6, Ta—D—1.5, 6 and Cun—1.14;

— fine disperse organic matter (graphite) in the sample Nagy—K—1.11;

— the abundant occurrence of Al-rich silicates (garnet, staurolite, $Al_2SiO_5$ modifications) generated as a result of Al-excess characteristic of the pelitic rocks;

— the strong fluctuation of the quartz-feldspar-phyllosilicate ratios relating to the varying mixtures of fine and coarse detrital sediments;

— the lack or the subordinate quantity of potash feldspar denying the granitic origin;

— the lack of carbonate minerals in the first progressive mineral assemblages.

Having evaluated the rocks with considerable amounts of potash feldspar, the migmatitization of paragneiss can be presumed in the case of the sample Cun—1.14 containing rounded zircon grains. The mylonites Kkut—2.4—9 formed from granitoid rocks or orthogneiss. Assuming the granitoid origin the primary sedimentary starting material can not be excluded in this case either.

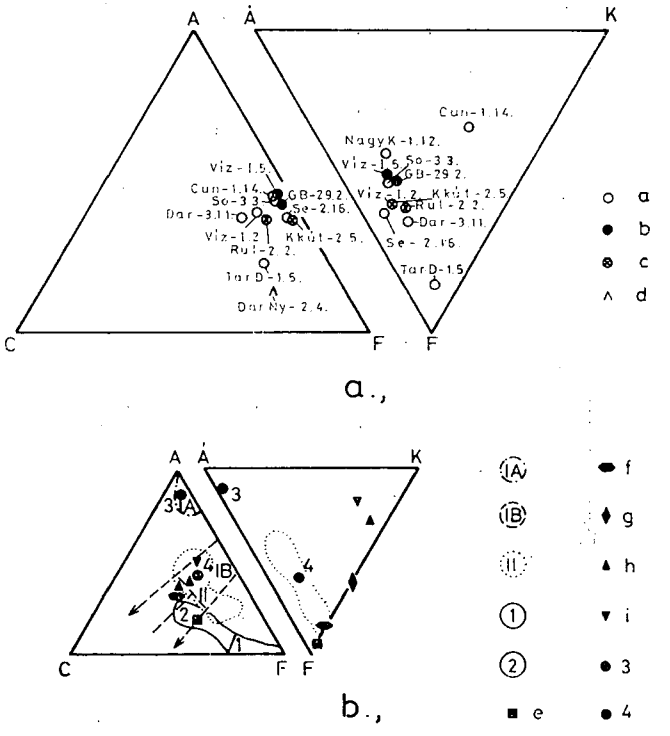


*Fig. 2. a:* Distribution of rocks of the crystalline basement in the ACF—ÁKF diagrams. Legend: *a)* gneiss *b)* mica schist *c)* blastomylonite *d)* amphibolite.

*b:* Distribution of the main rock types in the ACF—ÁKF diagrams after WINKLER [1976]. Legend: IA—Al-rich clays, IB — carbonate-free or max. 35% carbonate-bearing clays; between arrows: marls (with 35—65% carbonate content) II — greywackes, 1 — ultrabasic rocks, 2 — basic (basaltic) and andesitic rocks, e — basalt, f— tonalite, g — granodiorite, h — calc-alkaline granite, i — alkali granite, 3 — continental clay, 4 — marine clay.

TABLE 4

*Chemical composition of the polymetamorphic samples (weight percent)*
(Analysed by J. LEFLER and GY. HANGYÁS)

| | So—3. 3. | Víz—I. 2. | Víz—I. 5. | Tar D—1. 5. | Rul—2. 2. | GB—29. 2. | Dar Ny—2.4. | Dar—3. 11. | Se—2. 16. | Cun—1. 11. | Cun—1. 14. | Kut—2. 15. | Nagy K—1.12. | K kut—2. 5. |
|---|---|---|---|---|---|---|---|---|---|---|---|---|---|---|
| $SiO_2$ | 63.05 | 65.82 | 51.64 | 54.79 | 60.98 | 73.66 | 46.30 | 74.73 | 67.39 | 12.42 | 74.09 | 21.07 | 68.28 | 61.91 |
| $TiO_2$ | 0.38 | 0.65 | 0.65 | 0.43 | 0.46 | 0.43 | 1.26 | 0.43 | 0.37 | 0.17 | 0.17 | 1.11 | 0.38 | 0.56 |
| $Al_2O_3$ | 16.16 | 15.00 | 23.87 | 10.26 | 14.93 | 12.25 | 12.80 | 11.68 | 13.74 | 3.53 | 11.32 | 8.70 | 12.66 | 16.61 |
| $Fe_2O_3$ | 2.22 | 3.02 | 2.72 | 4.27 | 2.23 | 0.86 | 4.27 | 1.61 | 1.34 | 0.00 | 1.45 | 3.03 | 3.69 | 2.09 |
| FeO | 3.75 | 2.18 | 5.24 | 5.70 | 2.53 | 3.05 | 9.66 | 2.44 | 4.48 | 0.62 | 1.13 | 7.58 | 1.49 | 3.74 |
| MgO | 2.81 | 3.34 | 4.60 | 5.05 | 3.87 | 2.17 | 10.34 | 1.60 | 3.15 | 6.94 | 1.28 | 14.75 | 1.77 | 3.57 |
| MnO | 0.09 | 0.23 | 0.18 | 0.23 | 0.12 | 0.16 | 0.44 | 0.25 | 0.17 | 0.07 | 0.08 | 0.96 | 0.17 | 0.23 |
| CaO | 0.96 | 1.82 | 1.10 | 3.72 | 1.81 | 0.44 | 6.98 | 1.96 | 0.91 | 29.49 | 0.48 | 15.55 | 1.39 | 0.62 |
| $Na_2O$ | 2.21 | 3.01 | 1.89 | 1.33 | 2.16 | 1.10 | 3.86 | 2.75 | 1.64 | 0.14 | 0.64 | 0.64 | 1.60 | 3.59 |
| $K_2O$ | 2.91 | 1.91 | 4.93 | 2.14 | 2.83 | 2.85 | 0.32 | 1.38 | 2.08 | 1.36 | 6.27 | 1.07 | 2.60 | 2.47 |
| $+H_2O$ | 1.80 | 2.43 | 2.44 | 2.36 | 2.24 | 1.42 | 1.81 | 0.82 | 3.43 | 1.51 | 2.02 | 1.38 | 1.79 | 2.37 |
| $-H_2O$ | 0.00 | 0.04 | 0.00 | 0.16 | 0.21 | 1.30 | 0.40 | 0.08 | 0.14 | 0.18 | 0.28 | 0.62 | 0.07 | 0.12 |
| $CO_2$ | 2.62 | 0.48 | 1.41 | 9.78 | 4.88 | 0.86 | 0.83 | 1.03 | 0.33 | 6.03 | 0.00 | 21.12 | 4.32 | 1.40 |
| $P_2O_5$ | 0.24 | 0.15 | 0.18 | 0.09 | 0.22 | 0.06 | 0.19 | 0.23 | 0.22 | 0.15 | 0.14 | 2.76 | 9.11 | 0.16 |
| Total: | 99.20 | 100.08 | 100.85 | 100.31 | 99.47 | 100.61 | 99.46 | 100.99 | 99.39 | 99.52 | 99.35 | 100.34 | 100.32 | 99.44 |

TABLE 5

*Trace element concentrations of rock samples* (ppm)
(Analysed by O. TOMSCHEY)

| Sample | B | Co | Cr | Ga | Mn | Ni | Pb | Ti | V | Zn |
|---|---|---|---|---|---|---|---|---|---|---|
| So—3.3 | 15 | 11 | 150 | 11 | 367 | 62 | 5 | 3550 | 45 | 63 |
| Víz—I.2 | 19 | 10 | 350 | 34 | 835 | 50 | 9 | 3500 | 97 | 58 |
| Víz—I.3 | 8 | 3 | 32 | 9 | 353 | 15 | 3 | 2020 | 40 | 8 |
| Víz—I.5 | 24 | 12 | 138 | 45 | 1060 | 49 | 9 | 3320 | 173 | 124 |
| Víz—I.6 | 8 | 6 | 66 | 40 | 453 | 13 | 6 | 1660 | 12 | 11 |
| Tar—D—1.5 | 20 | 11 | 112 | 28 | 2030 | 32 | 8 | 3230 | 45 | 63 |
| Tar—D—1.6 | 16 | 20 | 135 | 31 | 673 | 34 | 12 | 3080 | 68 | 87 |
| Rul—2.2 | 48 | 13 | 157 | 60 | 650 | 67 | 53 | 4030 | 155 | 88 |
| Rul—3.2 | 23 | 8 | 103 | 34 | 320 | 27 | 9 | 2050 | 47 | 31 |
| GB—29.2 | 16 | 8 | 89 | 27 | 920 | 21 | 11 | 3330 | 52 | 41 |
| GB—29.4 | 11 | — | 8 | 11 | 190 | — | 4 | 630 | 13 | 12 |
| GB—K—9.15 | 15 | 3 | 21 | 9 | 310 | 8 | 4 | 1630 | 24 | 8 |
| Dar—Ny—2.4 | 17 | 16 | 95 | 19 | 2070 | 27 | 5 | 3620 | 300 | 34 |
| Dar—3.11 | 15 | — | 68 | 17 | 740 | 15 | 9 | 2480 | 22 | 24 |
| Fel—I.15 | 7 | — | 2 | 23 | 230 | 4 | 8 | 530 | 7 | 18 |
| Se—2.16 | 10 | — | 60 | 8 | 180 | 9 | 6 | 1650 | 27 | — |
| Se—2.18 | 140 | 7 | 140 | 30 | 510 | 94 | 6 | 3170 | 77 | — |
| Cun—1.14 | 24 | — | 1 | 14 | 97 | — | 7 | 447 | 6 | — |
| Szta—2.30 | 7 | — | 41 | 5 | 527 | 11 | 3 | 1240 | 17 | 8 |
| Kut—2.16 | 70 | 28 | 182 | 70 | 1030 | 86 | 21 | 5830 | 273 | 85 |
| Nagy—K—1.10 | 60 | 15 | 99 | 31 | 193 | 21 | 9 | 2320 | 75 | 35 |
| Nagy—K—1.11 | 110 | 12 | 130 | 42 | 920 | 53 | 12 | 3030 | 153 | 83 |
| Nagy—K—1.12 | 42 | 8 | 138 | 33 | 837 | 38 | 11 | 3920 | 137 | 42 |
| Nko—2.11 | 42 | 8 | 138 | 31 | 667 | 33 | 8 | 3100 | 72 | 33 |
| Kkút—2.4 | 15 | — | 4 | 62 | 893 | 12 | 14 | 820 | 60 | 65 |
| Kkút—2.5 | 45 | 24 | 212 | 59 | 910 | 87 | 11 | 3370 | 113 | 101 |
| Kkút—2.8 | 17 | — | 7 | 46 | 393 | 8 | 14 | 833 | 12 | 16 |
| Kkút—2.9 | 11 | — | 5 | 23 | 237 | 7 | 9 | 497 | 10 | — |

Samples GBK—9.15 and Fel—I.15 differ from the gneiss group in their high quartz+feldspar and low phyllosilicate contents. These may be the metamorphic derivates of dioritic magmatites or of feldspar-rich sandstones.

The petrochemical (main element) data support the conclusions above concerning the para origin. Plotting the petrochemical data (Table 4) in the ACF—ÁKF diagrams *(Fig. 2a)* these were compared with the average values and fields of the main sedimentary and igneous rock types determined by WINKLER [1976, 1979] shown in *Fig. 2b*. It can be stated that

— except two samples the rocks of the gneiss — mica schist and related mylonite — blastomylonite groups lie in the field of the marine carbonate-free clays and graywacke, far off the igneous trend, i.e. these are of para (pelitic-psammitic) origin. Out of the exceptions the position of the sample Tar—D—1.5 was displaced towards the C-edge due to the secondary carbonate mineral formation. In the ÁKF diagram the sample Cun—1.14 is of transitional position between the clastic sediments and granites indicating the granizitation process.

— The amphibolite sample (Dar—Ny—2.4) falls out of the marl region and corresponds to the basaltic part of the igneous differentiation trend, i. e. it is presumably of ortho origin. The projection point of the investigated amphibolite coincides also with the ortho field in the MgO—CaO—FeO discrimination diagram of WALKER *et al.* [1960].

PLATE I

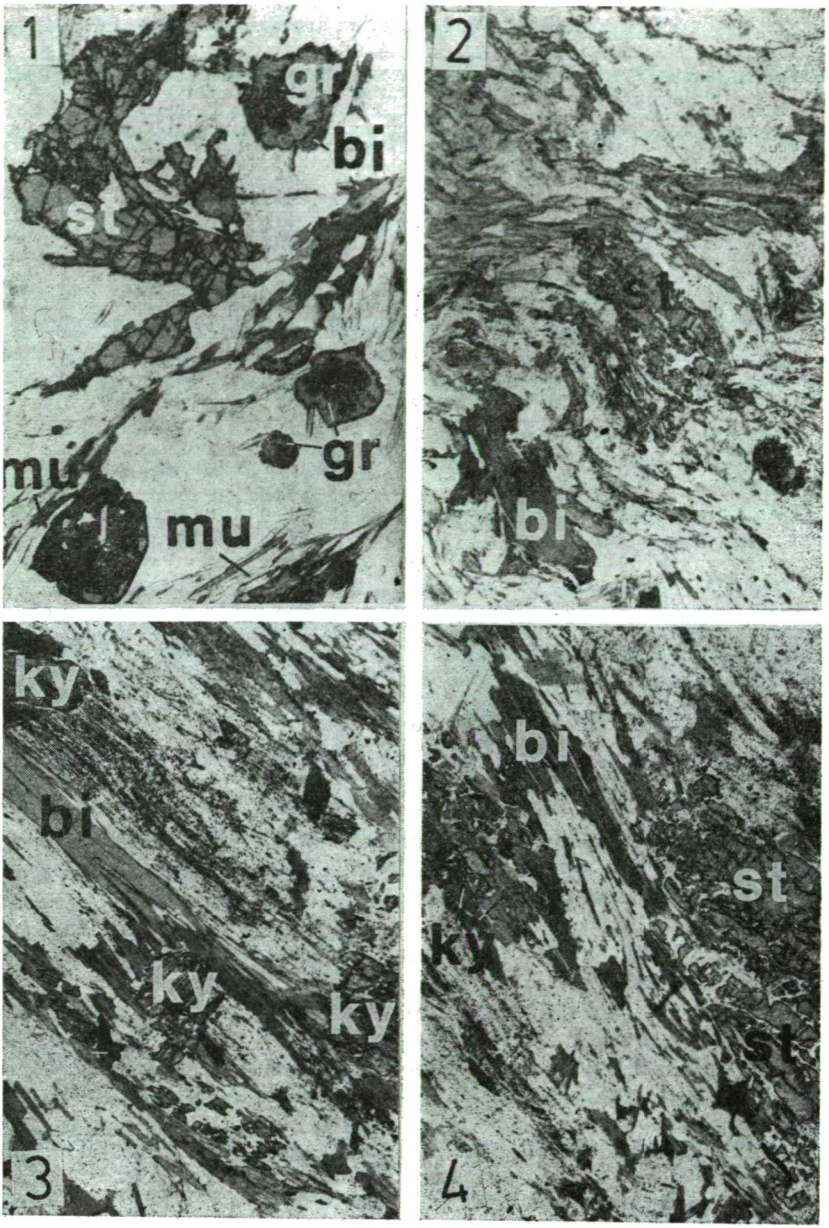

The considerable fluctuations of the trace element contents of the gneiss — mica schist and mylonite — blastomylonite groups (Table 5) also indicate that these rocks were recrystallized from not homogenized detrital sediments of varying compositions within wide limits. In the trace element concentrations of the rocks mentioned above there are no remarkable, systematic differences.

The trace element ratios of the amphibolite sample fall in the ortho fields of the discrimination diagrams using the Ni—Co and Ni—Cr ratios [WALKER *et al.*, 1960] as well as the V—Cr ratio [SCHWEDER, 1968]. Taking into account the main element composition and the lack of the carbonate rocks in the basement, the amphibolite seems to be more of basic igneous than of sedimentary (marly) origin.

## RECRYSTALLIZATION PHASES, METAMORPHIC EVOLUTION

The mineral assemblage of the first detectable progressive metamorphism in the gneiss — mica schist and the mylonite — blastomylonite groups consists of quartz, plagioclase (oligoclase), muscovite, biotite ± garnet, staurolite, kyanite, sillimanite and potash feldspar.

Applying the Winkler's classification [1976, 1979] this mineral assemblage involves the whole range of medium-grade metamorphism, and is assigned in the facies classification of WINKLER [1967] to the medium-pressure (Barrovian) almandine-amphibolite facies (staurolite-almandine and kyanite-almandine-muscovite subfacies). Out of the metamorphic grade indicating minerals the garnet (Plate I.1) is the most abundant. Staurolite is less frequent (Plate I.1, 2, 4). while kyanite (Plate I.3, 4) and sillimanite occur only in one-one samples. Their associations are: garnet; garnet-staurolite; garnet-staurolite-kyanite and garnet-staurolite-sillimanite.

Based on the reaction isograde system of metapelites [WINKLER, 1976, 1979] the probable temperature interval of the first progressive metamorphism is about 560—620 °C, the pressure ($P_{H_2O}=P_S$) is more than 6 kbar. (Temperature and pressure were estimated on the basis of the field bordered by the "staurolite-in" isograde and the initial anatexis, and of the field above the $Al_2SiO_5$ tripple point, respectively.)

The progressive metamorphic mineral assemblage of amphibolite is hornblende, plagioclase (oligoclase), quartz, biotite, garnet, epidote. The temperature of the metamorphism might have been between the Winkler's "hornblende-in" and "$An_{17}$+ +hornblende" isograde, i.e. about 500—520 °C, which is somewhat lower than the value estimated for the gneiss — mica schist group.

---

**Plate I**

1. Textural picture of garnetiferous staurolitic muscovite-biotite schist (sample GB—29.2).

Legend: gr — garnet, st — staurolite, bi — biotite, mu — muscovite. 1 nicol, the picture width corresponds to 2 mm.

2. Syn-tectonic staurolite (st) and biotite (bi) grains in gneiss (samples So—3.3). 1 nicol, the picture width corresponds to 2 mm.

3. Post-tectonic kyanite grains (ky) in garnetiferous staurolitic kyanitic muscovite-biotite gneiss (sample Nagy—K—1.11). 1 nicol, picture width is 2 mm.

4. Staurolite and kyanite in gneiss (sample Nagy—K—11). Legend: ky — kyanite, st — staurolite, bi — biotite. 1 nicol, picture width is 2 mm.

In order to determine the physical parameters of the first progressive metamorphic event more precisely, different *geothermometric and geobarometric methods* were used. The cation numbers per unit cells necessary to the computations were calculated from the coexisting minerals analysed by means of electron microprobe (Table 6). To satisfy the requirements of the thermodynamic equilibrium, the analytical data of adjoining or close-lying mineral grains were used, the homogeneity of the chemical composition within the rock and within the individual grains was also studied. In case of minerals with chemical zoning (garnets) the composition of grain's margin was taken into account.

TABLE 6

*Average chemical composition of rock forming and accessory minerals*
(electron microprobe data in weight percent and numbers of cations per unit cell)
(Analysed by G. NAGY and G. DOBOSI)

*1. Garnet analyses*

| | 1. | 2a | 2b | 3a | 3b | 4a | 4b | 5a | 5b | 6a | 6b |
|---|---|---|---|---|---|---|---|---|---|---|---|
| $SiO_2$ | 37,84 | 36,57 | 36,89 | 37,63 | 37,80 | 37,17 | 37,32 | 38,40 | 38,43 | 36,77 | 37,41 |
| $TiO_2$ | 0,15 | 0,04 | 0,05 | n. d. | n. d. | 0,06 | 0,03 | 0,19 | 0,12 | 0,21 | 0,23 |
| $Al_2O_3$ | 21,39 | 20,84 | 21,17 | 21,49 | 21,40 | 21,37 | 21,35 | 21,21 | 21,64 | 21,10 | 21,11 |
| *FeO | 32,82 | 34,36 | 34,43 | 33,27 | 36,36 | 30,59 | 32,23 | 30,03 | 32,29 | 23,42 | 28,64 |
| MnO | 0,99 | 1,55 | 2,12 | 2,05 | 0,53 | 1,80 | 1,57 | 2,11 | 0,38 | 6,70 | 1,16 |
| MgO | 3,59 | 2,33 | 2,41 | 1,79 | 2,85 | 2,62 | 2,99 | 1,23 | 3,47 | 1.00 | 1,38 |
| CaO | 4,28 | 3,57 | 3,31 | 3,70 | 0,90 | 6,74 | 5,03 | 8,95 | 5,90 | 11,14 | 11,37 |
| $K_2O$ | 0,00 | 0,03 | 0,02 | n. d. | n. d. | n. d. | n. d. | n. d. | n. d. | n. d. | n. d. |
| $Na_2O$ | 0,01 | 0,03 | 0,00 | n. d. | n. d. | 0,01 | 0,11 | n. d. | n. d. | 0,03 | 0,03 |
| Total | 101,07 | 99,32 | 100,40 | 99,93 | 99,84 | 100,36 | 100,63 | 102,12 | 102,23 | 100,37 | 101,33 |

Numbers of cations on the basis of 24 O

| | | | | | | | | | | | |
|---|---|---|---|---|---|---|---|---|---|---|---|
| Si | 5,977 | 5,953 | 5.941 | 6,040 | 6,068 | 5,929 | 5,945 | 6,025 | 5,984 | 5,889 | 5.919 |
| Al | 3.983 | 3.998 | 4.018 | 4,065 | 4,049 | 4,017 | 4.009 | 3.922 | 3.971 | 3,983 | 3,938 |
| Ti | 0,017 | 0,005 | 0,005 | n. d. | n. d. | 0,007 | 0,003 | 0,003 | 0,023 | 0,024 | 0,027 |
| *$Fe^{2+}$ | 4.335 | 4.678 | 4,637 | 4,467 | 4,881 | 4,084 | 4,295 | 3,940 | 4,205 | 3,137 | 3,791 |
| Mn | 0,132 | 0,214 | 0,288 | 0,278 | 0,073 | 0,242 | 0,211 | 0,280 | 0,051 | 0,909 | 0,156 |
| Mg | 0,845 | 0,565 | 0,579 | 0,430 | 0,682 | 0,625 | 0,710 | 0,287 | 0,805 | 0,239 | 0,326 |
| Ca | 0,723 | 0,622 | 0,571 | 0637 | 0,153 | 0,150 | 0,857 | 1,505 | 0,985 | 1,913 | 1,927 |
| K | 0,001 | 0,011 | 0,008 | n. d. | n. d. | n. d. | n. d. | n. d. | n. d. | n. d. | n. d. |
| Na | 0,005 | 0,007 | 0,001 | n. d. | n. d. | 0,003 | 0,036 | n. d. | n. d. | 0,011 | 0,009 |
| Total | 16,018 | 16,053 | 16,048 | 15,917 | 15,906 | 16,057 | 16,066 | 15,982 | 16,014 | 16,105 | 16,093 |

1. So—3.3: gneiss, $n=3$; 2. Viz—I.5: mica schist, a) core ($n=3$) and b) edge ($n=3$) of the grains; 3. GB—29,2: mica schist, a) core ($n=3$), b) edge ($n=3$); 4. Dar—3.11: gneiss, a) core ($n=3$), b) edge (n=3); 5. Nagy—K—1.11: gneiss, a) core ($n=2$), b) edge ($n=2$); 6. Dar—Ny—2.4; amphibolite, a) core ($n=2$), b) edge ($n=2$).

* Total Fe calculated as FeO and $Fe^{2+}$, respectively
$n$=number of analyses
n. d.=not determined

In case of the gneiss and mica schist samples the complex plagioclase-biotite-garnet-muscovite thermobarometer elaborated by GHENT and STOUT [1981] was used. Results are found in *Fig. 3* and Table 7. The temperature and pressure intervals of 550—600 °C and 5.9—8.9 kbar obtained for the first progressive metamorphism correspond fairly well to the values estimated from the mineral assemblage on the basis of Winkler's reaction isograde system, as well as to the values of 510 °C and 7.3 kbar obtained for the amphibolite of Dar—Ny—2.4 by the amphibole-plagioclase thermobarometer elaborated by PLYUSNINA [1981, 1982: *Fig. 4*].

TABLE 6 (continued)

2. Plagioclase analyses

| | 1. | 2. | 3. | 4. | 5. | 6. |
|---|---|---|---|---|---|---|
| $SiO_2$ | 64,14 | 61,57 | 65,40 | 60,05 | 64,57 | 65,63 |
| $Al_2O_3$ | 23,14 | 22,32 | 21,31 | 24,09 | 23,27 | 22,72 |
| CaO | 4,57 | 4,77 | 2,13 | 5,88 | 3,89 | 2,85 |
| $Na_2O$ | 9,00 | 8,93 | 10,78 | 8,55 | 9,48 | 9,95 |
| $K_2O$ | 0,09 | 0,07 | 0,14 | 0,03 | 0,08 | 0,10 |
| Total | 100,94 | 97,66 | 99,76 | 98,60 | 101,29 | 101,25 |
| | Numbers of cations on the basis of 8 O | | | | | |
| Si | 2,806 | 2,791 | 2,886 | 2,708 | 2,812 | 2,903 |
| $Al^{iv}$ | 1,193 | 1,192 | 1,108 | 1,280 | 1,194 | 1,111 |
| Ca | 0,215 | 0,231 | 0,101 | 0,284 | 0,182 | 0,126 |
| Na | 0,763 | 0,785 | 0,922 | 0,748 | 0,800 | 0,800 |
| K | 0,005 | 0,005 | 0,008 | 0,002 | 0,005 | 0,006 |
| Total | 4,982 | 5,004 | 5,025 | 5,022 | 4,993 | 4,946 |

1. So—3.3: gneiss, $n=3$; 2. Víz—I.5: mica schist, $n=3$;
3. GB—29.2: mica schist, $n=3$; 4. Dar—3.11: gneiss, $n=3$;
5. Nagy—K—1.11: gneiss, $n=3$; 6. Dar—Ny—2.4: amphibolite, $n=6$

*3. Hornblende analyses*
(Dar—Ny—2.4: amphibolite, $n=8$)

| | Weight % | | Cation numbers (23 O) |
|---|---|---|---|
| $SiO_2$ | 43,28 | Si | 6,480 |
| $TiO_2$ | 0,60 | $Al^{iv}$ | 1,520 |
| $Al_2O_3$ | 12,50 | | |
| *FeO | 17,52 | $Al^{vi}$ | 0,686 |
| MnO | 0,27 | Ti | 0,068 |
| MgO | 10,68 | $*Fe^{2+}$ | 2.194 |
| CaO | 10,37 | Mn | 0,034 |
| $Na_2O$ | 2,03 | Mg | 2,448 |
| $K_2O$ | 0,29 | | |
| Total | 97,54 | | |
| | | Ca | 1,664 |
| | | Na | 0,589 |
| | | K | 0,054 |
| | | Total | 15,737 |

* Total Fe calculated as FeO and $Fe^{2+}$

TABLE 6 (continued)

*4. Biotite analyses*

| | 1. | 2. | 3. | 4. | 5. |
|---|---|---|---|---|---|
| $SiO_2$ | 36,10 | 34,81 | 36,16 | 39,07 | 35,97 |
| $TiO_2$ | 1,78 | 1,79 | 1,83 | 1,71 | 1,88 |
| $Al_2O_3$ | 20,99 | 17,93 | 19,63 | 18,87 | 19,84 |
| *FeO | 16,56 | 22,07 | 20,35 | 15,77 | 16,78 |
| MnO | 0,11 | 0,10 | 0,17 | n. d. | 0,05 |
| MgO | 10,94 | 8,37 | 8,92 | 11,56 | 11,71 |
| CaO | 0,00 | 0,04 | n. d. | n. d. | 0,06 |
| $Na_2O$ | 0,23 | 0,06 | 0,36 | 0,19 | 0,19 |
| $K_2O$ | 9,17 | 8,93 | 8,91 | 8,93 | 8.19 |
| Total | 95,88 | 94,10 | 96,33 | 96,10 | 94,67 |
| Numbers of cations in the basis of 22 O | | | | | |
| Si | 5,355 | 5,437 | 5,439 | 5,700 | 5,389 |
| $Al^{iv}$ | 2,645 | 2,563 | 2,561 | 2,300 | 2,611 |
| $Al^{vi}$ | 1,024 | 0,737 | 0,918 | 0,967 | 0,893 |
| Ti | 0,198 | 0,211 | 0,207 | 0,188 | 0,212 |
| $*Fe^{2+}$ | 2,055 | 2,884 | 2,559 | 1,935 | 2.105 |
| Mn | 0,015 | 0,013 | 0,022 | n. d. | 0,007 |
| Mg | 2,421 | 1,949 | 2,001 | 2,526 | 2,615 |
| Ca | 0,000 | 0,006 | n. d. | n. d. | 0,009 |
| Na | 0,067 | 0,019 | 0,104 | 0,054 | 0,055 |
| K | 1,736 | 1,780 | 1,709 | 1,669 | 1,565 |
| Total | 15,516 | 15,599 | 15,520 | 15,339 | 15,461 |

1. So—3.3: gneiss, $n=2$; 2. Víz—I.5: mica schist, $n=7$;
3. GB—29.2: mica schist, $n=5$; 4. Dar—3.11: gneiss, $n=3$;
5. Nagy—K—1.11: gneiss, $n=4$.

* Total Fe calculated as FeO and $Fe^{2+}$

n. d. = not determined.

*5. Muscovite analyses*

| | 1. | 2. | 3. | 4a | 4b | 5. |
|---|---|---|---|---|---|---|
| SiO | 44,50 | 45,85 | 46,93 | 45,76 | 46,20 | 46,34 |
| $TiO_2$ | 0,40 | 0,51 | n. d. | 0,61 | 0,46 | 0,51 |
| $Al_2O_3$ | 34,81 | 33,57 | 34,94 | 34,21 | 33,86 | 34,74 |
| *FeO | 0,65 | 1,15 | 0,83 | 1,07 | 1,85 | 1,20 |
| MnO | 0,02 | 0,01 | n. d. | 0,04 | 0,01 | 0,01 |
| MgO | 0,60 | 0,86 | 0,66 | 1,06 | 1,46 | 0,91 |
| CaO | 0,00 | 0,02 | 0,05 | 0,01 | 0,00 | 0,01 |
| $Na_2O$ | 1,16 | 1,09 | 1,56 | 1,06 | 0,39 | 1,23 |
| $K_2O$ | 9,59 | 9,64 | 9,45 | 9,69 | 9,95 | 9,47 |
| | 91,73 | 92,70 | 94,42 | 93,51 | 94,18 | 94,42 |

TABLE 6 (continued)

| | Numbers of cations on the basis of 22 O | | | | | |
|---|---|---|---|---|---|---|
| Si | 6,125 | 6,224 | 6,260 | 6,190 | 6,220 | 6,198 |
| $Al^{iv}$ | 1.875 | 1,776 | 1,740 | 1,811 | 1,780 | 1,802 |
| $Al^{vi}$ | 3,772 | 3,656 | 3,756 | 3,644 | 3,593 | 3,674 |
| Ti | 0,041 | 0,053 | n. d. | 0,063 | 0,046 | 0,052 |
| $*Fe^{2+}$ | 0,074 | 0,132 | 0,093 | 0,122 | 0,208 | 0,135 |
| Mn | 0,003 | 0,001 | n. d. | 0,005 | 0,002 | 0,001 |
| Mg | 0,124 | 0,176 | 1,131 | 0,214 | 0,293 | 0,182 |
| Ca | 0,000 | 0,003 | 0,008 | 0,001 | 0,001 | 0,002 |
| Na | 0,308 | 0,289 | 0,403 | 0,278 | 0,103 | 0,320 |
| K | 1,684 | 1,687 | 1,608 | 1,672 | 1,709 | 1,617 |
| Total | 14,006 | 13,997 | 13,999 | 14,000 | 13,955 | 13,992 |

1. So—3: gneiss, $n=2$; 2. Viz—I.5: mica schist, $n=4$;
3. GB—29.2: mica schist, $n=3$; 4. Rul—3.2: phyllonitic blastomylonite, a) large porphyroclasts, $n=2$, b) small sericite flakes, $n=3$; 5. Nagy—K—1.11: gneiss, $n=8$.

* Total Fe calculated as FeO and $Fe^{2+}$
n. d. = not determined

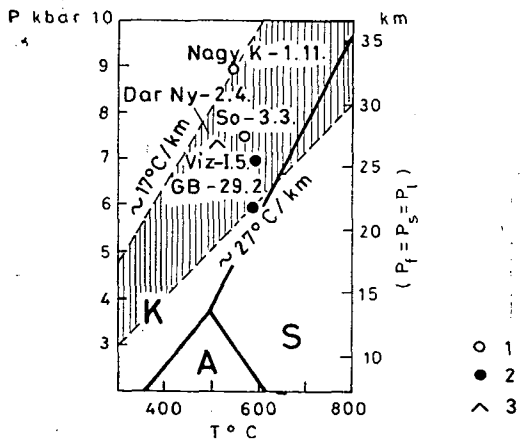


*Fig. 3.* P—T conditions and geothermal gradient-range of the first progressive metamorphism of the crystalline basement based on the geothermobarometer of GHENT and STOUT [1981] showing also the values obtained by the method of PLYUSNINA [1981 1982] for amphibolites.
Legend: 1 — gneiss, 2 — mica schist, 3 — amphibolite, A — andalusite, K — kyanite S — sillimanite.

This latter thermobarometer is based on the P—T dependent changes of the anorthite content of the plagioclase and of the Al-content of hornblende in zoisite-epidote containing assemblages.

Presuming the pressure relations $P_f = P_s \approx P_l$ (which is generally accepted for the amphibolite facies conditions, [see WINKLER, 1976, 1979] and using an average rock density value, the pressure — depth — temperature relationship is demonstrated in *Fig. 3* ($P_f$ — fluid pressure, $P_s$ — pressure acting on the solid phases and $P_l$ — lithostatic or load pressure). Accordingly, the first progressive metamorphism was going

TABLE 7

*Temperature and fluid pressure conditions of the first progressive metamorphic event*

| Sample | Rock type | Thermobarometers | | | |
|---|---|---|---|---|---|
| | | plagioclase-biotite garnet-muscovite (Ghent and Stout, 1981) | | amphibole-plagioclase (Plyusnina, 1981, 1982) | |
| | | T [°C] | $P_f$ [Kbar] | T [°C] | $P_f$ [Kbar] |
| So—3.3 | sillimanite-staurolite-garnet-biotite-muscovite-gneiss | 564 | 7,5 | — | — |
| Víz—I.5 | garnet-biotite-muscovite schist | 598 | 6,9 | — | — |
| GB—29.2 | staurolite-garnet-muscovite-biotite schist | 582 | 5,9 | — | — |
| Dar. Ny—2.4 | garnet-epidote-biotite amphibolite | — | — | 510 | 7,3 |
| Nagy—K-1.11 | kyanite-staurolite-muscovite-biotite gneiss | 551 | 8,9 | — | — |

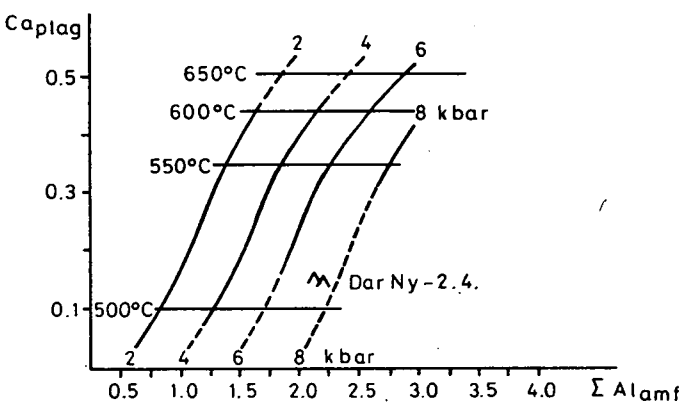


*Fig. 4.* P—T conditions of amphibolite metamorphism according to the geothermobarometer of PLYUSNINA [1981, 1982] for amphibole-plagioclase.

on in a system with a geothermal gradient interval of 17—27 °C/km. This result supports the former statement of LELKES-FELVÁRI, SASSI *et al.* [1981] giving the first quantitative data on the geothermic regime of the metamorphism. This gradient interval is characteristic of the medium pressure range (Barrovian) facies series. The garnet, staurolite, kyanite, and according to the thermobarometric analysis of the sample So—3.3, the sillimanite were generated by this metamorphism.

Traces of anatectic or potash-metasomatic migmatite formation could not be evidenced in the samples except a few uncertain cases. Nevertheless, the plagioclase (oligoclase) porphyroblasts are common and characteristic in the rocks. The formation of plagioclase porphyroblasts (more precisely: poikiloblasts containing the often resorbed inclusions of quartz, biotite, muscovite and garnet, see Plate II.2) together

with the rarely observable mirmekite formation can be evaluated as a phase directly preceeding the anatexis in the course of the recrystallization.

The presence of andalusite in one sample indicates that in addition to the Barrovian metamorphic event an other (low-pressure) amphibolite facies metamorphism of >34 °C/km gradient also acted in certain, restricted parts of the Somogy—Drava Basin. The relationship between andalusite and kyanite is unknown. As in the studied sample of Kut—2.16 the andalusite is younger than the mostly syntectonic garnet+staurolite assemblage (the andalusite contains resorbed staurolite inclusions, see Plate II.1), it can be assumed that the medium pressure kyanitic type recrystallization was overprinted by a low-pressure andalusite-type metamorphism in a subsequent tectonophase or -cycle. (Because of the weathered state of the andalusite-bearing sample the thermobarometric method could not be used.)

Presumably this second (andalusitic) metamorphic event can be related to the Hercynian granitization of the Mecsek Mountains and of the Danube—Tisza Interfluve from spatial, temporal and genetic points of view as well.

The two metamorphic events outlined above were followed by a younger, low-temperature retrograde metamorphism. Its temperature did not reach the biotite isograde ($\sim$ <450 °C, see WINKLER, 1976, 1979) and might be 200—400 °C corresponding to the anchizone and the low temperature part of the greenschist facies (chlorite-zone, epizone). Its mineral assemblages consisting of quartz, sericite, chlorite, calcite, siderite and dolomite can not be or can only be hardly distinguished from the products of the subsequent weathering processes. The illite crystallinity parameters of the not weathered or slightly weathered, biotite-free retrograde metamorphic samples indicate mostly epizonal (greenschist facies) conditions. The fluid pressure of the retrograde metamorphism can be estimated only on the basis of the $b_0$ average of the white micas ($\bar{x}$=8.996 Å, n=3) which presumes low-pressure conditions. The carbonate minerals being always present in these assemblages indicate that the $CO_2$ in addition to the $H_2O$ might have played an important role in the fluid system of the retrograde recrystallization.

Locally, the retrograde metamorphism was connected (most probably somewhat preceeded) by cataclastic metamorphism (mylonite formation): samples Rul—2.2, Rul—3.2, GB—29.4, Se—2.18, Kkut—2.4—9 (Plate II.4). The mineral assemblages of the "static type" retrograde metamorphism characterized above and the assemblages of the weak matrix-recrystallization (blastomylonite formation) subsequent to the dynamic mylonitization are the same. There is a considerable difference in the phengite content of muscovite generated by the first progressive metamorphism and of sericite generation produced by blastomylonite formation (see Table 6 point 5).

When summing up the conclusions the *evolution of the metamorphic basement* can be divided in the phases below, in relative time scale:

*A)* the oldest event was a Barrovian medium pressure, medium-grade (almandine-amphibolite facies) regional metamorphism with a geothermal gradient range of 17 to 27 °C/km. This was followed by

*B)* and andalusite-type (low-pressure, >34 °C/km gradient) amphibolite facies overprint, and

*C)* a predominantly low-pressure, low-temperature, anchi-, epizonal regional metamorphism (<450 °C), locally with cataclastic (mylonitic, blastomylonitic) character.

By means of geothermometric and geobarometric methods only the physical parameters of the event *A)* could be determined: 510—600 °C and 5.9—8.9 kbar.

PLATE II

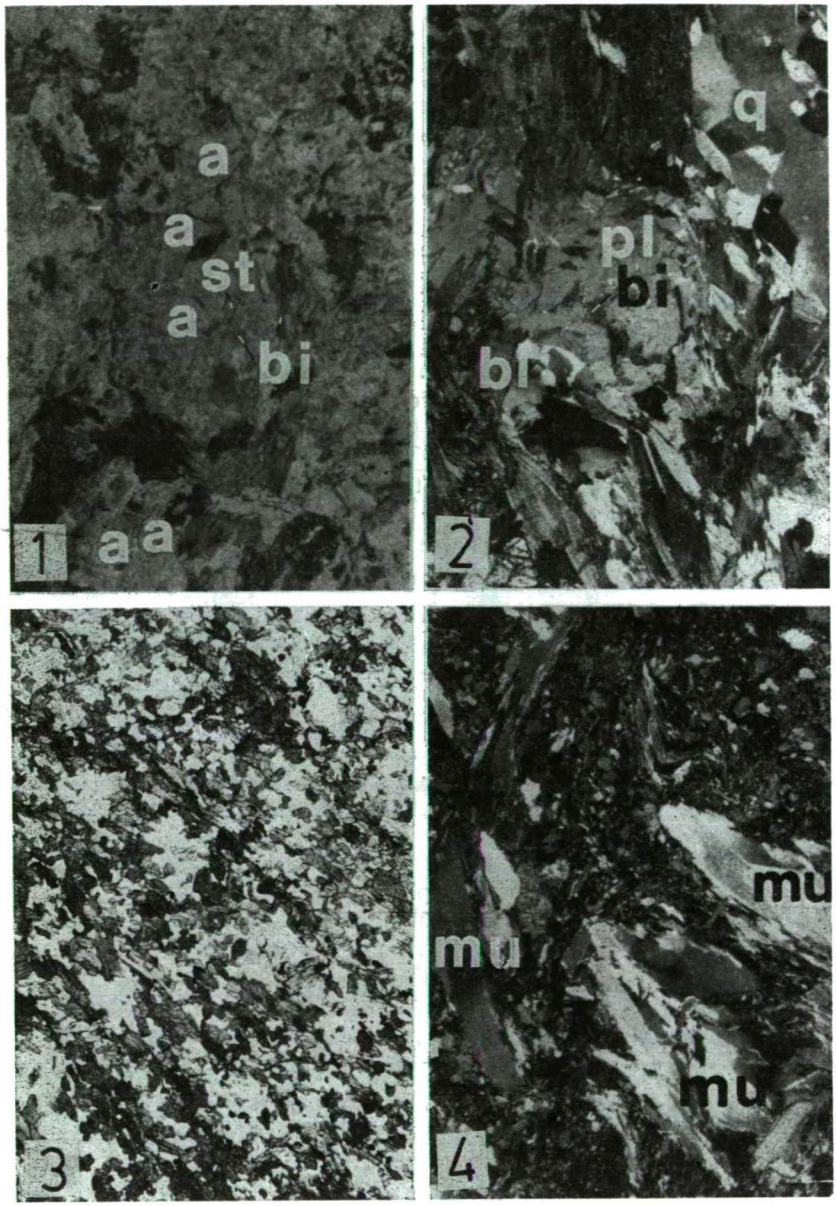

Having no isotope geochronological data and counting with the chronological uncertainties of the metamorphic and granitoid rocks of the Mecsek Mountains adjoining to the investigated area, the chronological classification of the metamorphic events can be made on the bases of farther and presumed analogies. Consequently, several hypothetic models can be established. The possibilities exemplified by the Eastern Alps (FRANK, PURTSCHELLER *et al.*, in NIGGLI 1978] are as follows:

1) *A)* Caledonian, *B)* Hercynian and *C)* Hercynian and/or Alpine:

2) *A)* older Hercynian, *B)* younger Hercynian and *C)* younger Hercynian and/or Alpine.

Based on the models of the Carpatho-Pannonian region [SZÁDECZKY-KARDOSS, ÁRKAI *et al.*, 1976]:

3) *A)* Dalslandian = Early Baikalian, *B)* Hercynian and *C)* Hercynian and/or Alpine.

Out of these models the varieties 1 and 2 seem to be the most probable. To prove them, however, further detailed and systematic isotope geochronological investigations are required.

## WEATHERING

By means of the usual microscopic investigations the retrograde metamorphic mineral assemblages consisting of sericite, chlorite, quartz and carbonate minerals can not be distinguished from the similar mineral parageneses formed by surficial or near-surface chemical weathering of the crystalline basement rocks by the migration of low-temperature solutions. Thus, concerning the effects of weathering conclusions could be drawn only from the qualitative and quantitative relations of clay minerals forming under low-temperature conditions, and from the illite crystallinity indices of the biotite-free samples.

Based on the clay mineral assemblages (Table 2) it can be stated that in the samples investigated the degradation process being progressively parallel with increasing weathering was incomplete. Out of the members of the illite→kaolinite→ →mixed layer clay mineral→smectite degradation (weathering) series determined by RIEDMÜLLER [1978] for phyllosilicate bearing metamorphic rocks only kaolinite and illite could be detected in the crystalline basement of the Somogy—Drava Basin. Out of the samples investigated, ten samples contained kaolinite between trace and

---

**Plate II**

1. Andalusite (a) with inclusions of staurolite (st) and biotite (bi) in gneiss sample Kut—2,16. 1 nicol, picture width is 1 mm.

2. Plagioclase poikiloblast (pl) containing resorbed biotite (bi) inclusions in mica schist (sample GB—29.2). Legend: q — quartz. Crossed nicols, picture width is 2 mm.

3. Textural picture of amphibolite (sample Dar—Ny—2.4). 1 nicol, picture width is 2 mm.

4. Textural picture of blastomylonite of gneissic origin with muscovite (mu) porphyroclasts. — crossed nicols, picture width is 2 mm.

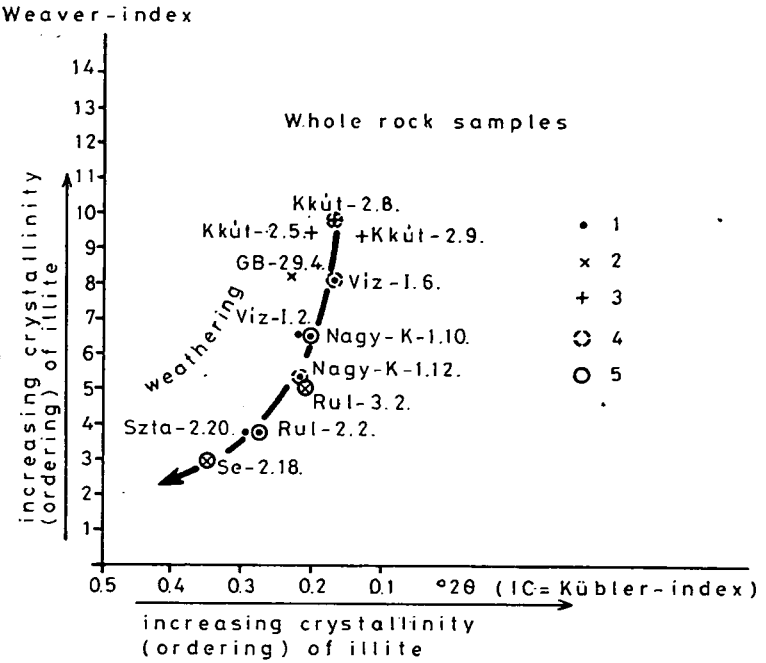


*Fig. 5.* Effect of weathering on the illite crystallinity indices of the biotite-free metamorphic rock Legend: 1 — gneiss and mica schist, 2 — mylonite, 3 — blastomylonite, 4 — trace — 5% kaolinite 5 — >5% kaolinite content.

5%, and five samples between 5 and 15%, thus regarding the quality, the chemica weathering was partial and initial, and concerning the quantitative relations, only o minor significance.

In the samples not containing biotite the illitization producing low-temperature disordered lattice can be detected only by the illite crystallinity indices, first of all by the Weaver-index. The results of this unusual, novel application of illite crystallinity methods used so far only to distinguish the progressive stages of the diagenesis and incipient metamorphism, are shown in *Figs. 5* and *6*.

It can be seen in *Fig. 5* that in the initial stage of weathering (when the samples contain small quantities of poorly crystallized, disordered illite) the Weaver-index considerably decreases while the Kübler-index remains nearly the same as in the not weathered samples. This phenomenon can be explained by a mixture of the muscovite having good crystallinity and of illite with not perfect, disordered structure. The increasing illitization is usually accompanied by the appearance of kaolinite and by its increasing amount. A tendency similar to that observed in the bulk rock samples can be observed in the fractions of less than 2 microns too *(Fig. 6)*.

It can be also assumed that at least a part of the chlorite was generated also by weathering. Its proof, however, needs further investigations.

The carbonate minerals generated by retrograde metamorphism and formed also in the subsequent surficial or near-surface weathering can not be distinguished

either. The carbonate formation took place in several phases from the diffuse imbibition up to the fissure filling with sharp boundaries producing the formation of calcite, dolomite and siderite.

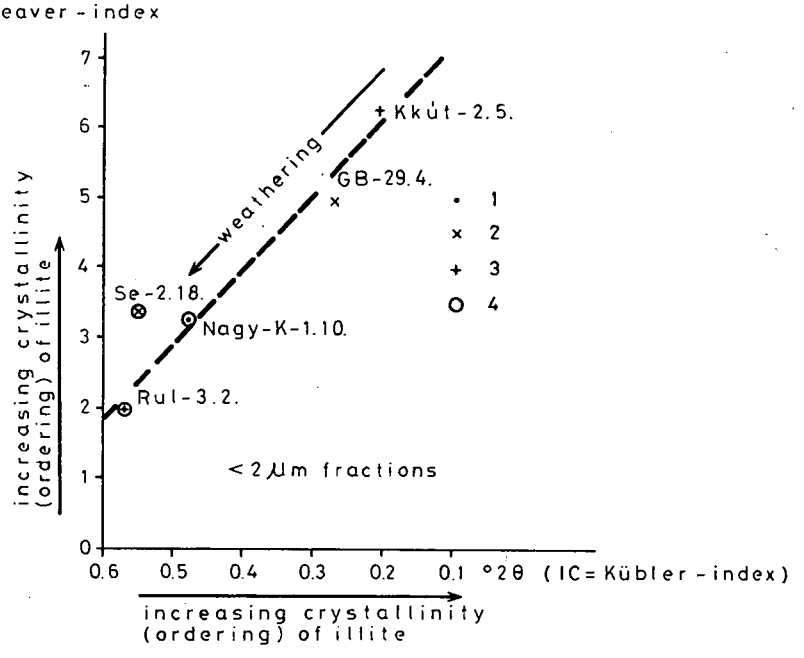


*Fig. 6.* Effect of weathering on the changes of illite crystallinity of the fractions of less than 2 microns in relation with the kaolinite content of the whole rock samples.
Legend: 1 — gneiss, mica schist, 2 — mylonit,e 3 — blastomylonite, 4 — >5% kaloinite content.


## ACKNOWLEDGEMENTS

Author is indebted to DR. V. DANK, geologist-in-chief (National Oil and Gas Industrial Trust, Budapest), to DR. B. BARDÓCZ, geologist-in-chief and to I. TORMÁSSY, Head of Department (Oil and Gas Mining Enterprise, Nagykanizsa) for initiating and financial supporting of the investigations, for the availability of the fundamental geological data and for the permission for publications.

Last, but not least thanks are due to DR. G. DOBOSI, GY. HANGYÁS, J. LEFLER, DR. G. NAGY, DR. O. TOMSCHEY and M.N. TÓTH, co-workers of the Laboratory for Geochemical Research of the Hungarian Academy of Sciences for their analytical works.


## REFERENCES


ÁRKAI, P. [1973]: Pumpellyite-prehnite-quartz facies Alpine metamorphism in the Middle Triassic volcanogenic-sedimentary sequence of the Bükk Mountains, Northeast Hungary. Acta Geol. Acad. Sci. Hung., **17**, 67—83.

ÁRKAI, P. [1983]: Very low- and low-grade Alpine regional metamorphism of the Paleozoic and Mesozoic formations of the Bükkium, NE—Hungary. Acta Geol. Acad. Sci. Hung., **26**, 83—101.

ÁRKAI, P., Z. A. HORVÁTH, M. TÓTH [1981]: Transitional very low- and low-grade regional metamorphism of the Paleozoic formations, Uppony Mountains, NE—Hungary. Acta Geol. Acad. Sci. Hung., **24**, 265—294.

ÁRKAI, P., T. SZEDERKÉNYI [1979]: Javaslat a szénhidrogénkutatások körében a metamorf képződmények és jelenségek egységes megnevezésére (Proposal to the uniform terminology of metamorphic formations and phenomena in hydrocarbon exploration). — OKGT Publication-Budapest.

BALÁZS, E. [1968]: A dél-dunántúli metamorf és mélységi magmás képződmények genetikája és el, terjedése a szénhidrogénkutató fúrások alapján (Genetics and extension of the metamorphic and igneous formations of South Transdanubia on the basis of hydrocarbon exploratory wells). OGIL Műsz. Tud. Közl. **51—55**.

BALÁZS, E. [1980]: Összefoglaló magvizsgálati jelentés a Barcs—Ny—1 kutatófúrásról (Final report on the core sample investigations from the Barcs—Ny—1 borehole). OKGT Adattár, Budapest.

BARDÓCZ, B. *et al.*, [1973]: A Délnyugat-Dunántúli medencerész előkutatási programja (Exploration program for the basin part of Southwest Transdanubia). — OKGT Dunántúli Kutató és Feltáró Üzem, Nagykanizsa.

BÁRDOSSY, GY. [1966]: A bauxit ásványos összetételének röntgendiffrakciós vizsgálata (X-ray diffraction investigation of the mineral composition of bauxite). Koh. Lapok. **8**, 355—363.

BUDA, GY. [1972]: Magyarországi granitoid kőzetek genetikai és tektonikai csoportosítása, különös tekintettel a földpátok vizsgálatára (Genetic and tectonic classification of Hungarian granitoid rocks with special regard to the feldspar studies). — MTA X. Oszt. Közl., **5**, 21—26.

FRANK, W., F. PURTSCHELLER *et al.*, [1978]: Eastern Alps. In: NIGGLI E. (editor): Metamorphic map of the Alps. Subcommission for the Cartography of the Metamorphic Belts of the World, Leiden.

GHENT, E. D., M. Z. STOUT [1981]: Geobarometry and geothermometry of plagioclase-biotite-garnet-muscovite assemblages. Contrib. Mineral. Petrol., **26**, 92—97.

GUIDOTTI, C. V., F. P. SASSI [1976]: Muscovite as a petrogenetic indicator mineral in pelitic schists. N. Jb. Miner. Abh., **127**, 97—142.

JANTSKY, B. [1976]: Geologische Entwicklungsgeschichte des präkambrischen und paläozoischen Untergrundes im Pannonischen Becken. Nova Acta Leopoldina, Neue Folge **45**, 303—334.

JANTSKY, B. [1979]: A mecseki gránitosodott kristályos alaphegység földtana (Geology of the granizited basement of the Mecsek Mountains). — MÁFI Évkönyv **60**, 1—385.

KOVÁCS, S. [1982]: Problems of the „Pannonian Median Massif" and the plate tectonic concept. Geologische Rundschau **71**, 617—640.

KÜBLER, B. [1968]: Evaluation quantitative du metamorphisme par la cristallinité de l'illite. Bull. Centre Rech. Pau — SNPA, **7**, 385—397.

KÜBLER, B. [1975]: Diagenese — anchimetamorphisme et metamorphisme. Inst. National de la recherche sci. — Petrole, Quebec.

LELKES-FELVÁRI, GY., F. P. SASSI *et al.* [1981]: Outlines of the pre-Alpine metamorphism in Hungary. IGCP Project No. 5 Newsletter No. **3**, 89—99.

NAGY, E., K. SZEPESHÁZY: [1971]: Magyarország mélyföldtani térképe a paleozóikumnál fiatalabb képződmények elhagyásával (Deep geological map of Hungary omitting the formations younger than Paleozoic). — Explanatory text, manuscript, MÁFI, Budapest.

NÁRAY-SZABÓ, I., T. PÉTER [1967]: Die quantitative Phasenanalyse in der Tonmineralforschung. Acta Geol. Acad. Sci. Hung., **11**, 347—356.

PLYUSNINA, L. P. [1981]: Eksperimental'noe izutshenie zavisimosti glinozemistosti rogovih obmanok ot PT-uslovij in obrozovanija. Izv. Adak. Nauk SzSzSzR. Szer. Geol., No. **7**, 19—28.

PLYUSNINA, L. P. [1982]: Geothermometry and geobarometry of plagioclase-hornblende bearing assemblages. Contrib. Mineral. Petrol., **80**, 140—146.

RIEDMÜLLER, G. [1978]: Neoformations and transformations of clay minerals in tectonic shear zones. Tschermaks Miner. Petr. Mitt., **25**, 219—242.

RISCHÁK, G., I. VICZIÁN [1974]: Agyagásványok bázisreflexiójának intenzitását meghatározó ásványtani tényezők (Mineralogical factors determining the base reflexion intensity of clay minerals). — MÁFI Évi jel. 1972, 229—256.

SASSI, F. P. [1972]: The petrological and geological significance of the $b_0$ values of potassic white micas in low-grade metamorphic rocks. Tschermaks Miner. Petr. Mitt., **18**, 105—113.

SCHWEDER, P. [1968]: Geochemische Untersuchungen im Kiffhäuser-kristallin. Chemie der Erde **72**, No. 1.

SZÁDECZKY-KARDOSS, E., Á. JUHÁSZ *et al.* [1969]: Erläuterung zur Karte der Metamorphiten von Ungarn. Acta Geol. Acad. Sci. Hung., **13**, 27—34.

SZÁDECZKY-KARDOSS, E., P. ÁRKAI *et al.* [1976]: Map of metamorphites of the Carpatho-Balkan-Dinaride area. KBGA—KFH—MTA GKL, Budapest.

SZEDERKÉNYI, T. [1975]: A Délkelet-Dunántúl ópaleozóos képződményeinek ritkaelem kutatása (Trace element invesgations in the Early Paleozoic formations of Southeast Transdanubia) — Candidate theses, Budapest.
SZEDERKÉNYI, T. [1982]: Lithostratigraphic division of the crystalline mass in South Transdanubian and the Great Hungarian Plain. IGCP Project No. 5 Newsletter No. 4, 101—106.
SZEPESHÁZY, K. [1958]: A magyar medence aljzatának kristályos kőzetei (Crystalline rocks of the basement in the Hungarian Basin). — Report, OKGT, Labor Főo. Budapest.
SZEPESHÁZY, K. [1959]: Jugoszlávia É-i határvidékénél lemélyített fúrásokból előkerült metamorf kőzetminták vizsgálata (Investigation of metamorphic rock samples found in the boreholes drilled in the norther part of Jugoslavia). — Report, OKGT. Labor Főo. Budapest,
VICZIÁN, I., A. F. GHONEIM [1977]: X-ray studies on crystalline rocks of the Ófalu Group, Mecsek Mts., Hungary. Acta Miner. Petr. Szeged 23, 29—39.
WALKER, K. R., G. A. JOPLIN *et al.*, [1960]: Metamorphic and metasomatic convergence of basic igneous rocks and lime-magnesia sediments of the Precambrian of North-Western Queensland. J. Geol. Soc. Australia 6, No. 2.
WEAVER, C. E. [1960]: Possible uses of clay minerals in search for oil. AAPG. Bulletin 44, 1505—1518.
WEIN, GY. [1969]: Tectonic review of the Neogene-covered areas of Hungary. Acta Geol. Acad. Sci. Hung., 13, 399—436.
WINKLER, H. G. F.: Petrogenesis of metamorphic rocks. 2nd, 4th and 5th editions. Spinger, New York—Heidelberg—Berlin, 1967, 1976, 1979.

*Manuscript received, 29 August, 1983*

P. ÁRKAI
Laboratory for Geochemical Research
Hungarian Academy of Sciences
H-1112 Budapest, Budaőrsi út 45
Hungary

*Acta Mineralogica-Petrographica, Szeged, XXVI/2, 155—170, 1984*

# AN ATTEMPT FOR DISTINCTION OF AMPHIBOLITES BASED ON STATISTICAL ANALYSIS OF THEIR BULK COMPOSITION

J. GEIGER and T. SZEDERKÉNYI

ABSTRACT

Distinction between different amphibolite types usually is solvable by great number of discrimination diagrams based on chemical composition and trace element content. Using mathematical statistics (cluster analysis as well as hypothesis analysis) another method is presented in this paper This attempt proves a fairly good fitness of these statistical methods for the distinction of amphi bolites.

## INTRODUCTION

Due to their uniform mineralogical-petrographic and petrochemical characteristics as well as lithostratigraphic position, a distinction of different amphibolites of South Transdanubia and Great Hungarian Plain is very difficult. Having essential importance for the correlation, these amphibolite intercalations (lenses or beds) of thick and monotonous gneiss-mica-schist complexes, similarly to that of marble beds require an emphasized attention of the researchers.

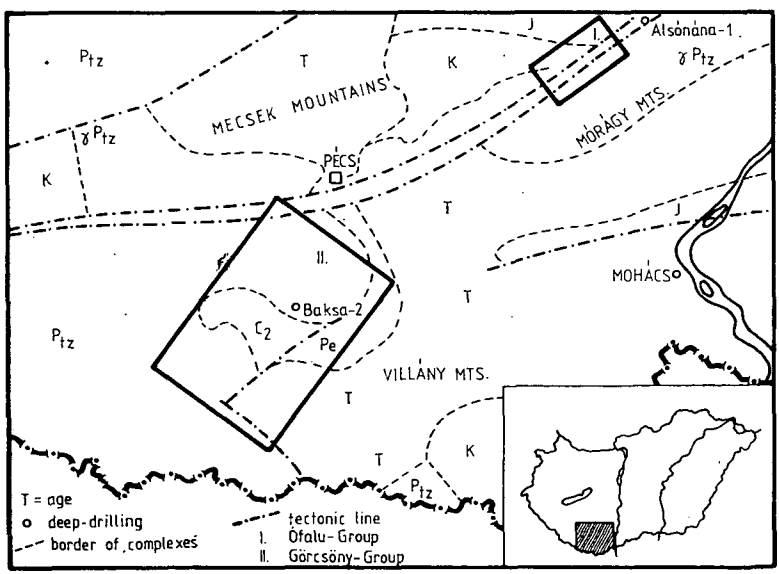


*Fig. 1.* Locality of the investigated complexes

The aim of this attempt is to develop a mathematical method for the evaluation which renders the long and sometimes gloomy graphical works (discrimination diagrams) shorter and makes it more understable. This attempt is based on numerous bulk composition data gained from amphibolites of South Transdanubian Görcsöny- and Ófalu Groups which has already been evaluated and interpreted by a traditional petrological method [SZEDERKÉNYI, 1982].

## REVIEW OF THE INVESTIGATED COMPLEXES

Metamorphics belonging to the crystalline groundfloor of Southeast Transdanubia *(Fig. 1)* are subdivided into two groups lithostratigraphically: (1) Görcsöny Group and (2) Ófalu Group [SZEDERKÉNYI, 1977], see *Fig. 1.* Both groups contain numerous amphibolite intercalations and show certain diversities in their lithology and metamorphic development as well as geochemistry, too. Their most important characteristics are as follows:

1. The *Görcsöny Group* is located on the southern foreground of Western Mecsek Mts. and consists of a well-developed sequence of Barrow-type metamorphics containing zones from chlorite up to sillimanite (and migmatization) with a well detected progressivity from SW to NE. Its characteristic rock-types are: chlorite schist, biotite-muscovite schists and gneisses with or without garnet, staurolite, kyanite, sillimanite minerals corresponding to the Barrovian zonality and amphibolite and actinolite schist intercalations as well as marble and/or dolomitic marble lenses together with calc-silicate rocks having regional polymetamorphic origin.

2. The *Ófalu Group* joints to the northern margin of the Mórágy granite mass. Its members form a strongly sheared and diaphtorized crystalline schist sequence which is developed by a greenschist-amphibolite grade of regional metamorphism and a considerable shearing. Its most important rock-types are: metagraywacke with basic and intermedier tuffs and lavas, chlorite schists, siliceous shales with chert, sericitized phyllonitic rocks, actinolite schists and amphibolite beds as well as a rather thick (30—70 m) crystalline limestone member having chlorite schist intercalations. Several parts of this strongly sheared and tectonically dissected sequence show a weak melting phenomenon connected with the shearing [SZEDERKÉNYI, 1974].

## METHODS OF STATISTICAL ANALYSIS

Requirements of the applied analytical technique are:

— to give a real genetical arrangement of samples by means of their geochemical features,

— to describe several geochemical connections among the genetical units obtained,

— to point out some genetical differences and similarities among these groups.

In the first step of this statistical work several possibilities of different grouping phrough the bulk chemical analysis of the amphibolites and their geological interpretation are examined. In the second step a mathematical modelling of applied cetrotectonic interpretations is attempted. The applied mathematical process is a combination of multiple hierarchical classification and hypothesis analysis as well as torrelation one, which is suitable for drawing several geological-geochemica inferences of particular importance for the geology of crystalline complexes of South Transdanubia and Great Hungarian Plain. For a better petrological interpretation

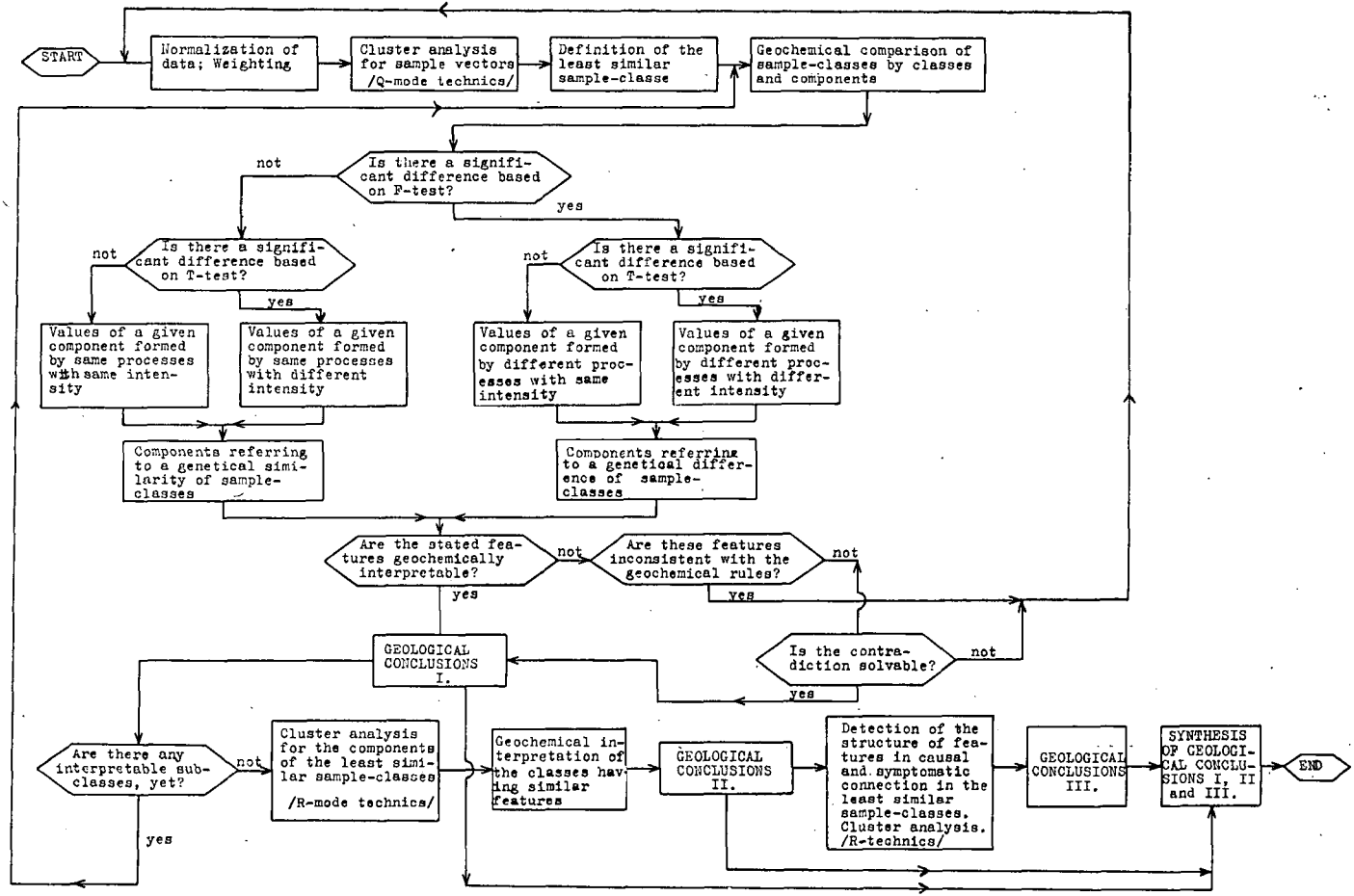


*Fig. 2.* Flow sheet of the examination applied

TABLE 1

*Chemical composition (calculated on volatile-free basis) of the Ófalu Group amphibolites as well as Görcsöny Group ones*

| No. of samples | Components | | | | | | | | | | | |
|---|---|---|---|---|---|---|---|---|---|---|---|---|
| | $SiO_2$ | $TiO_2$ | $Al_2O_3$ | $Fe_2O_3$ | FeO | MnO | MgO | CaO | $Na_2O$ | $K_2O$ | $P_2O_5$ | L.O.I. |
| Görcsöny Group | | | | | | | | | | | | |
| $V_1$ | 47.64 | 2.56 | 14.22 | 1.14 | 10.17 | 0.08 | 5.35 | 11.71 | 3.19 | 2.05 | 1.26 | 2.98 |
| $V_2$ | 47.89 | 2.55 | 13.95 | 1.60 | 10.46 | 0.11 | 5.23 | 10.69 | 3.19 | 1.80 | 1.38 | 2.73 |
| $V_3$ | 47.13 | 1.19 | 14.58 | 0.35 | 12.24 | 0.22 | 6.10 | 10.49 | 3.08 | 1.50 | 1.48 | 2.48 |
| $V_4$ | 48.62 | 2.05 | 14.89 | 0.35 | 12.05 | 0.18 | 5.22 | 9.57 | 3.59 | 1.23 | 0.23 | 2.36 |
| $V_5$ | 45.98 | 3.07 | 12.88 | 1.30 | 12.63 | 0.17 | 8.24 | 11.58 | 2.56 | 0.91 | 0.39 | 2.29 |
| $V_6$ | 47.49 | 2.87 | 14.83 | 0.52 | 12.21 | 0.16 | 6.35 | 9.22 | 3.43 | 1.37 | 0.29 | 2.42 |
| $V_7$ | 49.57 | 2.72 | 15.76 | 1.52 | 10.08 | 0.16 | 6.76 | 9.15 | 2.15 | 1.70 | 0.25 | 2.44 |
| $V_8$ | 47.31 | 2.82 | 13.77 | 1.18 | 11.11 | 0.10 | 6.50 | 11.32 | 2.92 | 1.20 | 1.09 | 2.38 |
| $V_9$ | 50.57 | 3.33 | 15.14 | 0.58 | 12.03 | 0.16 | 4.20 | 10.14 | 2.07 | 1.02 | 0.27 | 2.36 |
| $V_{10}$ | 46.47 | 3.23 | 14.57 | 0.99 | 10.67 | 0.21 | 7.42 | 10.97 | 2.60 | 1.31 | 1.16 | 2.87 |
| $V_{11}$ | 48.39 | 2.88 | 13.98 | 1.29 | 9.50 | 0.21 | 6.53 | 9.42 | 2.80 | 2.18 | 1.02 | 1.53 |
| $V_{12}$ | 46.61 | 3.13 | 14.23 | 0.98 | 11.29 | 0.26 | 7.36 | 10.35 | 2.63 | 1.39 | 1.13 | 2.13 |
| $V_{13}$ | 50.34 | 3.01 | 14.42 | 1.20 | 9.04 | 0.16 | 7.10 | 9.45 | 1.30 | 3.23 | 0.89 | 2.11 |
| $V_{14}$ | 47.65 | 3.00 | 14.45 | 0.54 | 10.64 | 0.18 | 7.54 | 10.40 | 2.83 | 1.16 | 1.05 | 2.40 |
| Ófalu Group | | | | | | | | | | | | |
| $V_{15}$ | 51.85 | 1.56 | 13.88 | 3.94 | 6.88 | 0.19 | 6.49 | 10.40 | 4.11 | 0.78 | 0.16 | 3.78 |
| $V_{16}$ | 47.93 | 1.27 | 15.48 | 1.02 | 12.80 | 0.17 | 7.38 | 11.02 | 2.34 | 0.31 | 0.22 | 4.17 |
| $V_{17}$ | 50.64 | 1.67 | 13.87 | 2.67 | 5.17 | 0.26 | 8.21 | 8.92 | 3.24 | 3.39 | 0.37 | 4.34 |
| $V_{18}$ | 51.47 | 1.88 | 13.42 | 3.13 | 10.74 | 0.18 | 8.17 | 0.57 | 2.48 | 0.99 | 0.19 | 4.03 |
| $V_{19}$ | 52.73 | 2.49 | 14.27 | 3.41 | 8.27 | 0.82 | 5.92 | 7.69 | 4.35 | 0.53 | 0.24 | 2.11 |
| $V_{20}$ | 51.27 | 2.44 | 15.59 | 4.24 | 8.47 | 0.23 | 4.92 | 9.80 | 2.89 | 0.34 | 0.46 | 2.62 |
| $V_{21}$ | 48.39 | 2.01 | 13.52 | 2.92 | 9.66 | 0.95 | 6,98 | 12.42 | 2.24 | 1.03 | 0.22 | 3.77 |
| $V_{22}$ | 50.24 | 0.68 | 15.99 | 3.16 | 7.73 | 0.25 | 8.80 | 9.60 | 2.78 | 0.70 | 0.33 | 3.05 |

TABLE 1

*Source of the investigated samples*

(continued)

| No. of the samples | | | |
|---|---|---|---|
| $V_1$ | Baksa No. 2. drilling, | 108,6 m | |
| $V_2$ | Baksa No. 2 drilling, | 118,0 m | |
| $V_3$ | Baksa No. 2 drilling, | 127.0 m | |
| $V_1$ | Baksa No. 2 drilling, | 108,6 m | |
| $V_2$ | Baksa No. 2 drilling, | 118.0 m | |
| $V_3$ | Baksa No. 2 drilling, | 127.0 m | |
| $V_4$ | Baksa No. 2 drilling, | 825.0 m | |
| $V_5$ | Baksa No. 2 drilling, | 845.3 m | |
| $V_6$ | Baksa No. 2 drilling, | 856,9 m | T. SZEDERKÉNYI [1982] |
| $V_7$ | Baksa No. 2 drilling, | 1065.1 m | |
| $V_8$ | Baksa No. 2 drilling, | 152,6 m | |
| $V_9$ | Téseny No. 1 1 drilling, | 169.2 m | |
| $V_{10}$ | Téseny No. 1 drilling, | 172.5 m | |
| $V_{11}$ | Gyód No. 3 drilling, | 130.0 m | |
| $V_{12}$ | Gyód No. 3 drilling, | 147.0 m | |
| $V_{13}$ | Gyód No. 4 drilling, | 75.2 m | |
| $V_{14}$ | Okorág No. 1 drilling | 1178.5 m | |
| $V_{15}$ | Bátaapáti, Kövespatak | | B. JANTSKY [1979] |
| $V_{16}$ | Alsónána No. 1 drilling, | 102.3 m | B. JANTSKY [1979] |
| $V_{17}$ | Ófalu, Sheep-fold Valley | | T. SZEDERKÉNYI [1982] |
| $V_{18}$ | Ófalu, Goldgrund | | |
| $V_1$ | Ófalu, Studer Valley | | |
| $V_{20}$ | Bátaapáti, Kövespatak | | M. A. F. GHONEIM., T. SZEDERKÉNYI [1977] |
| $V_{21}$ | Erdősmecske, village | | |
| $V_{22}$ | Erdősmecske, village | | |

of the results obtained in close connection with the geological considerations, a few quantitative checking points are enclosed into the mathematical process (see *Fig. 2)*.

In the first step of the analysis, each sample is represented by 12 dimensional vectors derived from the chemical components (Table 1) belonging to the given sample (more exactly: each value of all parameters is divided with the standard deviation of the given parameter. This methods liquidates the mistakes derived from the differences of the order magnitude. The classifying algorithm has been carried out this rescaled sample). A classification of the points of the sample-space is carried out by group average method of cluster analysis [MICHENER, 1958]. A vectorial distance is regarded as a similarity parameter. Results of the analysis are displayed on a dendogram or dendograph *(Fig. 3)*. At the interpretation of dendograms it is important to consider that the horizontal lines having different similarity parameters and drawn in different heights on the graph, correspond to different hierarchy of the sample classes. (As synonyms of the sample class concept, the "cluster class" and "group", or "genetical unit" expressions are also used in this paper.) Consequently, according to their contents, only the sample classes having same similarity level can be set against with each other. Including a lower similarity level as well as a higher one of a sample class, the first one (the lower level) can be characterized as a special case of the second one (the higher level).

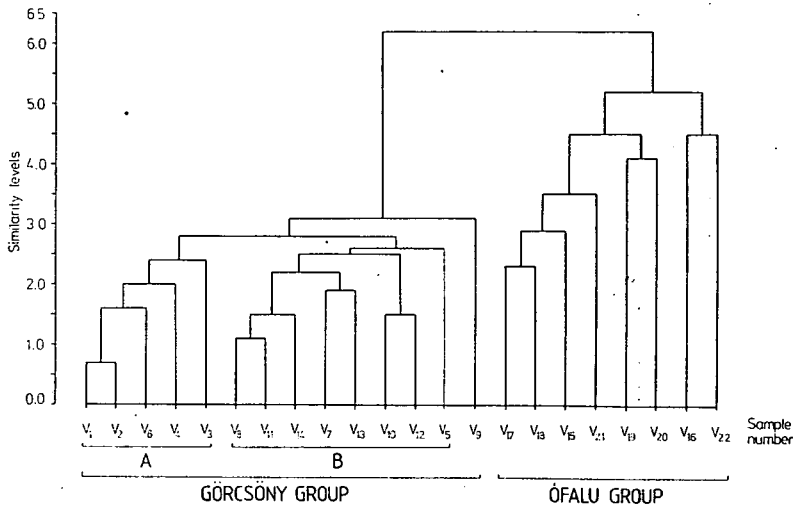


*Fig. 3.* Dendograph of the Görcsöny Group amphibolites as well as Ófalu Group ones

Since the cluster classes obtained are originated from the grouping of different sample-vectors, every cluster expresses some kind of genetical relationship of the samples contained by it. Theoretically, each different cluster represents several rock-types of heterogenous origin, or of the same origin showing the results of heterogenous geochemical events during their genesis. Consequently, degree of similarity of the obtained statistical sample classes appears as an image of some kind of genetical relationships of the examined rock-samples. The sample classes linked in the highest similarity level of a dendogram, represent a group of the most important rock-

TABLE 2

*Averages ($\bar{x}$) and related standard deviation values ($s$) of the chemical components of the Ófalu Group amphibolites as well as Görcsöny Group ones*

| Group | No. of samples | $SiO_2$ | $TiO_2$ | $Al_2O_3$ | $Fe_2O_3$ | FeO | MnO | MgO | CaO | $Na_2O$ | $K_2O$ | $P_2O_5$ | L. O. I. | |
|---|---|---|---|---|---|---|---|---|---|---|---|---|---|---|
| Görcsöny Group | 14 | 1.392 | 0.553 | 0.681 | 0.425 | 1.112 | 0.049 | 1.112 | 0.871 | 0.601 | 0.603 | 0.460 | 0.351 | $s$ |
| Ófalu-Group | 8 | 1.666 | 0.601 | 1.023 | 0.974 | 2.356 | 0.315 | 1.303 | 3.610 | 0.796 | 0.999 | 0.103 | 0.801 | |
| Görcsöny Group | 14 | 47.976 | 2.744 | 14.405 | 0.967 | 11.009 | 0.168 | 6.421 | 10.319 | 2.739 | 1.575 | 0.849 | 2.391 | $\bar{x}$, wt% |
| Ófalu Group | 8 | 50.565 | 1.750 | 14.503 | 3.061 | 8.715 | 0.381 | 7.109 | 8.803 | 3.054 | 1.009 | 0.274 | 3.484 | |

genetical units. The sample classes are defined only up to the similarity level as far as they have still a precise geological-petrological content (see *Fig. 3)*.

A geochemical comparison of the opposed cluster classes is carried out by hypothesis analysis of the parameters obtained *(Fig. 2)*. The aim of this comparison is to select several components which suffered different effects during their formation in the opposed sample classes. This operation carried out by the sequence of so called "F-test" and "T-test"; the type of T-test depends on the result of F-one *(Fig. 2)*. If on a fixed level of significancy the result of the F-test demonstrates appreciable differences in the values of the standard deviation (with a certain reservation) it can be inferred on some qualitative differences in the geochemical events during the rock genesis. A significant deviation of the mean-values shown by the T-test suggests quantitative differences in the events [NAGY, 1969]. *Fig. 2* [after NAGY, 1969] also presents some geological interpretations belonging to different variational possibilities. Geochemical components which can characterize several cluster classes *(Figs.* 3, 7, 10, 11) are granted by this figure. At the same time, a geochemical interpretability of the obtained results also gives a checking-point for the series. Geological conclusions are originated from here *(Fig. 2)*.

After the definition of all geologically interpretable sample classes, the next task is to describe each group. It can be carried out by the revelation of the particular relationships of the chemical components. Firstly, the related component-groups are determined in the sample classes by the "R-test" of cluster analysis. The strength of dependence between the chemical components is measured by the correlation coefficient, and the hierarchic classification is made again by the "group-average method" *(Figs. 4, 5)*. Since in this algorithm the causal relations and/or symptomatic ones are reflected in a hidden-way, a structure of relations existing between parameters is developed by the so called "ramifying linkage method" [TYRON, 1939; CATTEL, 1944; GEIGER, 1982]. Further on, these structures will be regarded as geochemical (correlation) profiles *(Fig. 6)*. The correlatable features are signed by a straight line on *Fig. 6*. The number being close to this line expresses a value of a correlation and its sign gives a direction for this correlation. The geochemica

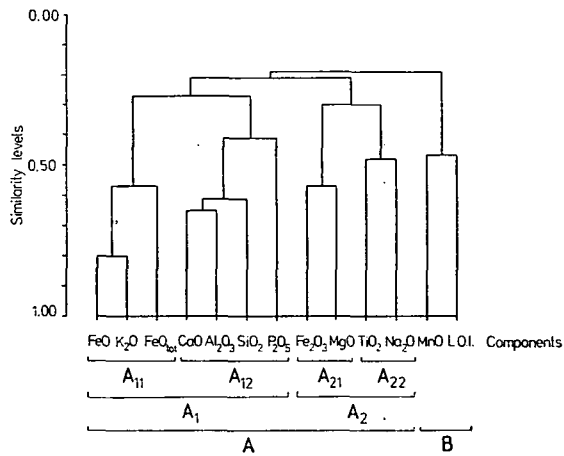


*Fig. 4.* Dendograph of the Görcsöny Group amphibolites based on the correlation coefficients existing between chemical components

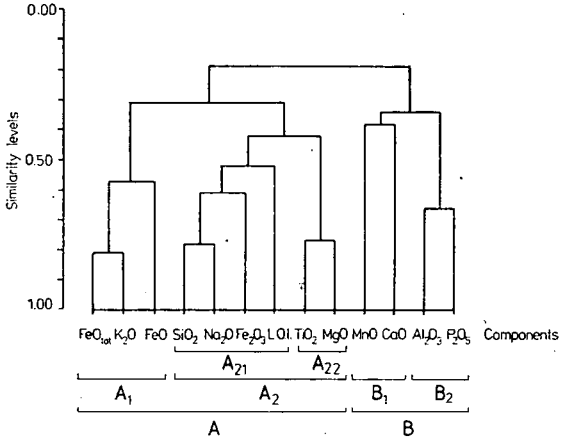


*Fig. 5.* Dendograph of the Ófalu Group amphibolites based on the correlation coefficients existing between chemical components

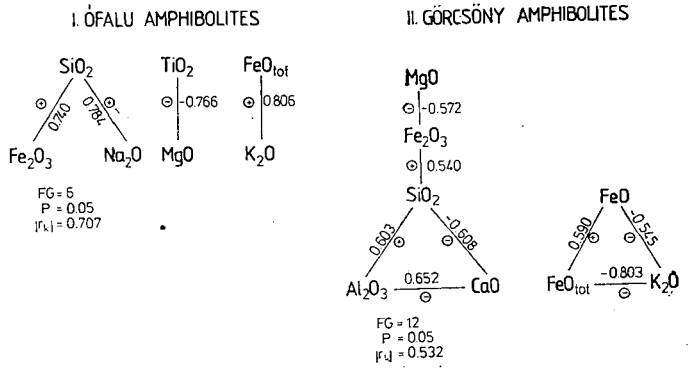


*Fig. 6.* Geochemical correlation profiles of the Ófal ≈ Group amphibolites (I) as well as Görcsöny Group ones (II).
Legend: FG = numbers of degree of the freedoms
P = level of the significancy
($r_k$) = critical value of the correlation coefficient

interpretation related to several genetical units of the rock samples is given by the evaluation of the geochemical correlation profile, as well as similar groups of the components. Moreover, the correlation profile is also suitable for the realization of different geological conclusions obtained from the second and third levels of *Fig. 2.*

Chemical components showing the same evolution within a genetical unit are also selected. The obtained results offer numerous useful complementary information for the analysis of the progress of development. The way of this process is the F-test and T-one of the hypothesis analysis.

Finally, a complete analysis of series of the geochemical data is completed by the synthesis of several geological conclusions obtained from the first, second and third levels in *Fig. 2.*

## INTERPRETATION OF THE RESULTS

One of the most important results of the cluster analysis is a perfect separation of the samples of Görcsöny and Ófalu amphibolites based on the similarity level No. 6,4 of the dendogram *Fig. 3* (which is calculated and compiled by chemical analyses in Table 1). Consequently, amphibolites originated from both groups have a fairly divergent evolution. This separation can be interpreted as different origin, or site, or a possibly another premetamorphic and/or metamorphic history, etc.

The separated cluster-class of the Görcsöny Group in the *Fig. 3* shows a further division possibility into two subclasses (named A and B) on the similarity level No: 2, 6. A sample signed $V_9$ may be regarded as a supplementary class of the Görcsöny Group, but being a single element it should rather be considered as a variation. Due to its little sample-number a similar subdivision cannot be made in the Ófalu Group.

According to the hypothesis analysis of the mean values andstandard deviations, it is obvious that the $Al_2O_3$, MgO, $Na_2O$ $K_2O$, $SiO_2$ $TiO_2$ componeots mathematically show the same evolution but the $Fe_2O_3$, FeO, $P_2O_5$ MnO, CaO, and the "loss of ignition (L. O. I.)" parameters are formed by different ones in the amphibolites of the Ófalu and Görcsöny Groups *(Fig. 7)*. The components derived in the sameway, are suitable for a further differentiation based on their T-test. Morevoer, the *Fig. 7*

| | $SiO_2$ | $TiO_2$ | $Al_2O_3$ | $Fe_2O_3$ | FeO | MnO | MgO | CaO | $Na_2O$ | $K_2O$ | $P_2O_5$ | L.O.I. |
|---|---|---|---|---|---|---|---|---|---|---|---|---|
| F - test | • | • | • | | | | • | | • | • | | |
| t - test | | | • | | | • | • | • | • | • | | |

*Fig. 7.* Hypothesis analysis of the chemical components of the Ófalu Group amphibolites as wel as Görcsöny Group ones.
Legend: ● no significant difference pointed out in the development of the investigated features on significancy level $P=0.05$ (F-test) and in the medium intensity of the process produced by the investigated features (T-test).

shows a perfect genetical identity (i.e. same evolution and same intensity) in the features of the $Al_2O_3$, MgO, $Na_2O$ and $K_2O$. But in spite of the same evolution, the $SiO_2$ content of the Görcsöny amphibolites is significantly lower, and the $TiO_2$ content is significantly higher than that of Ófalu ones. $Fe_2O_3$, FeO, $P_2O_5$ and L.O.I. components represent a total genetical difference between both groups (divergent evolution characterized by different intensity). But, the values of MnO and CaO were formed by divergent processes with the same intensity. After all, the most important geochemical differences between Ófalu and Görcsöny amphibolites are given by the formation of $Fe_2O_3$, FeO, $P_2O_5$ and L.O.I. parameters. The caracteristic and extreme high $P_2O_5$ content of the Görcsöny amphibolites suggest magmatically and essentia difference in the parent rocks of both amphibolite groups.

Further differences can be traced by results of cluster analysis, too. A dendograph drawn on the basis of the chemical components of Görcsöny amphibolites *(Fig. 4)* shows a bipartition among them as it is mentioned before (subclasses A and B). The B subclass is represented by MnO and L.O.I. components (where the correlation coefficient is smaller between them than the critical but still acceptable value: see *Fig. 4* B and *Fig. 6* II). All other components belong to the A subclass. A similar bipartition can be observed on the graph of the Ófalu amphibolites *(Fig. 5)*. The A subclass is determined by MnO, CaO and $Al_2O_3$, but all other chemical components to the subclass B. Common features of both graphs (*Fig. 4* and *Fig. 5*) are: (1) further

differentiation occurs only in the subclasses A, (2) FeO, $FeO_{tot}$ and $K_2O$ establish the same members in both A subclasses.

Geochemical correlation profiles of both amphibolite groups show fairly sharper genetical differences between them than the dendographs do. *Fig. 6* shows four no-correlatable systems in the Ófalu amphibolites. MnO, CaO and L.O.I. data (from 13 components) have no significant correlation either with each other, or with other components. In the Görcsöny amphibolites (*Fig. 6* II) the parameters $TiO_2$, MnO, $Na_2O$, $P_2O_5$ and L.O.I. show the same picture. Geochemical (correlation) profile of these amphibolites contains two no-correlatable systems with three mutually acting components: $Al_2O_3$—CaO—$SiO_2$ triad influenced by $Fe_2O_3$ through the $SiO_2$, as well as the FeO — $FeO_{tot}$ — $K_2O$ one.

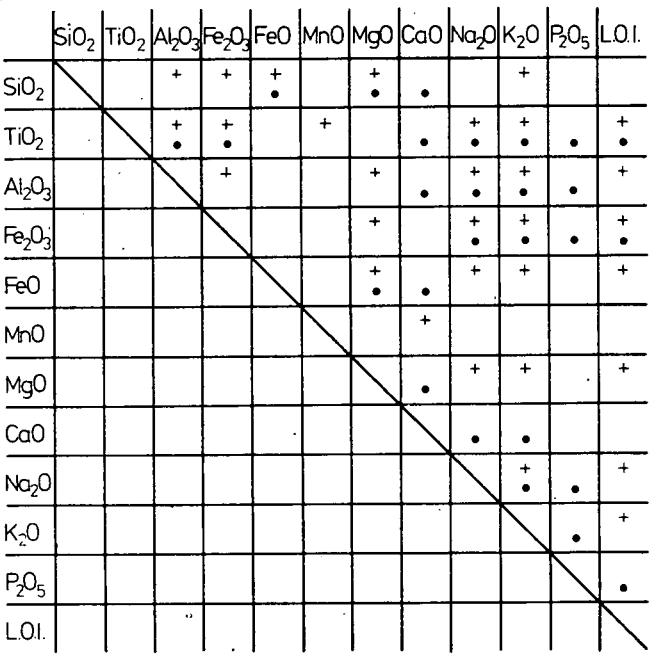


*Fig. 8.* Result of the F-test hypothesis analysis of the Ófalu Group amphibolites as well as Görcsöny Group ones based on chemical data.
Legend: + no significant difference pointed out in the development of both variables on the significancy level P=0.05 in the Ófalu Group amphibolites
● The same for the Görcsöny Group amphibolite

In *Figs. 8* and *9* a paired hypothesis analysis of the examined parameters of both groups are presented. Based on the results of this operation, several component-pairs having a common origin are pointed out. These pairs in the Görcsöny amphibolites are: $TiO_2$ — $K_2O$, $Fe_2O_3$ — $Na_2O$, $Fe_2O_3$ — L.O.I., FeO — MgO and $Na_2O$ — L.O.I. pairs in the Ófalu amphibolites. The rock-evolutional interpretation of these pairs is rather complicated and in many cases uncertain. Triads having the same origin are much more interpretable. E. g. in the Ófalu amphibolites an $Fe_2O_3$ — $Na_2O$ — L.O.I. system exists as a triad showing the same origin, but such a triad is missing from the Görcsöny amphibolites.

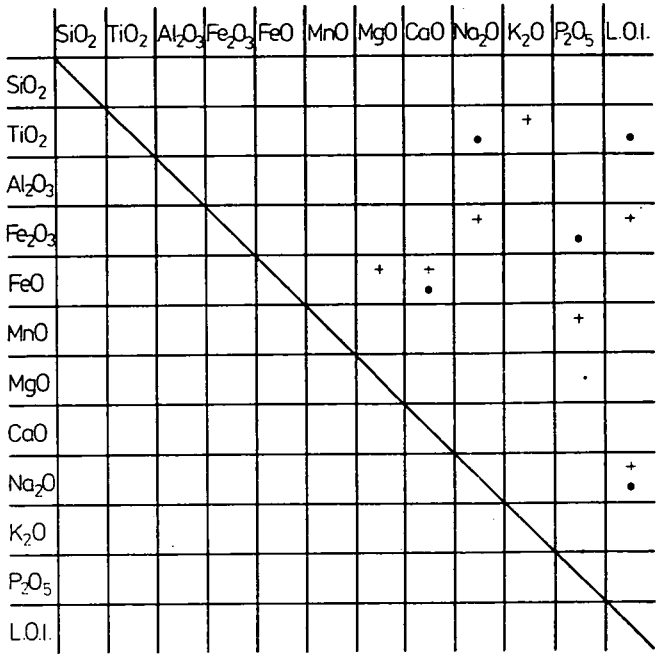


*Fig. 9.* Result of the T-test hypothesis analysis of the Ófalu Group amphibolites as well as Görcsöny Group ones based on chemical data.
Legend: The same as that of *Fig. 7.*

This feature of the Ófalu amphibolites follows partly from the spilitic character of their parent-rocks and partly from the effect of a considerable shearing and diaphtoresis. The lack of this character from the Görcsöny amphibolites can be explained by non-spilitic parent-rocks and the absence of shearing. A further difference between two amphibolite groups appears in the individual behaviour of MnO in the Görcsöny Group, as well as in a similarly unique evolution of $P_2O_5$ in the Ófalu Group contributing to the confirmation of the main result of the cluster analysis, namely: the Görcsöny and Ófalu Groups have different origin.

Due to a higher rock-sample number, the Görcsöny amphibolites are suitable for a further detailed analysis. According to a comparative hypothesis analysis of its subclasses A and B (originated from the dendogram in *Fig. 3*) show conspicuous differences between them. Thus, the mean-values of $TiO_2$, MgO and $Na_2O$ are significantly higher in the B subclass than that of in A one (Table 3). Precursors of these amphibolites represent the most mafic parent-rock types of the pre-metamorf sequence. Otherwise, according to their parameters, each sample of the Görcsöny amphibolites can be regarded homogeneous in the evolutional point of view *(Fig. 10)*. Simultaneously, it means fairly constant evolutional circumstances within this group (i.e. the same magmatype and same grade of metamorphism, etc.). Some small but observable differences existing between them can be attributed to a varying grade of epidotizational effect of the aplitic veins wich dissect all the mass of the Görcsöny Group.

*Figs. 11* and *12* show some results of the paired hypothesis analysis carried out between the parameters of subclasses A and B of the Görcsöny amphibolites. The

TABLE 3

*Averages ($\bar{x}$) and related standard deviation values (s) calculated from the chemical data of the Görcsöny Group amphibolites (subclasses A and B) based on cluster analysis*

| Group | No. of samples | $SiO_2$ | $TiO_2$ | $Al_2O_3$ | $Fe_2O_3$ | FeO | MnO | MgO | CaO | $Na_2O$ | $K_2O$ | $P_2O_5$ | L.O.I. | |
|---|---|---|---|---|---|---|---|---|---|---|---|---|---|---|
| Görcsöny Group A class | 5 | 0.56 | 0.66 | 0.40 | 0.56 | 1.02 | 0.06 | 0.53 | 0.98 | 0.21 | 0.33 | 0.62 | 0.26 | $s$ |
| Görcsöny Group B class | 8 | 1.54 | 0.17 | 0.81 | 0.29 | 1.12 | 0.05 | 0.59 | 0.92 | 0.53 | 0.75 | 0.35 | 0.38 | |
| Görcsöny Group A class | 5 | 47.75 | 2.24 | 14.49 | 0.79 | 11.43 | 0.15 | 5.65 | 10.34 | 2.30 | 1.59 | 0.93 | 2.59 | $\bar{x}$ wt% |
| Görcsöny Group B class | 8 | 47.79 | 2.98 | 14.26 | 1.13 | 10.62 | 0.18 | 7.18 | 10.33 | 2.47 | 1.64 | 0.87 | 2.27 | |

| | $SiO_2$ | $TiO_2$ | $Al_2O_3$ | $Fe_2O_3$ | FeO | MnO | MgO | CaO | $Na_2O$ | $K_2O$ | $P_2O_5$ | L.O.I. |
|---|---|---|---|---|---|---|---|---|---|---|---|---|
| F-test | • | • | • | • | • | • | • | • | • | • | • | • |
| t-test | • | | • | • | • | • | | • | | • | • | • |

*Fig. 10.* Hypothesis analysis of the chemical components of the Görcsöny Group amphibolites (subclasses A and B).
Legend: The same as that of *Fig. 7.*

| | $SiO_2$ | $TiO_2$ | $Al_2O_3$ | $Fe_2O_3$ | FeO | MnO | MgO | CaO | $Na_2O$ | $K_2O$ | $P_2O_5$ | L.O.I. |
|---|---|---|---|---|---|---|---|---|---|---|---|---|
| $SiO_2$ | | • | +<br>• | • | +<br>• | | • | +<br>• | | • | • | • |
| $TiO_2$ | | | • | +<br>• | • | | • | • | | • | • | |
| $Al_2O_3$ | | | | • | + | | +<br>• | +<br>• | +<br>• | +<br>• | • | • |
| $Fe_2O_3$ | | | | | • | | • | • | + | • | +<br>• | +<br>• |
| FeO | | | | | | | +<br>• | +<br>• | | + | • | |
| MnO | | | | | | | | | | | | |
| MgO | | | | | | | | +<br>• | +<br>• | +<br>• | +<br>• | +<br>• |
| CaO | | | | | | | | | + | + | • | |
| $Na_2O$ | | | | | | | | | | +<br>• | + | +<br>• |
| $K_2O$ | | | | | | | | | | | • | • |
| $P_2O_5$ | | | | | | | | | | | | +<br>• |
| L.O.I. | | | | | | | | | | | | |

*Fig. 11.* Hypothesis analysis of the chemical components of the Görcsöny Group amphibolites (subclasses A and B); F-test.
Legend: ● no significant difference pointed out in the development of both variables on the significancy level $P=0.05$ in the subclass A.
\+ The same in the subclass B.

component pairs of the subclasse A are: $TiO_2$ — $K_2O$, $Fe_2O_3$ — $P_2O_5$ and $K_2O$ — $P_2O_5$. Apart from the $TiO_2$ — $K_2O$ pair, the $Fe_2O_3$ — $K_2O$ — $P_2O_5$ triad also suggest the same origin. It is rather difficult to give an acceptable explanation for the behaviour of $K_2O$ in the presented relations. Its close contact with some immobile components can be reflected on a special alkaline basalt origin of amphibolites belonging to the subclass A. Moreover, these amphibolite samples are collected from a definite lithostratigraphic unit of the Görcsöny Group. The connected component pairs of the subclass B are: $Fe_2O_3$ — $P_2O_5$, FeO — CaO and $Na_2O$ — L.O.I. The last of them signs a weak Na metasomatism produced by greenschist grade of retrograde metamorphism. These rock-samples belong to another lithostratigraphic unit of the Görcsöny Group and mineralogically consist mainly of actinolite-hornblende mixture and subordinate chlorite and epidote.

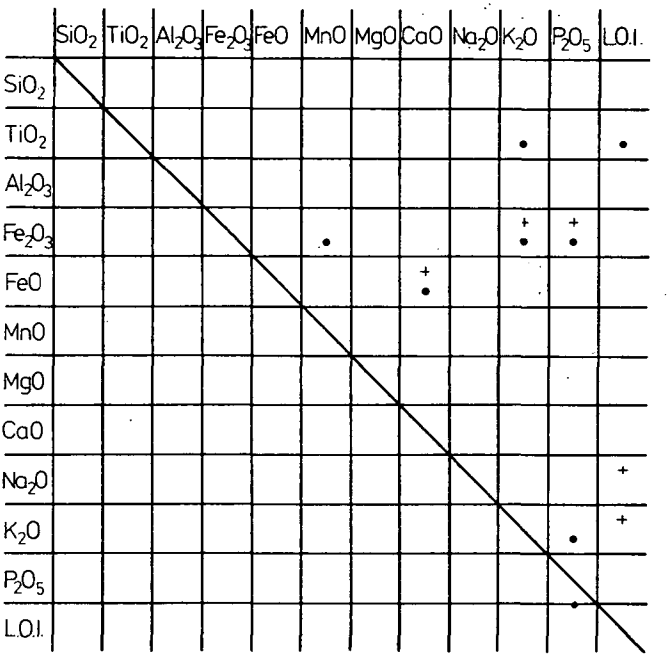


*Fig. 12.* Hypothesis analysis of the chemical components of the Görcsöny Group amphibolites (subclasses A and B); T-test.
Legend: ● no significant difference pointed out in the medium tendencies of the processes produced both variables on the significancy level P=0.05 in the subclass A.
\+ The same in the subclass B.

Finally, *Figs. 13* and *14* show a comatative hypothesis analysis of subclasses A and B of the Görcsöny amphibolites together with the Ófalu ones according to every component of their bulk composition. A difference between both subclasses A of the Görcsöny as well as Ófalu amphibolites is recognized in their $P_2O_5$ evolution. Differences between B classes are manifested by $TiO_2$, MnO and CaO components.

| | $SiO_2$ | $TiO_2$ | $Al_2O_3$ | $Fe_2O_3$ | FeO | MnO | MgO | CaO | $Na_2O$ | $K_2O$ | $P_2O_5$ | L.O.I. |
|---|---|---|---|---|---|---|---|---|---|---|---|---|
| F-test | • | • | • | • | • | • | • | • | • | • | | • |
| t-test | | • | • | | | • | | • | • | • | | |

*Fig. 13.* Hypothesis analysis of the chemical components of the Görcsöny Group amphibolites subclass A as well as the Ófalu amphibolites.
Legend: The same as that of *Fig. 7.*

| | $SiO_2$ | $TiO_2$ | $Al_2O_3$ | $Fe_2O_3$ | FeO | MnO | MgO | CaO | $Na_2O$ | $K_2O$ | $P_2O_5$ | L.O.I. |
|---|---|---|---|---|---|---|---|---|---|---|---|---|
| F-test | • | | • | • | • | | • | | • | • | • | • |
| t-test | | | • | | • | • | • | • | • | • | | |

*Fig. 14.* Hypothesis analysis of the chemical components of the Görcsöny Group amphibolites subclass B as well as Ófalu Group amphibolites.
Legend: The same as that of *Fig. 7.*

These results also comfirm the genetical diversities existing between Görcsöny and Ófalu amphibolites which formerly were already pointed out by discrimination diagrams [SZEDERKÉNYI, 1982] and now by cluster analysis, respectively.

## CONCLUSIONS

The most important result of this attempt is the demonstration of fitness of hypothesis analysis together with cluster one for the distinction of amphibolites based on their bulk composition. Comparing the results of this operation to that of discriminant diagrams of the same rock-samples [SZEDERKÉNYI, 1982] the statistical methods applied can give more remarkable pictures about similarities or differences existing among the rock-samples and can offer a more exact and well computerizable method for the distinction. Explanation of the differences obtained by such a statistical analyses still requires further considerations and conciliations with the experiences of "classical" petrochemical as well as petrotectonic interpretations. It is important to take into consideration that these statistical methods are founded on an enlargement of the differences existing between the same chemical components of the samples examined. Therefore these methods strictly require correct chemical data.

## REFERENCES


CATELL, R. B. [1944]: A note on correlation clusters and cluster search methods. Psychometrika 9/3, 169—184.

GEIGER, J. [1982]: Diagenizált törmelékes üledékek szemcseeloszlásának ősföldrajzi értékelése; a Szeged—2. telep vizsgálata — Kőolaj és Földgáz. (Paleogeographic interpretation of grain-size distribution of diagenized clastic sediments; investigation of the Szeged No. 2 bed — Crude oil and natural gas.) SzKFI Műsz. Tud. Közl., **1**, 13—17.

GHONEIM, M. A. F., T. SZEDERKÉNYI [1977]: Preliminary petrological and geochemical studies of the area Ófalu, Mecsek Mountains, Hungary. Acta Miner. Petr., Szeged, **XXIII**/1, 15—28.

JANTSKY, B. [1979]: A mecseki kristályos alaphegység földtana. (Geology of the crystalline basement of Mecsek Mountains.) Year-book of Hung. Geol. Survey, Budapest.

MELTON, M. A. [1958]: Correlation structure of morphometric properties of drainage system and their controlling agents. J. Geol., **66**, 442—460.

MICHENER, C. D. [1958]: A statistical method for evaluating systematic relationships. Univ. Kansas Sci. Bull., **38**, 1409—1438.

SZEDERKÉNYI, T. [1974]: Paleozoic magmatism and tectogenesis in Southeast Transdanubia. Acta Geol. Ac. Sci. Hung., **18**, 305—313.

SZEDERKÉNYI, T. [1983]: Origin of amphibolites and metavolcanics of crystalline complexes of South Transdanubia, Hungary. Acta Geol. Ac. Sci. Hung., **26**, 103—136.

TYRON, R. C. [1939]: Cluster Analysis. Edwards Bros. Co., Ann Arbor, Michigan.



*Manuscript received, 20 June, 1983*



J. GEIGER
Sediment Laboratory of Hungarian
Hydrocarbon Institute
H-6701 Szeged, Pf. 30, Hungary
T. SZEDERKÉNYI
Institute of Mineralogy, Geochemistry and
Petrography, Attila József University
H-6722 Szeged, Egyetem u. 2—6.
Hungary

*Acta Mineralogica-Petrographica, Szeged, XXVI/2, 171 — 186, 1984*

# CONTRIBUTIONS TO THE PETROCHEMISTRY AND GEOCHEMISTRY OF SOME QUATERNARY BASALTIC ROCKS, NORTHERN AND SOUTHERN YEMEN

MAHMOUD LOTFY KABESH, ABDEL-KARIM AHMED SALEM
and MOHAMED H. A. HIGAZY

## ABSTRACT

Petrochemical and geochemical characteristics of some basaltic rocks from Sirwah-Marib and Dhamar-Rad'a volcanic fields (Northern Yemen) as well as Shuqra volcanic field (Southern Yemen), all of Quaternary age are presented. The relation of major elements together with other petrochemical indices and normative minerals have been discussed and the chemical characterization of the examined basaltic rocks is elucidated. The distribution and behaviour of selected trace elements in the examined rocks are also studied.

## INTRODUCTION

The present study deals with the petrochemistry and geochemistry of some basaltic rocks from Sirwah-Marib and Dhamar-Rad'a volcanic fields (Northern Yemen) of Quaternary age. These form two of three major recent volcanic fields in the Yemen Arab Republic (Northern Yemen), previously grouped by GEUKENS [1966] into:

1. Sana'a-Amran (Hamdan).
2. Sirwah-Marib.
3. Dhamar-Rad'a.

Comparison, on a chemical basis with Shuqra volcanic field (Southern Yemen, Yemen People's Republic) of Quaternary age has also been attempted *(Fig. 1)*. Also,

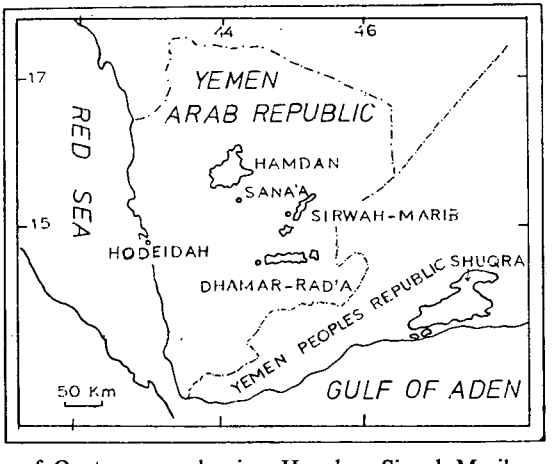


*Fig. 1.* Location map of Quaternary volcanics: Hamdan Sirwah-Marib and Dhamar Rad'a in Yemen Arab Republic and Shuqra in Yemen People's Republic

the only Egyptian olivine tholeiitic basalt from St. John's Island of Quaternary age has been compared with the Quaternary basaltic rocks of Yemen [EL-SHAZLY *et al.*, 1974, ABDEL-MONEM and HEIKAL, 1981]. However, few workers previously contributed to the chemistry of these volcanics, among whom may be mentioned SHUKRI and BASTA [1955], GEUKENS [1966], KABESH and GHOWEBA [1976], COX *et al.*, [1977], KABESH and HEGAB [1978], and KABESH *et al.*, [1980, 1981]. KABESH *et al.*, [1980] discussed some major and trace element relations of basaltic rocks which form part of the volcanics of Dhamar Rad'a. On the other hand, KABESH *et al.*, [1981] discussed some chemical features and the classification of Sirwah Marib basaltic rocks. However, no geochemical work is included in that study. COX *et al.*, [1977] advanced the general geology structure and petrography of part of Shuqra volcanic field. These authors (op. cit.) also mentioned data of major elements, normative values as well as some trace element abundances for 4 basaltic rock samples in Southern Yemen.

## PETROCHEMISTRY

Major element data mentioned in the present study are essentially derived from previous studies of Dhamar-Rad'a volcanics (3 samples Table 1), [KABESH *et al.*, 1981], Sirwah-Marib basaltic rocks (12 samples Table 1), [KABESH *et al.*, 1981] while major element data of Shuqra volcanics, (4 samples, Table 1) are quoted from COX *et al.*, [1977] and 2 samples of St. John's Island (Egypt) after EL-SHAZLY *et al.*, [1974]. These data were recalculated and processed in the present work following several chemical parameters.

## MAJOR ELEMENT CHEMISTRY

The chemistry of major elements is discussed through different variation diagrams.

*Fig. 2* shows the relation between $SiO_2$ and FeO*/MgO, all in weight percent. It is evident that all the examined basaltic rocks from Northern, Southern Yemen and St. John's Island (Egypt) plot within the field of tholeiite according to the classification of MIYASHIRO [1974].

*Fig. 3* shows the relation $FeO^* = FeO + 0.899 \times Fe_2O_3/MgO$ and FeO, all samples of Sirwah Marib and Dhamar Rad'a fall within field (3), tholeiitic basalt, while those of Shuqra and St. John's plot within field (2) mildly calc-alkalic rocks with the exception one sample from Shuqra which plots in the field calc-alkalic rocks. On the other hand, *Fig.* 4 shows the relation between FeO/MgO and $TiO_2$. It is evident from this figure that all the examined basaltic rocks from Northern and Southern Yemen plot within the field of tholeiitic basalt according to the classification of MIYASHIRO [1974] with the exception of one sample from St. John's Island falling in the field 1, calc-alkaline rocks.

MIYASHIRO (op. cit.) suggested that tholeiitic basaltic rocks are characterized by slower rate of increase of $SiO_2$ content and higher enrichement of FeO* (total iron as FeO) and titanium with advancing fractional crystallization than the calc-alkaline basalt. The advance in fractional crsytallization is measured by increase in FeO/MgO.

On the basis of $K_2O$ and $Na_2O$ contents in the igneous rocks MIDDLEMOST [1975] classified the alkali rocks into four main types comprising Na-series, K-series, high K-series and phonolitic basalts. *Fig. 5* shows that the basaltic rocks of Sirwah—

TABLE 1

*Chemical analyses of the investigated basaltic rocks Sirwah-Marib (Northern Yemen)*

| | 1 | 2 | 3 | 4 | 5 | 6 | 7 | 8 | 9 | 10 | 11 | 12 |
|---|---|---|---|---|---|---|---|---|---|---|---|---|
| $SiO_2$ | 46.90 | 47.30 | 50.50 | 43.10 | 50.90 | 44.40 | 44.40 | 43.50 | 46.20 | 46.10 | 45.60 | 45.50 |
| $Al_2O_3$ | 15.90 | 15.80 | 13.90 | 16.50 | 14.10 | 16.40 | 16.40 | 16.50 | 16.13 | 16.12 | 16.20 | 16.20 |
| $Fe_2O_3$ | 2.39 | 2.31 | 2.76 | 3.46 | 2.60 | 3.40 | 3.38 | 3.42 | 3.30 | 3.30 | 3.34 | 3.35 |
| FeO | 8.67 | 8.61 | 9.20 | 8.60 | 9.07 | 8.30 | 8.13 | 8.57 | 7.89 | 7.90 | 7.94 | 7.96 |
| MgO | 5.60 | 5.59 | 6.31 | 6.27 | 6.22 | 6.10 | 6.10 | 6.21 | 5.80 | 5.80 | 5.90 | 5.90 |
| CaO | 9.42 | 9.28 | 10.40 | 10.60 | 10.30 | 10.60 | 10.50 | 10.60 | 10.20 | 10.20 | 10.40 | 10.40 |
| $Na_2O$ | 2.55 | 2.56 | 2.22 | 3.25 | 2.21 | 3.20 | 3.22 | 3.25 | 3.14 | 3.15 | 3.19 | 3.20 |
| $K_2O$ | 3.87 | 3.87 | 1.11 | 2.86 | 1.13 | 2.53 | 2.52 | 2.79 | 2.17 | 2.18 | 2.22 | 2.23 |
| MnO | 0.18 | 0.18 | 0.17 | 0.34 | 0.17 | 0.30 | 0.30 | 0.35 | 0.29 | 0.30 | 0.30 | 0.30 |
| $TiO_2$ | 3.21 | 3.17 | 2.09 | 3.35 | 2.08 | 3.27 | 3.26 | 3.34 | 3.30 | 3.30 | 3.31 | 3.32 |
| $P_2O_5$ | 0.31 | 0.29 | 0.23 | 0.57 | 0.23 | 0.49 | 0.50 | 0.58 | 0.58 | 0.59 | 0.57 | 0.58 |
| $H_2O$ | 0.82 | 0.87 | 0.79 | 0.89 | 0.79 | 0.93 | 0.94 | 0.85 | 0.94 | 0.94 | 0.93 | 0.96 |
| Total | 99.82 | 99.83 | 99.68 | 99.79 | 99.79 | 99.92 | 99.83 | 99.96 | 99.94 | 99.88 | 99.90 | 99.90 |
| FeO/MgO | 1.93 | 1.91 | 1.85 | 1.87 | 1.88 | 1.85 | 1.84 | 1.87 | 1.86 | 1.88 | 1.85 | 1.86 |
| $TiO_2/P_2O_5$ | 10.35 | 10.93 | 9.09 | 6.23 | 9.04 | 6.67 | 6.52 | 5.76 | 5.69 | 5.59 | 5.81 | 5.72 |
| $K_2O+Na_2O$ | 6.42 | 6.43 | 3.33 | 6.11 | 3.34 | 5.73 | 5.74 | 6.04 | 5.31 | 5.33 | 5.41 | 5.43 |
| $\frac{K_2O \times 100}{K_2O+Na_2O}$ | 60.28 | 60.19 | 33.33 | 46.81 | 33.83 | 44.15 | 43.90 | 46.19 | 40.87 | 40.90 | 41.04 | 41.11 |
| $\frac{K_2O+Na_2O \times 100}{K_2O+Na_2O+CaO}$ | 40.53 | 40.93 | 24.25 | 36.56 | 24.49 | 35.09 | 35.34 | 36.30 | 34.24 | 34.32 | 34.22 | 34.30 |

TABLE 1 (continued)

| | Dhamar-Rad'a (Northern Yemen) | | | Shuqra (Southern Yemen) | | | | St. John's Island | |
|---|---|---|---|---|---|---|---|---|---|
| | 13 | 14 | 15 | 16 | 17 | 18 | 19 | 20 | 21 |
| $SiO_2$ | 46.63 | 47.73 | 49.90 | 47.39 | 45.63 | 44.42 | 44.35 | 47.52 | 48.44 |
| $Al_2O_3$ | 14.39 | 13.86 | 14.78 | 16.80 | 17.58 | 16.16 | 15.07 | 15.94 | 13.56 |
| $Fe_2O_3$ | 3.25 | 4.93 | 3.62 | 1.09 | 4.64 | 1.99 | 2.52 | 2.32 | 1.56 |
| FeO | 10.17 | 10.61 | 9.11 | 8.52 | 5.37 | 7.63 | 8.25 | 8.95 | 8.24 |
| MnO | 0.14 | 0.19 | 0.18 | 0.18 | 0.17 | 0.16 | 0.18 | 0.17 | 0.20 |
| $TiO_2$ | 2.11 | 1.99 | 2.56 | 2.03 | 2.32 | 2.31 | 2.07 | 1.40 | 1.12 |
| MgO | 7.09 | 7.70 | 6.35 | 6.72 | 7.17 | 9.79 | 11.71 | 7.39 | 8.76 |
| CaO | 9.81 | 8.93 | 9.74 | 9.10 | 9.50 | 11.08 | 10.91 | 10.72 | 12.33 |
| $Na_2O$ | 2.96 | 2.51 | 2.21 | 3.97 | 4.04 | 3.28 | 3.01 | 3.27 | 2.50 |
| $K_2O$ | 0.49 | 0.30 | 0.25 | 1.15 | 1.46 | 1.10 | 1.02 | 0.27 | 0.27 |
| $P_2O_5$ | 0.36 | 0.27 | 0.36 | 0.57 | 0.66 | 0.40 | 0.57 | 0.87 | 0.37 |
| $H_2O$ | 1.95 | 0.85 | 0.99 | 2.76 | 1.37 | 0.78 | 1.12 | 1.42 | 1.74 |
| Total | 99.35 | 100.07 | 100.05 | 100.28 | 99.91 | 99.09 | 100.06 | 100.24 | 99.09 |
| FeO*/MgO | 1.84 | 1.95 | 1.94 | 1.41 | 1.33 | 0.96 | 0.90 | 1.49 | 1.10 |
| $TiO_2/P_2O_5$ | 5.86 | 7.37 | 7.11 | 3.56 | 3.51 | 4.77 | 3.63 | 1.61 | 3.03 |
| $K_2O+Na_2O$ | 3.45 | 2.81 | 2.46 | 5.12 | 5.50 | 4.38 | 4.03 | 3.54 | 2.77 |
| $\frac{K_2O \times 100}{K_2O+Na_2O}$ | 14.20 | 10.67 | 10.16 | 22.46 | 26.54 | 25.11 | 25.31 | 7.62 | 9.75 |
| $\frac{K_2O+Na_2O \times 100}{Na_2O+K_2O+CaO}$ | 26.02 | 23.93 | 20.16 | 36.00 | 36.67 | 28.33 | 26.97 | 24.82 | 18.34 |

$FeO^* = FeO + 0.899 \times Fe_2O_3$.

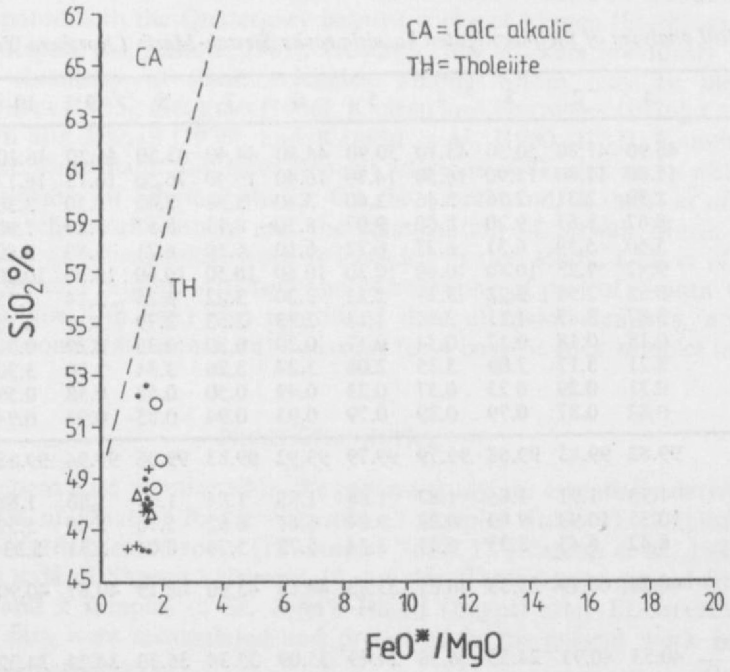


*Fig. 2.* Variation of $SiO_2$ *vs* FeO*/MgO after MIYASHIRO [1974].
● Sirwah-Marib
⊙ Dhamar Rad'a
\+ Shuqra
△ St. John's Island

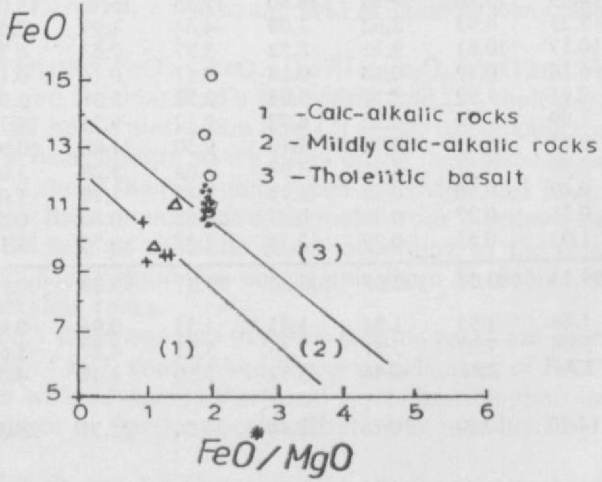


*Fig. 3.* Variation of FeO % *vs* FeO*/MgO after MIYASHIRO [1974]. Symbols as in *Fig. 2*.
FeO* = FeO + 0.899 $Fe_2O_3$
⊙ superimposed two or three points.

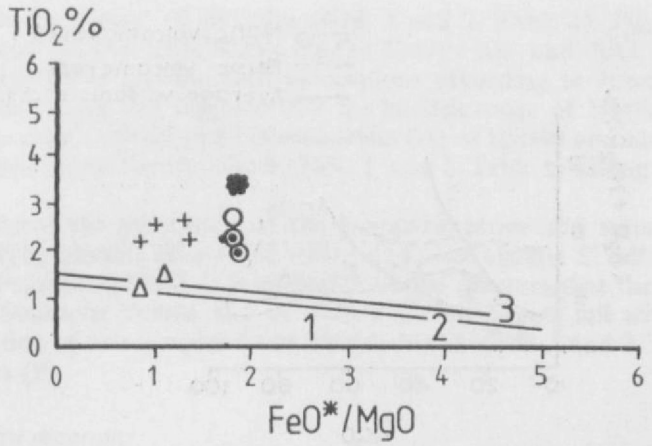


*Fig. 4.* Variation of $TiO_2$ *vs* FeO*/MgO after MIYASHIRO [1974]. Symbols as in *Fig. 2.*
1. Calc-alkalic rocks
2. Mildly calc-alkalic rocks
3. Tholeiitic basalt
⊙ superimposed two points

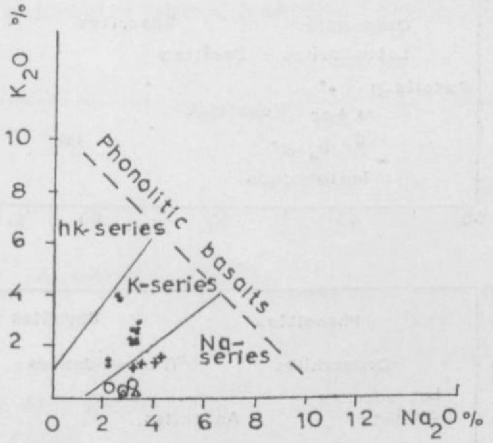


*Fig. 5.* $K_2O$—$Na_2O$ diagram [MIDDLEMOST, 1975]. Symbols as in *Fig. 2.*

Marib plot within the K-series while those of Dhamar-Rad'a, Shuqra and St. John's Island fall within the Na-series.

An evidence of possible alkali metasomatism is shown by plotting total alkalies ($Na_2O+K_2O$) against alkali index ($K_2O/Na_2O+K_2O)\times 100$ in *Fig.* 6) advanced by HUGHES [1973]. In the diagram three main field are present comprising mafic and felsic volcanics in addition to an igneous field which is characterized by typical values of alkalies.

The diagram shows that the basaltic rocks of Dhamar-Rad'a, Shuqra as well as those of St. John's Island fall within the field of mafic volcanics. The mafic volcanics possess low values of alkalies (2.46—5.54) and alkali index (7.62—26.54). On the

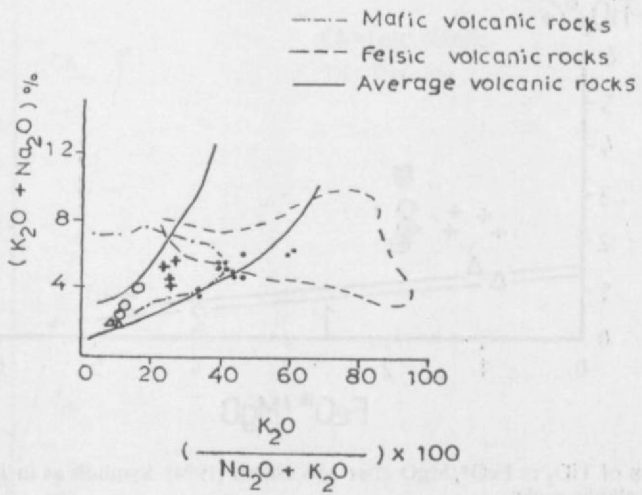


*Fig. 6.* Variation of $K_2O+Na_2O$ (%) *vs* $K_2O/K_2O+Na_2O$ after HUGHES. [1973]. Symbols as in *Fig. 2.*

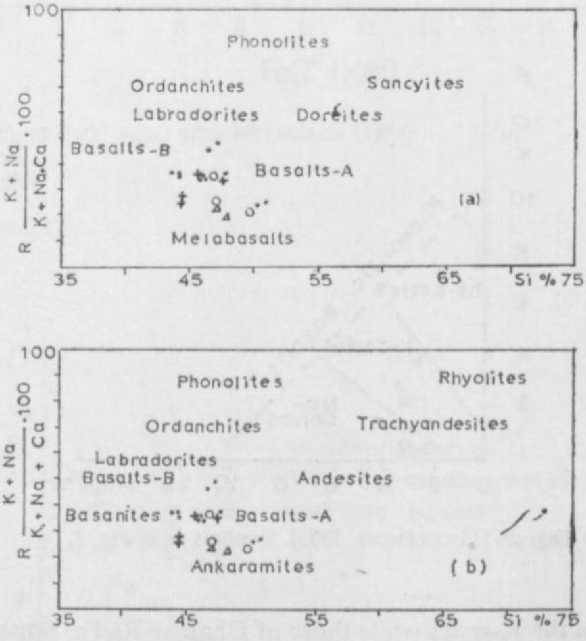


*Fig. 7. a)* Si—R diagram of the magmatic series: *A* saturated and *B* unsaturated after JUNG and BROUSSE [1966].
*b)* Si—R diagram of the magmatic series: *A* saturated and *B* unsaturated after VATIN—PERIGNON [1968]. Symbols an in *Fig. 2.*

other hand, the basaltic rocks of Sirwah-Marib show a wide range both in the total alkalies (3.33—6.43) and the alkali index (33.33—60.28). Consequently these basalts fall partly within the mafic volcanics, partly within the felsic volcanics and partly within the average igneous rocks. However, the two samples falling within the felsic

volcanics show the highest alkali index (Nos. 1 and 2, Table 1). *Fig. 7a* shows the relation between $(K_2O+Na_2O/K_2O+Na_2O+CaO)\times 100$ and $SiO_2$ which distinguishes several types of igneous rock associations according to JUNG and BROUSSE [1962]. It is clear from the diagram that the basaltic rocks of Northern, Southern Yemen and St. John's Island plot between series (A) of basalts and metabasalts with only two samples from Sirwah-Marib (Nos. 1 and 2, Table 1) falling near series (B) of basalts.

*Fig. 7b* shows the separation of the magmatic series into saturated (A) and unsaturated (B) by plotting $(K+Na/K+Na+Ca)\times 100$ against Si (all in weight percent), (VATIN-PERIGNON, 1968). It is evident from the diagram that the basaltic rocks of Northern, Southern Yemen and St. John's Island (Egypt) fall within series (A) with the exception of two samples from Sirwah-Marib (Nos. 1 and 2, Table 1) which plot near series (B).

*Alkali-silica diagram:*

This diagram *Fig. 8* has been established to distinguish alkalic and tholeiitic rocks as shown by MACDONALD [1968] dividing line with IRVINE and BARAGAR's curve [1971]. In this method $Na_2O+K_2O$ are plotted against $SiO_2$ (all in weight percent). According to the diagram the basaltic rocks of Dhamar-Rad'a and St. John's Island fall within the sub-alkaline field because of the absence of normative nepheline, those of Shuqra fall close to the alkaline field with the exception of two samples (Nos. 3 and 4, Table 2) devoid of normative nepheline and falling within the subalkaline field.

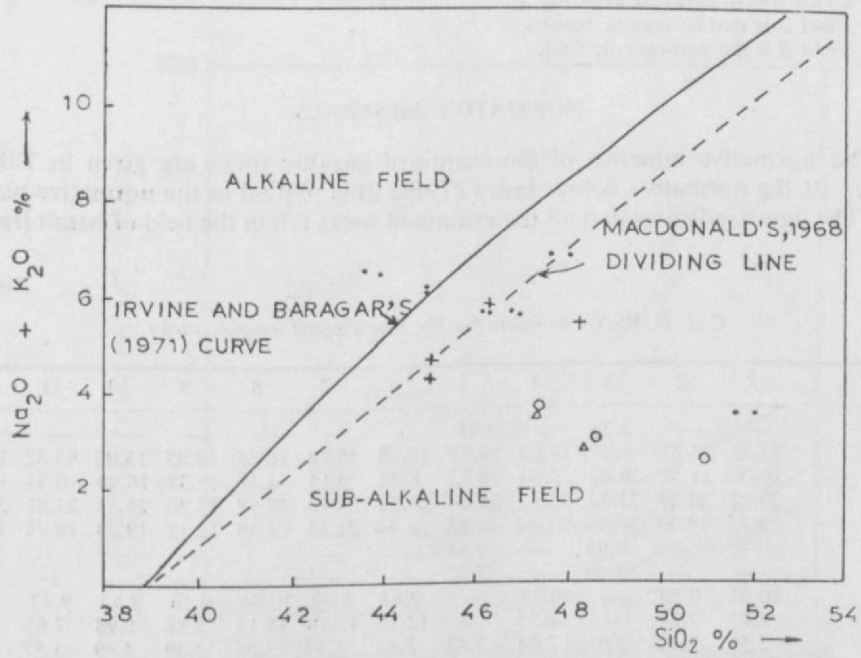


*Fig. 8.* Alkalies-silica diagram. Dashed line is MacDonald's [1968] dividing line for Hawaiian tholeiitic and alkaline rocks. The solid curve is the line proposed by IRVINE and BARAGAR [1971] to divide the alkaline and sub-alkaline compositions. Symbols as in *Fig. 2.*

*Fig. 9* plot for the examined basalts using $P_2O_5$, $TiO_2$ and $K_2O$ (all in weight percent) discrimination diagram of PEARCE and CANN, [1973]. The diagram shows that the basaltic rocks of Northern, Southern Yemen and St. John's Island (Egypt) plot within the field of non-oceanic basalts with the exception two samples from Dhamar-Rad'a falling in the field of oceanic basalts.

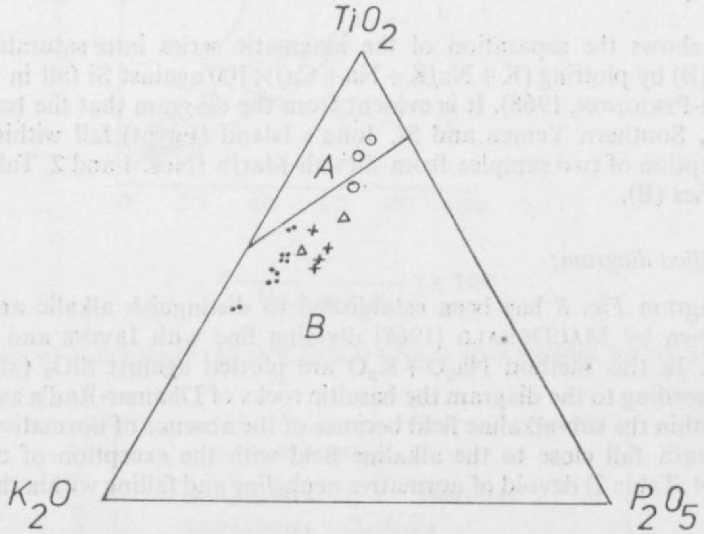


*Fig. 9.* $TiO_2$—$P_2O_5$—$K_2O$ triangular diagram showing the plots for the basalts after PEARCE and CANN [1973]. Symbols as in *Fig. 2*.
Field *A* is that of oceanic basalts.
Field *B* is the non-oceanic field.

## NORMATIVE MINERALS

The normative minerals of the examined basaltic rocks are given in Table 2 In *Fig. 10* the normative colour index (Table 2) is plotted *vs* the normative plagioclase. The figure indicates that all the examined rocks fall in the field of basalt [IRVINE

TABLE 2

*C. I. P. W-Norm values for the investigated basaltic rocks*

| | 1 | 2 | 3 | 4 | 5 | 6 | 7 | 8 | 9 | 10 | 11 | 12 |
|---|---|---|---|---|---|---|---|---|---|---|---|---|
| Q | — | — | 2.35 | — | 3.01 | — | — | — | — | — | — | |
| Or | 23.32 | 23.27 | 6.87 | 17.23 | 6.87 | 15.20 | 15.28 | 16.65 | 13.05 | 13.06 | 13.32 | 13.33 |
| Ab | 10.00 | 11.42 | 20.62 | 2.44 | 20.32 | 8.83 | 9.13 | 4.41 | 19.37 | 18.99 | 16.44 | 16.24 |
| An | 20.92 | 20.57 | 25.34 | 22.32 | 26.04 | 23.32 | 23.20 | 22.57 | 23.98 | 23.85 | 23.81 | 23.81 |
| Di | 19.75 | 19.49 | 20.96 | 21.84 | 20.15 | 21.44 | 21.13 | 21.59 | 19.11 | 19.23 | 19.88 | 19.89 |
| Fs | — | — | 9.98 | — | 9.88 | — | — | — | — | — | — | — |
| En | — | — | 7.46 | — | 7.62 | — | — | — | — | — | — | — |
| Ol | 10.22 | 10.36 | — | 10.24 | — | 9.64 | 9.82 | 10.06 | 9.56 | 9.53 | 9.47 | 9.39 |
| Ne | 8.01 | 7.28 | — | 16.33 | — | 12.17 | 12.18 | 15.13 | 5.58 | 5.98 | 7.65 | 7.78 |
| Mt | 2.55 | 2.47 | 3.01 | 3.64 | 2.83 | 3.65 | 3.57 | 3.64 | 3.49 | 3.49 | 3.57 | 3.57 |
| Ap | 0.66 | 0.61 | 0.46 | 1.21 | 0.46 | 1.06 | 1.06 | 1.20 | 1.21 | 1.21 | 1.21 | 1.21 |
| Il | 4.56 | 4.54 | 2.98 | 4.75 | 2.98 | 4.64 | 5.64 | 4.74 | 4.65 | 4.66 | 4.65 | 4.76 |
| N. C. I. | 37.08 | 36.86 | 44.39 | 40.47 | 43.46 | 39.37 | 40.16 | 40.03 | 36.81 | 36.91 | 37.57 | 37.61 |
| An. Con. | 67.66 | 64.30 | 55.13 | 90.14 | 56.17 | 72.53 | 71.76 | 85.99 | 55.32 | 55.67 | 59.15 | 59.45 |

TABLE 2 continued

| | Dhamar- Rad'a (Northern Yemen) | | | Shuqra (Southern Yemen) | | | | St. John's Island | |
|---|---|---|---|---|---|---|---|---|---|
| | 13 | 14 | 15 | 16 | 17 | 18 | 19 | 20 | 21 |
| Q | — | — | 5,79 | — | — | — | — | — | — |
| Or | 2,89 | 2,95 | 1,47 | 6,62 | 9,02 | 6,78 | 6,22 | 1,62 | 1,67 |
| Ab | 25,01 | 21,21 | 18,67 | 31,23 | 21,25 | 10,13 | 12,24 | 29,89 | 23,52 |
| An | 24,49 | 25,04 | 29,63 | 24,57 | 25,65 | 26,29 | 24,84 | 28,49 | 26,14 |
| Di Wo | 9,12 | 7,31 | 6,83 | | | | | 7,91 | 12,04 |
| Di Fs | 3,65 | 2,73 | 2,47 | 13,75 | 13,77 | 21,98 | 18,33 | 3,14 | 6,62 |
| Di En | 5,09 | 4,23 | 4,01 | | | | | 6,99 | 17,67 |
| Hy Fs | 2,63 | 8,90 | 7,33 | — | — | — | — | | |
| Hy En | 3,67 | 13,77 | 13,20 | — | — | — | — | | |
| Ol Fa | 4,97 | 0,62 | — | 15,79 | 10,25 | 16,73 | 22,39 | 5,34 | 2,46 |
| Ol Fo | 6,27 | 0,87 | — | | | | | 10,30 | 5,71 |
| Ne | — | — | — | 1,41 | 7,20 | 9,83 | 7,50 | — | — |
| Mt | 4,71 | 7,14 | 5,24 | 1,61 | 6,82 | 2,83 | 3,22 | 2,46 | 1,70 |
| Ap | 0,85 | 1,21 | 0,85 | 1,23 | 1,57 | 0,95 | 1,26 | 1,88 | 0,82 |
| Il | 4,00 | 3,78 | 4,86 | 3,77 | 4,47 | 4,49 | 4,01 | 1,98 | 1,63 |
| N. C. I | 44,96 | 50,56 | 44,79 | 36,15 | 36,88 | 46,98 | 49,21 | 40,00 | 48,65 |
| An. Con. | 49,47 | 54,14 | 61,34 | 44,03 | 54,69 | 72,18 | 66,99 | 48,80 | 52,64 |

and BARAGAR, 1971] and later defined by RASCHKA and MULLER [1974] for Hawaiian tholeiite.

A prominent chemical difference between more basic members of typical calc-alkaline and tholeiitic basalt is their alumina content. This difference is well illustrated by plotting $Al_2O_3$ *vs* normative plagioclase composition *(Fig. 11)* where a convenient

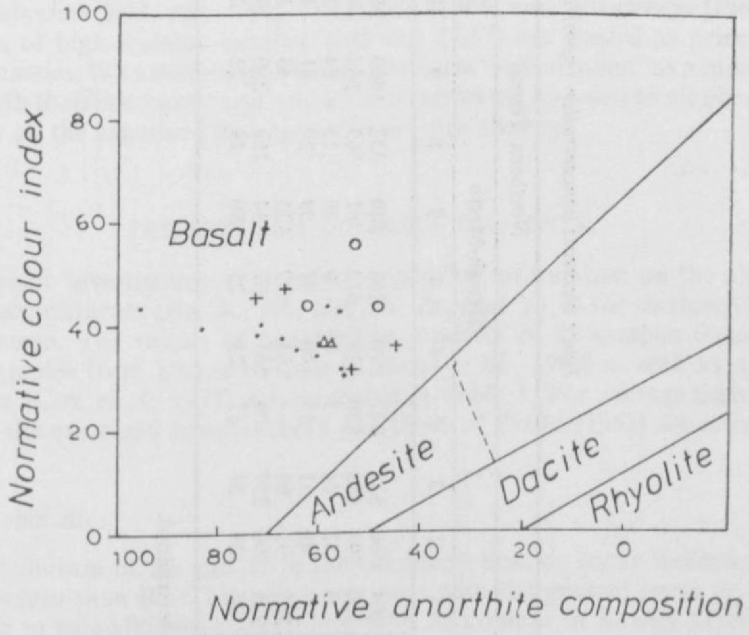


*Fig. 10.* Normative colour index against normative An content after IRVINE and BARAGAR [1971]. Symbols as in *Fig. 2.*

TABLE 3

*Trace elements concentration (ppm) of Northern and Southern Yemen basaltic rocks*

| | Northern Yemen | | | | | | | | | | | | | | | Southern Yemen | | | | Average of Prinz, (1967) |
|---|---|---|---|---|---|---|---|---|---|---|---|---|---|---|---|---|---|---|---|---|
| | Sirwah-Marib | | | | | | | | | | | | Dhamar-Rad'a | | | Shuqra | | | | |
| | 1 | 2 | 3 | 4 | 5 | 6 | 7 | 8 | 9 | 10 | 11 | 12 | 13 | 14 | 15 | 16 | 17 | 18 | 19 | |
| Ba | 204 | 406 | 535 | 947 | 270 | 264 | 440 | 332 | 1400 | 265 | 243 | 448 | 100 | 140 | 80 | n. d.* | n. d.* | n. d.* | n. d.* | 244 |
| Sr | 450 | 598 | 603 | 630 | 618 | 610 | 761 | 569 | 568 | 670 | 613 | 657 | 460 | 390 | 430 | 649 | 665 | 597 | 596 | 450 |
| Rb | 5 | 32 | 44 | 5 | 8 | 9 | 29 | 15 | 24 | 24 | 8 | 27 | 35 | 30 | 23 | 67 | 37 | 28 | 26 | 39 |
| Co | 77 | 49 | 31 | 13 | 40 | 41 | 39 | 20 | 41 | 42 | 43 | 41 | 40 | 50 | 40 | n. d.* | n. d.* | n. d.* | n. d.* | 39 |
| Ni | 243 | 92 | 69 | — | 181 | 159 | 135 | — | 45 | 138 | 143 | 182 | 65 | 60 | 50 | 99 | 99 | 159 | 256 | 85 |
| Zr | 235 | 300 | 257 | 109 | 263 | 267 | 234 | 159 | 280 | 207 | 219 | 233 | 96 | 80 | 125 | 230 | 218 | 171 | 160 | 108 |
| Y | 25 | 29 | 27 | 17 | 25 | 28 | 30 | 18 | 22 | 24 | 23 | 27 | n. d* | n. d* | n. d* | 26 | 27 | 25 | 25 | 32 |

* Not determined.

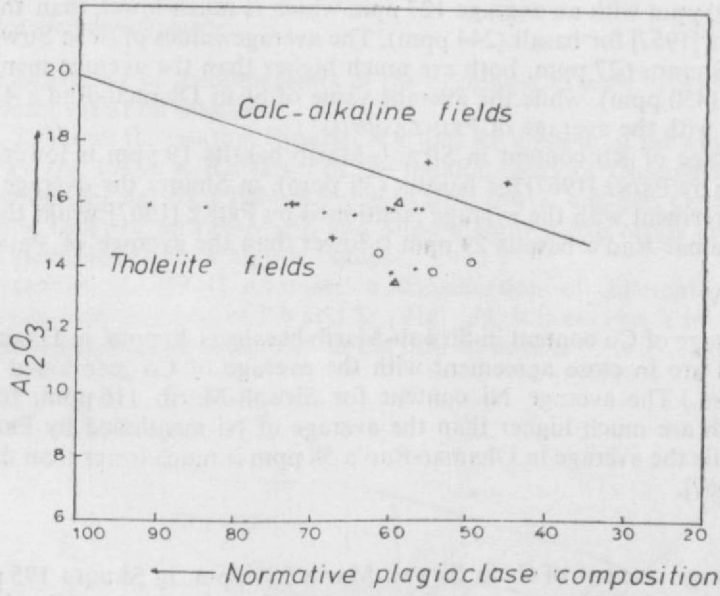


*Fig. 11.* $Al_2O_3$ wt per cent *vs* normative plagioclase composition for the basalts examined after IRVINE and BARAGAR [1971]. Symbols as in *Fig. 2.*

dividing line is drawn from very calcic-plagioclase down to about $An_{35}$. According to the diagram the majority of the examined basaltic rocks are classified as tholeiitic types, with the exception of two samples from Shuqra (Nos. 16 and 17, Table 1) falling in the calc-alkaline field. According to CHAYES [1966] and WILKINSON [1968], these two samples of high-alumina basalt (16.80 and 17.57) are treated as principally of calc-alkaline series. WILKINSON (op. cit.) used the term "sub-alkaline" as a more general name for both tholeiitic basalt and calc-alkaline series (as opposed to alkaline basalt). Accordingly all the examined basaltic rocks are sub-alkaline.

## DISTRIBUTION OF TRACE ELEMENTS

The present investigation is intended to provide information on the abundance of seven trace elements (Ba, Sr, Rb, Co, Ni, Zr, and Y) in the examined basaltic rocks of Yemen. The results of quantitative analysis of 12 samples from Sirwah-Marib, 3 samples from Dhamar-Rad'a [KABESH *et al.*, 1980] as well as 4 samples from Shuqra [COX *et al.*, 1977] are presented in Table 3. The average trace element contents of the examined basaltic rocks and those of PRINZ [1967] are also given in Table 3.

### *Ba, Sr, and Rb*

The distribution of Ba and Sr in the examined basaltic rocks indicates that Sr is more abundant than Ba. This is in agreement with the general trend of variation of Ba and Sr in calc-alkaline associations. The Ba content in Sirwah-Marib ranges from 204 ppm to 1400 ppm with an average 480 ppm which is higher than the average of PRINZ [1967] for basalt (244 ppm). In Dhamar-Rad'a the Ba content ranges from

80 ppm to 160 ppm with an average 127 ppm which is much lower than the average given by PRINZ [1967] for basalt (244 ppm). The average values of Sr in Sirwah-Marib 612 ppm, in Shuqra 627 ppm, both are much higher than the average mentioned by PRINZ [1967] (450 ppm), while the average value of Sr in Dhamar-Rad'a 427 ppm is in agreement with the average of PRINZ [1967].

The average of Rb content in Sirwah-Marib basalts 19 ppm is lower than the average given by PRINZ [1967] for basalts (39 ppm), in Shuqra the average of Rb 40 ppm is in agreement with the average mentioned by PRINZ [1967] while the average of Rb in Dhamar-Rad'a basalts 29 ppm is lower than the average of PRINZ [1967].

*Co and Ni*

The average of Co content in Sirwah-Marib basalts is 40 ppm, in Dhamar-Rad'a 43 ppm both are in close agreement with the average of Co mentioned by PRINZ [1967] 39 (ppm.) The average Ni content for Sirwah-Marib 116 ppm, for Shuqra 153 ppm both are much higher than the average of Ni mentioned by PRINZ [1967] (85 ppm), while the average in Dhamar-Rad'a 58 ppm is much lower than the average of PRINZ, [1967].

*Zr*

The average content of Zr in Sirwah-Marib 230 ppm, in Shuqra 195 ppm both are much higher than the average of PRINZ [1967] (1908 ppm), while the average in Dhamar-Rad'a 100 ppm is very close to the average of PRINZ [1967].

*Y*

The average content of Y in Sirwah-Marib (25 ppm), in Shuqra (26 ppm), both are close to the average mentioned by PRINZ [1967] (32 ppm).

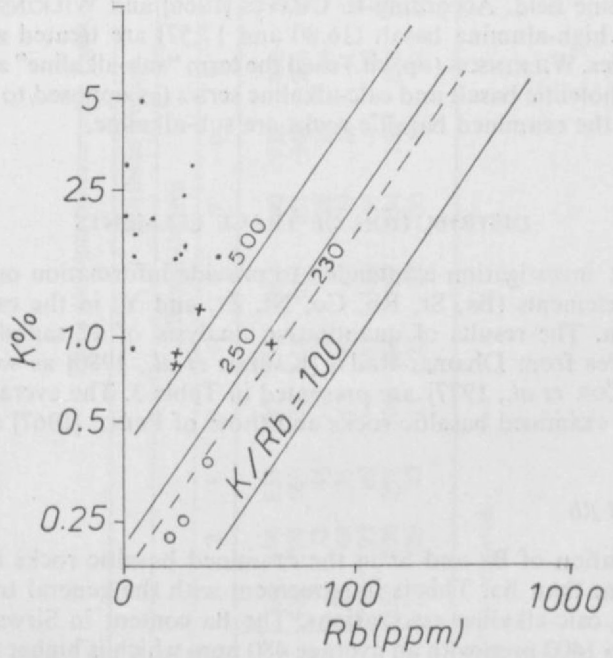


*Fig. 12.* K% *vs* Rb (ppm) after TAYLOR [1965]. Symbols as in *Fig. 2.*

*Trace element chemistry*

The behaviour of trace elements in the examined basaltic rocks is discussed by using several variation diagrams.

*Fig. 12* shows the relation between K% and Rb content of the examined basaltic rocks [TAYLOR, 1965]. K/Rb ratios of the basaltic rocks of Dhamar-Rad'a are relatively low ranging between 100—300 due to their low K content. On the other hand, the basaltic rocks of Sirwah-Marib and Shuqra show K/Rb ratios greater than 500 which is attributed to their high K content.

KISTLER *et al.*, [1971] advanced a classification of different volcanic rocks according ot their contents of Rb and Sr *(Fig. 13)*. It is evident from the figure that all the examined basaltic rocks plot in the field of basalt.

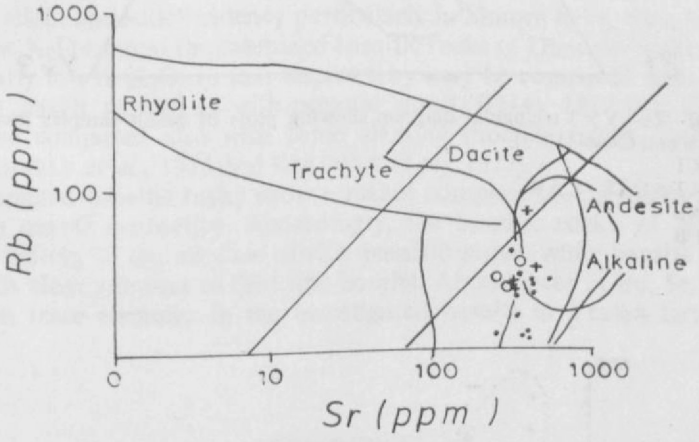


*Fig. 13.* Rb (ppm) — Sr (ppm) variation diagram after KISTLER *et al.*, [1971]. Symbols as in *Fig. 2*.

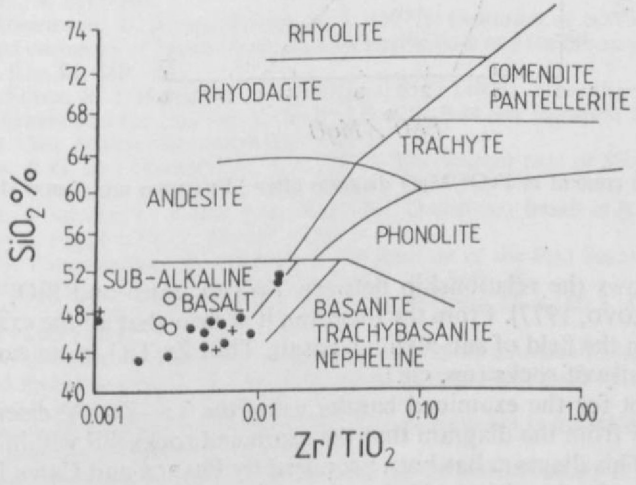


*Fig. 14.* $SiO_2$% *vs* $Zr/TiO_2$ diagram after WINCHESTER and FLOYD [1977]. Symbols as in *Fig. 2*.

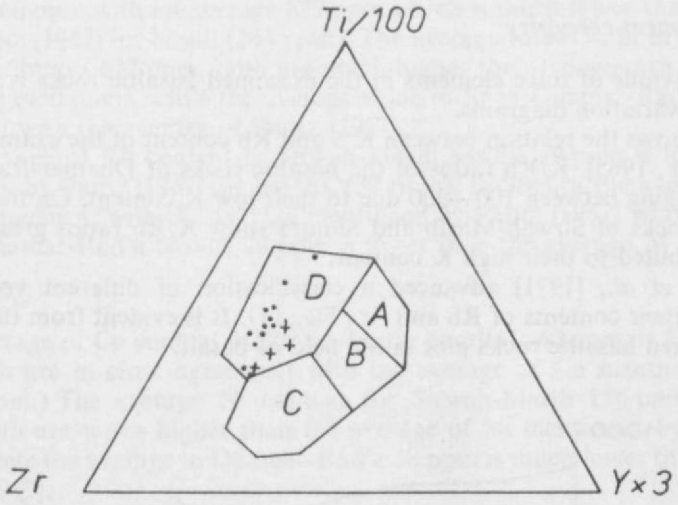


*Fig. 15.* Ti/100—Zr—Y×3 triangular diagram showing plots of basalt samples investigated after PEARCE and CANN [1973].
A: LKT
B: LKT+OFB+CAB
C: CAB
D: OFB

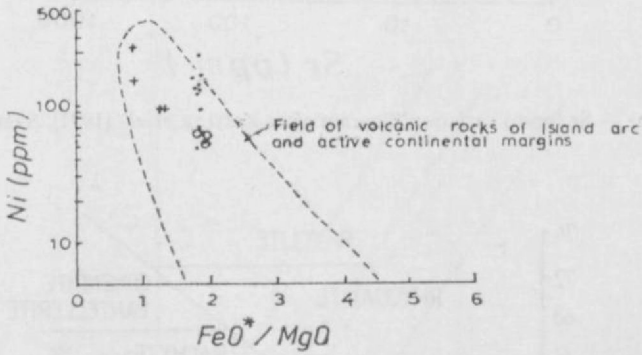


*Fig. 16.* Ni (ppm) content *vs* FeO*/MgO diagram after MIYASHIRO and SHIDO [1975]. Symbols as in *Fig. 2.*

*Fig. 14* shows the relationship between $Zr/TiO_2$ ratio and $SiO_2$ content [WINCHESTER and FLOYD, 1977]. From the diagram, it is clear that all the examined basaltic rocks fall within the field of sub-alkaline basalt. Thus $Zr/TiO_2$ ratio can be used as an index of alkalinity of rocks (op. cit.),

*Fig. 15* plot for the examined basalts using the Ti—Zr—Y discrimination diagram. It is clear from the diagram that the examined rocks fall within field D (within plate basalts). This diagram has been proposed by PEARCE and CANN [1973] as petrogenetic indicator for basaltic rocks.

*Fig. 16* shows the relation between Ni ppm and FeO/MgO ratio of basaltic rocks. It is evident from the figure that all the examined basaltic rocks fall within the field of volcanic island arc and active continental margins. However, two samples from Sirwah-Marib plot very close to this field. This diagram has been proposed by MIYASHIRO and SHIDO [1975].

## CONCLUSION

The basaltic rocks of Sirwah-Marib, Dhamar-Rad'a in Northern Yemen, Shuqra in Southern Yemen and of St. John's Island in Egypt, are petrochemically and geochemically evaluated. In terms of major oxides the examined basalts appear to have sub-alkaline characters with few alkaline affinities. According to the different systems of chemical classification, the examined basaltic rocks are classified as basalts with slight andesitic tendency particularly in Shuqra field, (Southern Yemen).

Based on $K_2O$ content the examined basaltic rocks of Dhamar-Rad'a and Shuqra are particularly low in $K_2O$. In this respect they may be compared with the Red Sea axial trough basalt as well as with oceanic basalt, [GASS, 1977 and CHASE, 1977]. They may be compared also with some alkaline tholeiite basalt from St. John's Island [EL-SHAZLY *et al.*, 1974 and COLEMAN *et al.*, 1977].

The examined basaltic rocks show a rather complete compositional range from nepheline to quartz normative. Accordingly, the basaltic rocks of Sirwah-Marib and Shuqra belong to the alkaline olivine basaltic series, while basalts of Dhamar-Rad'a possess close affinities to tholeiitic basalts. Abundances of Ba, Sr, Rb, Co, Ni Zr and Y an trace elements in the investigated basalts in Yemen have also been discussed.

## REFERENCES


ABDEL-MONEM, A. A. and HEIKAL, M. A. [1981]: Major element composition, magma type and tectonic environment of the Mesozoic to Recent basalts, Egypt: A rewiev. Bull. Fac. Earth Sci., K. A. U., **4**, 121—148.

BATIZA, A. R., ROSENDAHL, B. R. and FISHER, R. L. [1977]: Evolution of oceanic crust, Part III: Petrology and chemistry of basalts from the East Pacific Rise and the Siqueiros transform fault. J. Geophys. Res, **82**, 265—276.

COLEMAN, R. G., FLECK, R. J. HEDGE, C. E. and GHENT, E. D. [1977]: The volcanic rocks of south-west Saudi Arabia and the opening of the Red Sea. In Red Sea Research 1970—1975, Saudi Arabian Dir. Gen. Mineral Resources Bull., 22, 30.

COX, K. G., GASS, I. G. and MALLICK, D. I. J. [1977]: The western part of Shuqra volcanic field South Yemen. Lithos **10**, 185—191.

EL-SHAZLY, E. M., ROUFAIEL, G. S. and ZAKI, N. [1974]: Quaternary basalt in Saint John's Island, Red Sea, Egypt. Egypt J. Geol., **18**, 137—148.

GASS, I. G. [1970]: The evolution of volcanism in the junction of the Red Sea, Gulf of Aden and Ethiopian rifts. Philos. Trans. Roy. Soc. London A **267**, 369—381.

GEUKENS, F. [1966]: Geology of the Arabian Peninsula—Yemen. U. S. G. S. Geological Survey Professional Paper **560-B**.

HUGHES, C. J. [1973]: Spilites, keratophyrs and the igneous spectrum. Geol. Mag., **109**, 513—527.

IRVINE, T. N. and BARAGAR, W. R. A. [1971]: A guide to chemical classification of the common volcanic rocks. Can. J. Earth. Sci., **8**. 523—548.

JUNG, J. and BROUSSE, R. [1966]: Les provinces volcaniques neogenes et quaternaries de la France. Bull. Serv. Carte Geol. France **58**, 267—1.261.

KABESH, M. L. and GHOWEBA, A. M. [1976]: Remarks on the petrochemistry of some Quaternary basaltic rocks, Hamadan volcanic field Yemen Arab Republic. Chem. Erde **35**, 344—355.

KABESH, M. L. and HEGAB, O. A. [1978]: Contribution to the petrology of Hamadan Quaternary basaltic rocks, Y. A. R. Bull. Fac. Sci. Mansoura University **6**.
KABESH, M. L., MONIER, M. A. and HIGAZY, M. H. A. [1981]: Petrochemistry of some Quaternary basaltic rocks, Sirwah-Marib volcanic field, Yemen Arab Republic. Chem. Erde (in press).
KABESH, M. L., REFAAT, A. M. and ABDALLAH, Z. M. [1980]: Geochemistry of Quaternary volcanic rocks Dhamar Rad'a field Yemen Arab Republic. N. Jh. Miner. Abh., **138**, 292—311.
KISTLER, R. W., EVERNDEN, J. F. and SHAW, H. R. [1971]: Sierra Nevada plutonic cycle: Part 1, Origin of composite granitic batholiths. Geol. Soc. Am. Bull., **82**, 853—868.
MACDONALD, G. A. [1968]: Composition and origin of Hawaiian lavas. Geol. Soc. Amer. Mem., **116**, 477—522.
MIDDLEMOST, E. A. K. [1975]: The basalt Clan. Earth-Sci. Rev., **11**, 337—364.
MIYASHIRO, A. [1974]: Volcanic rock series in Island Arcs and active continental margins. Am. J. Sci., **274**, 321—335.
MIYASHIRO, A. and SHIDO, F. [1975]: Tholeiitic and calc-alkalic series in relation to the behaviours of titanium, vanadium, chromium and nickel. Am. Jour. Sci., **275**, 263—277.
PEARCE, J. A. and CANN, J. R. [1973]: Tectonic setting of basic volcanic rocks determined using trace elements analyses. Earth Planet. Sci. Lett., **19**, 290—300.
PRINZ, M. [1967]: Geochemistry of basaltic rocks: Trace Elements. In: Basalts V. I., HESS, H. H. and POLDERVAART, A. (edit): 271—323. Interscience, John Wiley and Sons, New York.
RASCHKA, H. and MULLER, P. [1974]: Contribution to the geochemistry of volcanics, Afar Region, Ethiopia. Proceedings of Inter. Symposium on Afar Region, Germany V. I, (ed.) A. PILGER and A. ROSLER.
TAYLOR, S. R. [1965]: The application of trace elements data to problem in petrology. Phys. Chem. Earth., **6**, 133—123.
SHUKRI, N. M. and BASTA, E. Z. [1955]: Petrography the alkaline volcanic rocks of Yemen. Bull. Inst. Egypt **XXXVI**, 129—164.
VATIN-PERIGNON, N. [1968]: Les formations eruptives et la structure de l'edifice volcanique au centre du Cantal (Massif Central Francais). Bull. Volcanol., **32**, 207—251.
WINCHESTER, J. A. and FLOYD, P. A. [1977]: Geochemical discrimination of different magma series and their differentiation products using. immobile elements. Chem. Geol., **70**, 325—343.
WILKINSON, J. F. G. [1968]: The petrology of basaltic rocks. In: Basalts, John Wiley and Sons, New York.

*Manuscript received, 10 September, 1983*

MAHMOUD LOTFY KABESH
ABDEL-KARIM AHMED SALEM
Earth Sciences Laboratory, National Research Centre
Dokki, Cairo, Egypt
MOHAMED H. A. HIGAZY
Geology Department, Al-Azhar University
Nasr City, Cairo, Egypt

*Acta Mineralogica-Petrographica, Szeged, XXVI/2, 187—205, 1984*

# PETROGRAPHY AND PETROCHEMISTRY OF WADI KAREIM IRON-BEARING FORMATION EASTERN DESERT, EGYPT

E. A. NIAZY, A. EL BAKRY and O. A. KAMEL


## ABSTRACT

The petrography of the Precambrian iron-bearing formation at Wadi Kareim proved that the formation consists of the following regionally metamorphosed rock types of the greenschist facies;

1. Graywackes (mainly volcanic grading to volcanic breccias, normal greywackes are less common).
2. Schists (chlorite, chlorite-calcite, and actinolite-epidote)
3. Volcanics (keratophyres, quartz-keratophyres, spilites, spilitic diabase and diabase).
4. Pyroclastics (lithoclastic and crystal tuffs, lapilli tuffs — mainly spilitic in composition).

The petrographic study is corporated with the results of eight new chemical analyses, representing the different rock types. The analysis of the basic metavolcanic is similar to the average world spilite, and that of the acid metavolcanic is comparable to the aphanitic keratophyre (Schirmeck-type) of the preorogenic Hercynian volcanics of Western Europe.

The recently suggested Al/3—K versus Al/3—Na and Si/3—(Na + K + 2Ca/3) *versus* K—(Na + + Ca) diagrams, the FMA and Na—K—Ca diagrams are adopted for the petrochemical presentation of the chemical data. It is suggested that most rock types either have a composition comparable to basalts or spilitic mineral assemblages. This mostly reflects the primary link of the spilitic rock with other volcanic and pyroclastic rocks, particularly keratophyres. The only exception, is the chlorite schist which has a composition similar to shales.


## INTRODUCTION

The iron ore deposit of Wadi Kareim lies on the northern side of Wadi Kareim, some 38 km southwest of Quseir on the Red Sea coast *(Fig. 1)*.

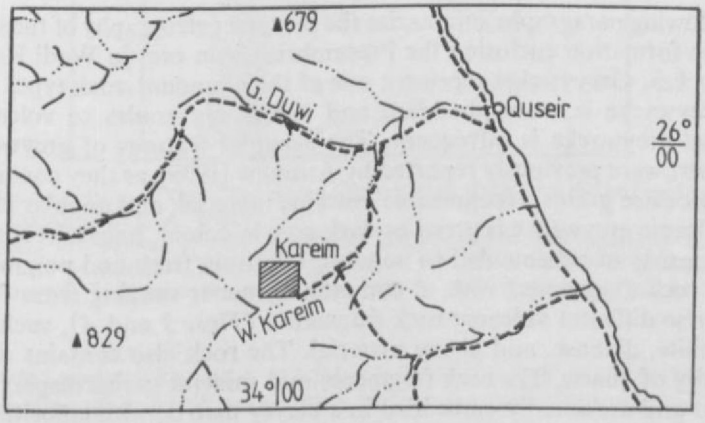


*Fig. 1.* Location map.

The geology, petrography and mineralogy of the Precambrian iron ores and their country rocks have been studied by many authors. Among whom may be mentioned; ABDEL NASSER and AFIA [1949]; NAKHLA, [1954]: EL-SHAZLY, [1957]; GINDY, [1957]; SIGAEV, [1959]; FRIED KRUPP, [1959]; AKAAD, [1959]; ABDEL AZIZ, [1968]; NIAZY, [1969]; HILMY *et al.*, [1972]; and KAMEL *et al.*, [1977].

The area of Wadi Kareim is covered by different basement rock units, which can be arranged chronologically as follows [HILMY *et al.*, 1972];

Top 5) Minor intrusions (mainly bostonite dykes)
4) Granodiorites
3) Igla Formation
2) Metavolcanics (keratophyres, quartz-keratophyres, spilites and diabases)
Base 1) Metasediments (mainly greywackes, schists and tuffs).

The iron-bearing formation in Wadi Kareim has been considered to consist of regionally metamorphosed: 1) geosynclinal sediments, 2) banded-siliceous iron ores, and 3) volcanic rocks [KAMEL *et al.*, 1977]. The Precambrian metasediments, metavolcanics and banded iron ores are paragenetically related to each other. The iron-bearing formation represents a large monoclinal fold, which is intersected by a major thrust fault, along which a highly sheared structural unit is displaced over the formation from the east [SIGAEV, 1959; HILMY *et al.*, 1972].

## PETROGRAPHY

The iron-bearing formation in Wadi Kareim, comprises different metasedimentary and metavolcanic rocks of the green schist facies. The geosynclinal metasediments and the associated volcanics are represented by the following rock types *(Fig. 2);* 1) graywackes, 2) schists, 3) metavolcanics, and 4) pyroclastics.

The formation represents the oldest rock unit in the studied area [NIAZY, 1969; KAMEL *et al.*, 1977]. Generally, the metamorphosed volcanogenic-sedimentary rocks of the formation have a pale brown colour, grading into pale green and greyish green colours. In some parts, the rocks are tough, however, they are commonly shattered and even friable. Most of the rock types are intersected by calcite veinlets.

The presence of pebbles and cobbles of different volcanic rocks in the metasediments was earlier recorded by SHUKRI *et al.*, [1959], EL-RAMLY and AKAAD [1960], and others in the different Precambrian iron ore occurrences of the central Eastern Desert.

The following paragraphs summarize the detailed petrography of the sedimentary-volcanogenic formation enclosing the Precambrian iron ores in Wadi Kareim.

*Greywackes*. Greywackes represent one of the abundant rock types in the area. Volcanic greywacke is more abundant and commonly grades to volcanic breccia, while normal greywacke is infrequent. The essential features of greywackes in the Eastern Desert were previously reported by ANDREW [1939], as they contain abundant detrital plagioclase grains, recognizable volcanic material, and angular clastic grains.

The volcanic greywacke is green or dark grey in colour, hard and coarse-grained. The rock consists of subrounded to angular, relatively fresh and polymictic mineral grains and rock fragments, with a common diameter ranging from 0.5 to 3 mm. They comprise different volcanic rock fragments *(Figs. 3* and *4)*, such as trachyte, andesite, spilite, diabase, and glassy material. The rock also contains other mineral grains, mainly of quartz. The rock fragments and mineral grains display sub-parallel arrangement and are usually embedded in a clayey matrix, with chlorite and sericite, that may show flow-banding.

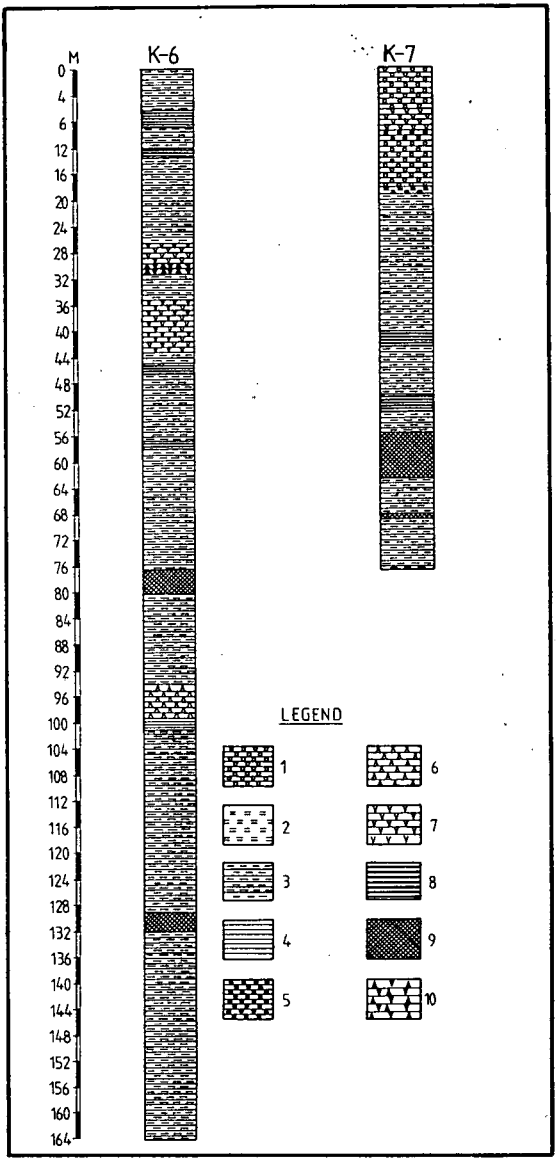


*Fig. 2.* Geologic succession of the iron-bearing formation as shown by the inclined wells K—6 and K—7, according to E. A. Niazy.
1: volcanic greywacke; 2: tuff; 3: chlorite, calcite-chlorite and actinolite schists; 4: graphite-calcite — actinolite schist; 5: garnet — actinolite schist; 6: meta-alkali-trachyte-(keratophyre); 7: diabase; 8: banded iron ore; 9: massive iron ore; 10: brecciation zone.

The normal greywacke has a greyish-green colour and is moderately compact. The rock consists of mineral grains and infrequent rock fragments. The essential clastic minerals are ill-sorted and consist of subangular quartz and fine orthoclase

*Fig. 3.* Photomicrograph of volcanic greywacke, composed of different subrounded rock fragments showing subparallel arrangement in a clayey-chloritic matrix. Plane light, 20×.

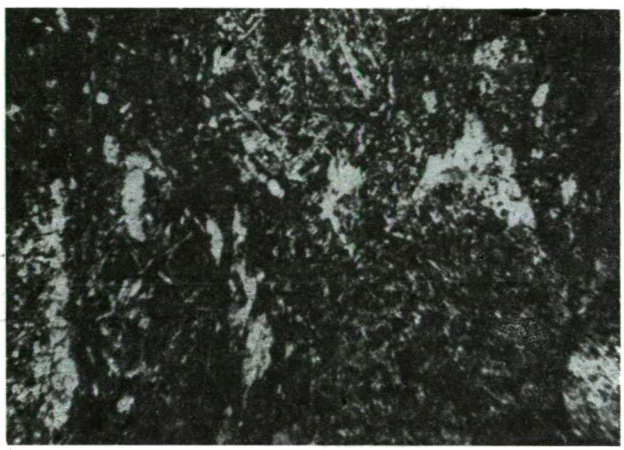

*Fig. 4.* Photomicrograph of volcanic greywacke, composed of spilite and other volcanic fragments in a similar groundmass. Crossed nicols, 20×.

grains *(Fig. 5)*. Flakes of muscovite are not uncommon. Grains of epidote, plagioclase, apatite, magnetite and tourmaline are rarely encountered. Coarse fragments of chert and greenstones are present, which diameter is about 0.5—1 mm. The mineral grains and rock fragments are embedded in a pasty matrix of chlorite, sericite and clayey material. The flaky minerals usually exhibit parallel arrangement to the rock cleavage.

*Schists.* Schists are represented by chlorite, chlorite-calcite and actinolite-epidote varieties which grade into each other imperceptibly. The schists are distinctly foliated with parallel allignment of flaky and prismatic minerals. Most of these schists belong to the same mineral assemblage.

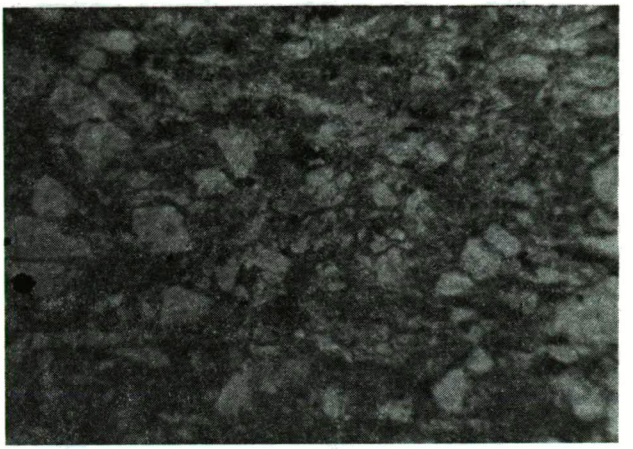

*Fig. 5.* Photomicrograph of normal greywacke, showing ill-sorted subangular quartz and feldspar grains in a matrix of chlorite and clayey material. Plane light, 20×.

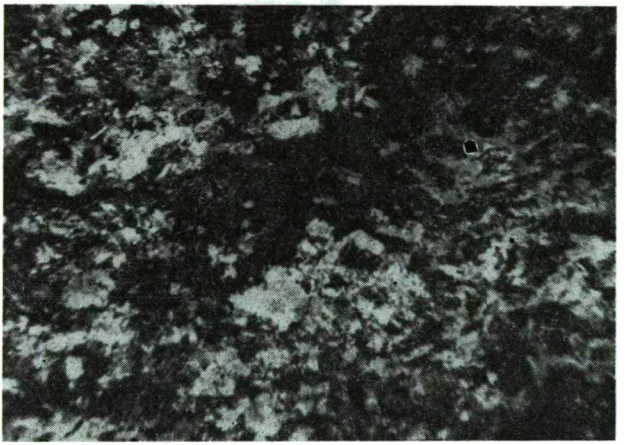

*Fig. 6.* Photomicrograph of chlorite schist, composed of chlorite (grey), quartz (colourless) and magnetite (black). Plane light, 20×.

The chlorite schist is greyish-green in colour, and fine to medium-grained. The rock is essentially composed of chlorite, quartz and calcite *(Fig. 6)*. Albite, magnetite, muscovite, epidote, actinolite and carbonaceous matter are less common. Chlorite is mainly represented by pennine, that forms fine twin aggregates of small andehral crystals. The mineral displays noticeable pleochroism ($Z$=green, $Y$=green, and $X$=yellowish green), with $n_\gamma = 1.575$, $n_\alpha = 1.572$, and anomalous interference. Clinochlore is less common and forms thin tabular crystals. Occasionally, brown stilpnomelane occurs as fine to coarse plates in subparallel bands of sheaflike aggregates *(Fig. 7)*, indicating high percentages of $K_2O$ in the rock. Quartz is subrounded, and occurs as fine aggregates between chlorite and calcite. The latter mineral forms fine-grained anhedral crystals, that may be aggregated in small patches and irregular

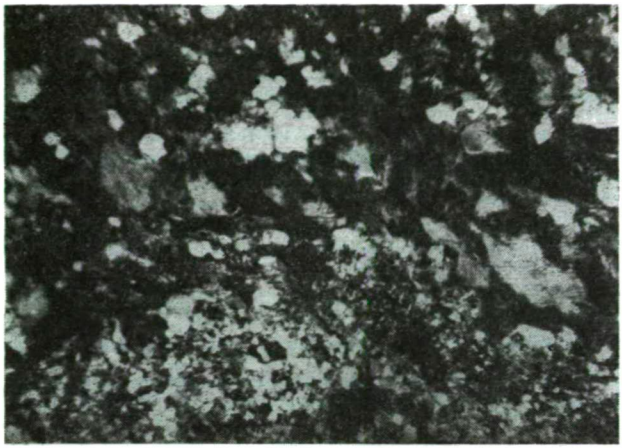

*Fig. 7.* Photomicrograph showing sheaflike aggregate of brown stilpnomelane in the chlorite schist. Plane light, 20×.

clots. Albite ($Ab_{95}$ $An_5$) is irregular, and displays albite twinning with $X' \wedge (010) = -16°$. Magnetite is disseminated in the rock. Chlorite schist is most probably the result of regional metamorphism of some pelitic and psammopelitic sediments. They belong to rocks of greenschist facies [TURNER and VERHOOGEN, 1960: TURNER, 1958].

The chlorite-calcite schists may be broadly referred to either original basic volcanic rocks or else calc-pelitic sediments. Schists derived from basic volcanics are dominant. They are essentially composed of chlorite, calcite, quartz and albite. Epidote, leucoxene, actinolite, magnetite and pyrite are uncommonly present. Remnants of the primary mafic minerals are still preserved. Magnetite forms clustered aggregates or scattered crystals. In some parts, the rock is traversed by quartz, chalcedony and calcite veinlets. Vein quartz is commonly associated with coarse pyrite cubes, which may be surrounded by microcrystalline quartz at the tapering parts of the veinlets. Later deformation of pyrite is sometimes observed accompanied by its partial replacement of quartz.

Chlorite-calcite schists derived from the calc-pelitic sediments are less abundant. They consist of carbonate laminae, bands, and lenses alternating with others of chlorite, quartz, magnetite and muscovite. The chlorite minerals are very similar to those of the chlorite schist. The carbonates are mainly calcite, dolomite associated with quartz, talc and tremolite. Coarse grains of detrital quartz are frequent at the boundaries of the carbonate and chlorite laminae. This quartz exhibits undulatory extinction and is optically biaxial. The rock is commonly traversed by calcite veinlets.

The actinolite-epidote schist has a light green colour, and consists essentially of actinolite, epidote and chlorite. Calcite, quartz, and albite are subordinate in abundance, while pyrite, magnetite, augite, apatite, sphene, muscovite and leucoxene are rarely observed. Actinolite forms fibrous aggregates of thin crystals. It is weakly pleochroic ($X$=light green, $X$=greenish yellow, and $Z$=green) with $c \wedge Z' = 15°$. The mineral is occasionally associated by anthophyllite. Pistacite is found accompanied by actinolite and chlorite. It is yellowish-green in colour and moderately pleochroic. The mineral usually forms small euhedral crystals and granular aggregates that display parallel extinction, with $n_\gamma = 1.737$ and $n_\alpha = 1.722$. Pennine forms

patches of fine anhedral crystals commonly associated by calcite. Feathery quartz is sometimes observed around the pyrite and magnetite porphyroblasts. The quartz crystals may show twisting indicating post-or syncrystallization rotation.

The described actinolite-epidote schists belong to the albite epidote hornfelses of the contact metamorphic facies [TURNER, 1958], They were, however, previously classified as actinolite-epidote hornfels subfacies [TURNER and VERHOOGEN, 1960]. It is reasonable to suggest that such schists were principally formed in sheared parts of the volcanic rocks and tuffs of the iron-bearing formation.

At the close contacts with granodiorite, the described schists are facially changed to a highly foliated reddish brown rock with papery appearance, where biotite replaces chlorite in the chlorite-biotite schist. Such a rock consists of biotite, quartz, chlorite, muscovite, actinolite and calcite. It may also contain disseminations of garnet, magnetite and pyrite, and the rock grades to chlorite-biotite-garnet schist. In some peripheral parts, however, the metasediments consist mainly of coarse crystalline calcite bands. Here, graphite is sometimes observed, where the mineral forms laminae, patches and streaks, and is associated with chlorite, epidote, phlogopite, anthophyllite, sodic plagioclase, and talc.

*Metavolcanics.* Metavolcanics include keratophyre, quartz-keratophyre, spilites, spilitic diabase and diabase. The metavolcanic rocks commonly form sheeted dyke and sill-like bodies which are often concordant with the schists, greywackes and tuffs. In many parts, keratophyres are in direct contact with the "banded-siliceous" iron ores.

It should be mentioned that along the upper reaches of the central wadi of the investigated area, a massive greyish-green, fine grained effusive rock grading to a coarser variety with abundant magnetite phenocrysts, which has a pillow-like structure *(Fig. 8),* is exposed intruding the greywackes, schists and tuffs. The rock is identified as possible keratophyre. The formation of such a rock is considered to be of probable submarine-effusive origin. Metamorphosed alkaline effusive rocks with spherulitic and trachytic textures are commonly encountered in many parts of Wadi Kareim, particularly, along adit No. 4 and borehole K—6 [NIAZY, 1969].

Keratophyre is hard, porphryitic *(Fig. 9)* with splintery fracture. The rock

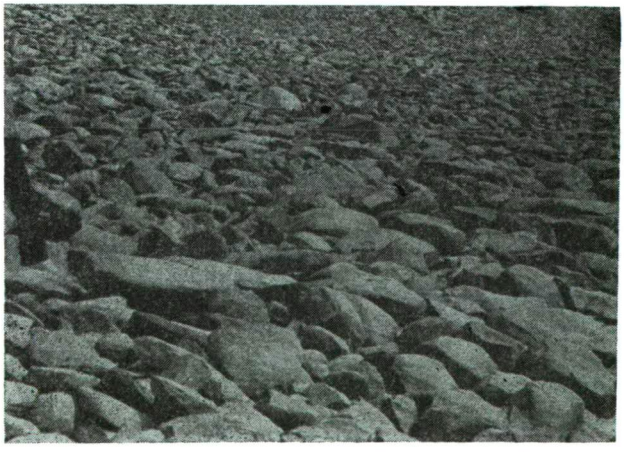

*Fig. 8.* Photograph of the central wadi in Kareim area, showing pillow-like bodies of a metavolcanic field.

displays sub-parallel arrangement of the mineral constituents. The phenocrysts consist of albite, oligoclase, and augite. The albite laths display both albite and Carlsbad twinning, and are often radially disposed and highly altered. The mineral microlites commonly show fluxional flow and trachytic fabric. Coarse augite ($c \wedge Z' = 38°$) is almost completely altered, however, their outlines and cleavage traces are occasionally preserved. The pyroxene mineral is usually altered to chlorite, actinolite and epidote. Potash feldspar commonly forms perthitic intergrowths with quartz, while sanidine is rare.

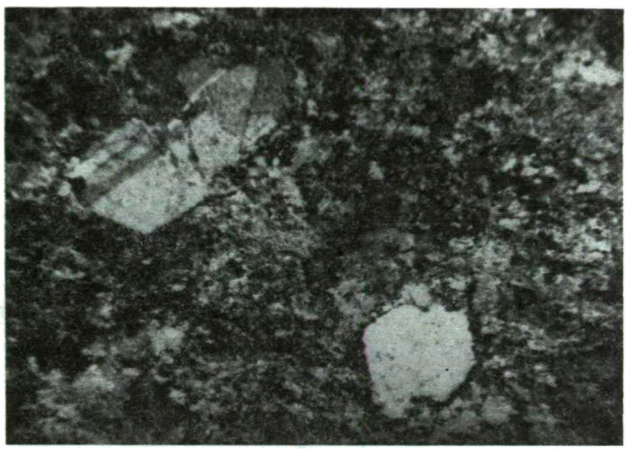

*Fig. 9.* Photomicrograph of porphyritic keratophyre. Phenocrysts are represented by quartz and sodic plagioclase in a trachytic groundmass. Plane light, 20×.

The quartz-keratophyre is marked by abundant quartz phenocrysts. Quartz is sometimes intergrown with sodic plagioclase in the groundmass. The rock is characterized by the presence of variolitic spherulites *(Fig. 10)* composed of radially arranged albite laths associated with fine-grained quartz. The spherulites are embedded

*Fig. 10.* Photomicrograph of keratophyre showing variolitic spherulites of radially arranged albite laths. Crossed nicols, 50×.

in a cryptocrystalline groundmass of minute albite microlites, quartz, chlorite, zoisite and microcrystalline silica. Apatite, sphene and talc are rare, while opaque minerals (magnetite, pyrite, ilmenite and leucoxene) are uncommon. Amygdales of quartz, chalcedony or calcite are also encountered.

In some parts, the keratophyres are associated with other effusive rocks, spilite [NIAZY, 1969], and spilitic diabase. The identification of spilite was earlier ascertained both by X-ray diffraction and chemical analysis [ABDEL AZIZ, 1968]. Spilite is hard, spotted and dark green. It consists of short thin albite laths ($\sim 70$ by volume) in a chlorite matrix *(Fig. 11)*. Relicts of unaltered augite are sometimes observed. The rock is marked by the radial arrangement of the albite laths and is characterized by the triangular disposal of the mineral in the mesostasis of altered pyroxene, chlorite, clinozoisite and epidote. Magnetite, ilmenite, actinolite, apatite and calcite are rarely present. Small pools of jasper and amygdales filled by chert, microcrystalline quartz or calcite are occasionally observed *(Fig. 12)*. Occasionally, the rock merges to a rather coarse-grained variety, i. e. spilitic diabase.

*Fig. 11.* Photomicrograph of spilite, composed of albite laths displaying intersertal texture in a chloritic groundmass. Crossed nicols, 20×.

The diabase is dark green, medium-grained and porphyritic. It is mainly composed of zone labradorite ($Ab_{44}$ $An_{56}$), augite and titaniferous augite showing ophitic and sub-ophitic textures. Calcite and chlorite are present in fair amounts, in the groundmass. Apatite, quartz, ilmenite and magnetite are rarely encountered. Generally, diabase is less affected by the regional metamorphism, and may show some contact effects with different rocks of the studied formation.

*Pyroclastics.* The pyroclastic rocks are represented by tuffs and lapilli tuff. The tuffs are fine-grained rocks, with light green, grey or even brown colours, and show banded texture *(Fig. 13)*. The tuff bands have regular, sharp and uniform contacts and their thickness varies between 0.5 and 2 mm. Sometimes, the bands are rather irregular and displaying gradation in grain size. In the studied area, both crystal and lithoclastic tuffs are encountered.

Crystal tuff is composed of angular to subangular crystals and ill-sorted glass particles embedded in a glassy, clayey or chloritic groundmass. The crystals may be cracked, corroded, and consist of sodic plagioclase, sanidine, potash feldspars,

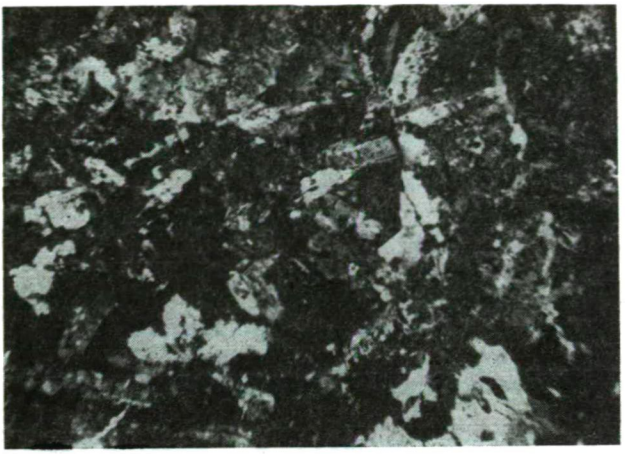

*Fig. 12.* Photomicrograph of spilitic diabase with small pools of jasper and chert. Crossed nicols, 20×.

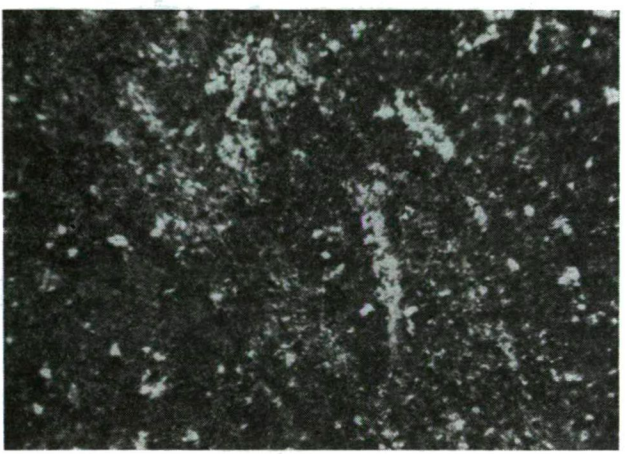

*Fig. 13.* Photomicrograph of fine-grained tuff with angular quartz grains and displaying banded texture. Plane light, 20×.

quartz, magnetite and leucoxene, some of the tuff bands are carbonate-rich or composed of pelitic material. Glassy material is normally altered to clay minerals, and the rock may be mistaken for "mudstone".

Lithoclastic tuff is also fine-grained, with common rock fragments of spilite, spilitic diabase, keratophyre and siliceous material. Frequently, the rock grades to lithoclastic lapilli tuff, with coarser rock fragments and lapilli. The most common variety is spilitic lithic tuff, where the lapilli are subangular to subrounded and composed mainly of spilitic rock fragments, about 0.2—1.5 cm in diameter, embedded in a groundmass of microcrystalline and cryptocrystalline spilite *(Fig. 14)*. Trachytic lithic tuff is also encountered, but in lesser amounts. The lithoclastic lapilli tuffs normally display flow-banding of the matrix and merge to the volcanic greywacke and volcanic breccia.

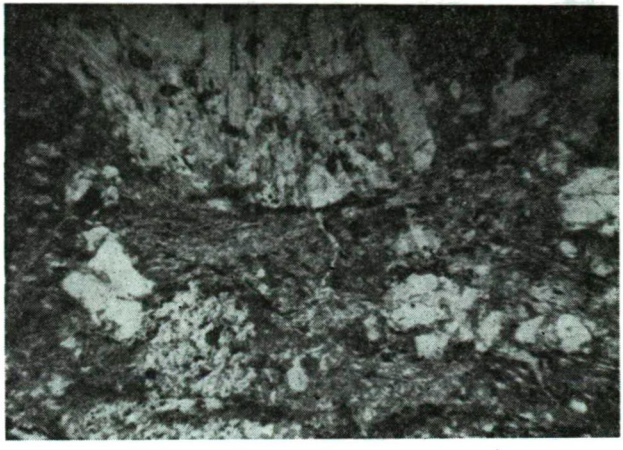

*Fig. 14.* Photomicrograph of spilitic lithic tuff, with lapilli of spilite in a groundmass of microcrystalline spilite. Plane light, 20×.

## PETROCHEMISTRY

The results of chemical analysis of newly analyzed eight samples from the iron-bearing formation of Wadi Kareim are given in Table 1. The average chemical analysis of spilite [VALLANCE, 1960], chemical analysis of aphanitic keratophyre [JUTEAU and ROCCI, 1974] are also cited for comparison.

TABLE 1

*Chemical analysis data of W. Kareim iron-bearing formation*

| Analysis No. | 1 | 2 | 3 | 4 | 5 | 6 | 7 | 8 | 9 | 10 |
|---|---|---|---|---|---|---|---|---|---|---|
| $SiO_2$ | 48,97 | 49,65 | 62,41 | 61,30 | 49,65 | 56,93 | 63,91 | 59,26 | 46,92 | 59,07 |
| $Al_2O_3$ | 16,86 | 16,00 | 14,11 | 18,20 | 16,78 | 10,73 | 13 94 | 12,70 | 13,63 | 17,10 |
| $Fe_2O_3$ | 1,96 | 3,85 | 2,06 | 6,76 | 1,94 | 7,97 | 2,99 | 2,12 | 2,16 | 4,22 |
| FeO | 9,07 | 6,08 | 5,29 | 3,34 | 5,87 | 9,47 | 8,37 | 4,22 | 3,95 | 2,86 |
| MnO | 0,23 | 0,15 | 0,19 | 0,20 | 0,18 | 0,21 | 0,13 | 0,23 | 0,27 | 0,16 |
| MgO | 3,41 | 5,10 | 2,75 | 2,46 | 6,81 | 4,80 | 2,31 | 1,98 | 3,30 | 3,73 |
| CaO | 6,56 | 6,62 | 3,36 | Tr. | 6,72 | 3,05 | 1,83 | 7,63 | 12,97 | 2,44 |
| $Na_2O$ | 3,54 | 4,29 | 3.13 | 5,12 | 2,93 | 0,23 | 0,47 | 2,83 | 2,86 | 5,80 |
| $K_2O$ | 1,17 | 1,28 | 1,39 | 1,78 | 0,66 | 0,24 | 0,92 | 1,54 | 1,81 | 0,42 |
| $TiO_2$ | 2,28 | 1,57 | 0,93 | 0,57 | 0,72 | 0,85 | 0,56 | 0,61 | 0,58 | 0,95 |
| $P_2O_5$ | 0,32 | 0,26 | 0,07 | — | 0,05 | 0,21 | 0,71 | 0,13 | 0,09 | 0,09 |
| L. O. I | 5,19 | 5,12 | 4,27 | — | 7,72 | 5,00 | 2,41 | 6,95 | 11,76 | 3,62 |
| | 99,56 | 99,97 | 99,96 | 99,73 | 100,03 | 99,69 | 100,55 | 100,20 | 100,30 | 100,46 |

1. Spilite, W. Kareim.
2. Average spilite (WALLANCE, 1960].
3. Keratophyre of intermediate composition, W. Kareim.
4. Aphanitic keratophyre (Schirmeck type) [JUTEAU and ROCCI, 1974].
5. Volcanic greywacke (spilitic lithic tuff), W. Kareim.
6. Normal greywacke, W. Kareim.

7. Chlorite schist derived from shale, W. Kareim.
8. Chlorite-calcite schist derived from calc-alk. dacite, W. Kareim.
9. Calcite-chlorite schist derived from calc-alk. dacite, W. Kareim.
10. Tuff, W. Kareim.

The associated albite-oligoclase and chlorite in the spilitic rocks is accompanied by increased proportions of $Na_2O$. FIALA [1967], suggested that 4% $Na_2O$ can be accepted as a dividing line for similar occurrences in Bohemia. This dividing line is not sharp, and gradational types with 3.5—4% $Na_2O$ and oligoclase as the main feldspar, sometimes with fresh augite are common. The value of the ratio $CaO/Na_2O+K_2O<2$ is accepted, as a rule, in analogy. The $K_2O$ content is generally very low in spilites [TURNER and VERHOOGEN, 1960).

Types enriched in $K_2O$ also exist, e. g. the weakly metamorphosed chlorite schists characterized by presence of stilpnomelane. These schists seem to be derived from some pelitic sediments. Ca-enriched varieties, e. g. calcite-chlorite schist do occur in some parts of the area, and a value of 12.97% CaO is also reached. In such varieties, the ratio $CaO/Na_2O+K_2O$ is deviated from the mentioned rule. Similar Ca enriched varieties with a CaO up to 16.42% were earlier reported by VALLANCE [1965].

*Al/3 — K versus Al/3 — Na diagrams*

The Al, Na, K diagram *(Fig. 15)* was first suggested by DE LA ROCHE [1966], and then adopted by DE LA ROCHE *et al.*, [1974] for the chemical presentation of spilitic rocks. The diagram is constructed by calculating the numbers of milliatoms-grams of each component in 100 grams. The diagram allows a clear distinction between the characteristic transition anorthite-albite during spilitization. It shows the disposal of the volcanic associations and their distribution fields against those of the sedimentary associations. Also, it is useful in the separation of sedimentary degradation *versus* the magmatic differentiation.

From the diagram, it is clear that analysis No. 1 (spilite) is plotted within the field of spilitic volcanics, which is also reflected in the chemical analysis of the sample and is very similar to the average spilite composition given by VALLANCE [1960], analysis No. 2. Analysis No. 3 (keratophyre) is plotted in the field of intermediate volcanics. The chemical composition of the rock is quite comparable to the aphanitic keratophyre [JUTEAU and ROCCI, 1974], analysis No. 4 (Schirmeck type). Analysis No. 5 (volcanic greywacke) has a plot very near to the field of spilitic volcanics and the domain of basalts. On the contrary, analysis No. 6 (normal greywacke) is plotted very near to the boundary line of greywackes and shales, within the sedimentary sector. Again, analysis No. 7 (chlorite schist) is plotted in the field of shales. Analyses No. 8 (chlorite-calcite schist), and No. 9 (calcite-chlorite schist), however, are plotted in the field of calc-alkaline Pacific tholeiitic volcanics and within the area specific for dacites. Lastly, analysis No. 10 (tuff) is plotted outside the fields of volcanic and sedimentary rocks, but rather near to the field of spilitic volcanics.

The Al, Na, K diagram *(Fig. 16)* was also suggested by DE LA ROCHE *et al.*, [1974]. The diagram shows the domain of basalts and the field of the spilitic mineral assemblage. It delineates a limited zone for basalts, within the sector of calcic plagioclase (labradorite-bytownite) and the point of origin of the axes near to the area of common pyroxenes and amphiboles.

However, the minerals characteristic for the spilitic assemblage (albite, chlorite, calcite, K-feldspar, augite, quartz, iron oxides) occupy a vast area covering the domain of basalts.

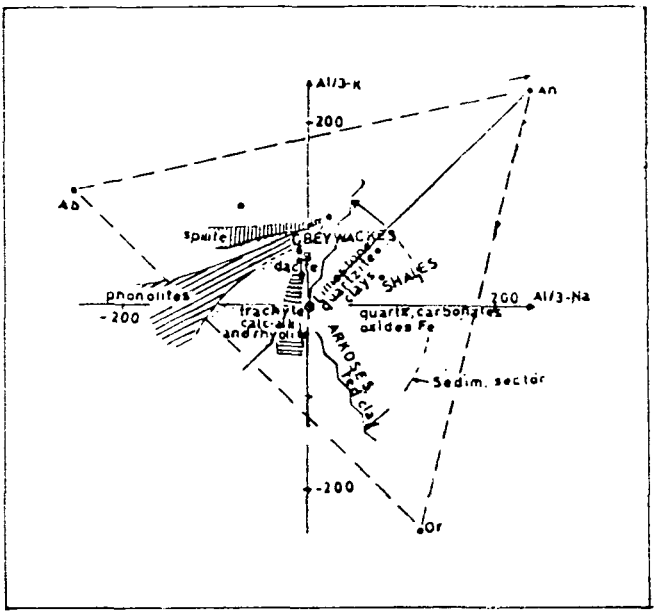


*Fig. 15.* Al—Na—K variation diagram showing general disposal of volcanic and sedimentary rock association in Wadi Kareim.

From the diagram, it is noticed that the analyzed samples of spilite, volcanic greywacke and chlorite-calcite schist have mineral composition comparable to basalts as their analyses are plotted in the domain of basalts. Also, the samples of keratophyre as their analyses are plotted in the domain of basalts. Also, the samples of keratophyre, calcite-chlorite schist, tuff and normal greywacke have mineral composition of spilitic mineral assemblage. The only exception is the analysis of chlorite schist as

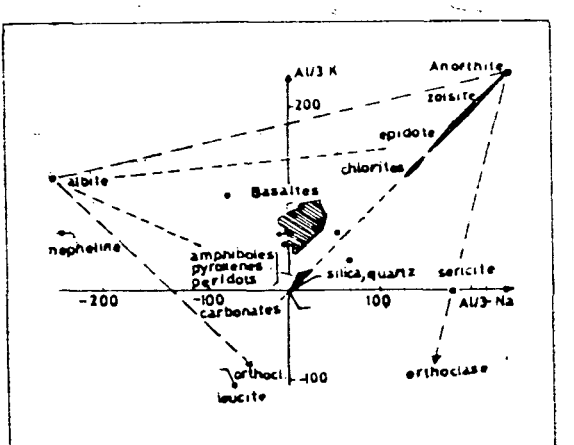


*Fig. 16.* Al—Na—K variation diagram showing domain of basalts and field of spilitic rock association.

its plot is located outside the area of spilitic assemblage. The disposal of plots of the different volcanics on the Al. Na, K, diagrams points to the primary link of the spilitic rocks with the other volcanic and pyroclastic rocks, particularly keratophyres.

*Si/3 — (Na+K+2Ca/3) versus K — (Na+Ca) diagram*

The Si, K, Na, Ca diagram *(Fig. 17)* was also adopted by DE LA ROCHE *et al.* [op. cit., 1974] for differentiation of the lithological types of the preorogenic Hercynian volcanics in Northern Europe. Distinction has been made into two evolution trends (Schirmeck-type and Lahn-Dill type) in relation with the paleogeography. A magmatism of folds (Schirmeck-type) to a magmatism of "grabens" (Lahn-Dill type) has been outlined by JUTEAU and ROCCI [1974] in their petrographic and chemical investigation of the Hercynian orogeny in Western Europe.

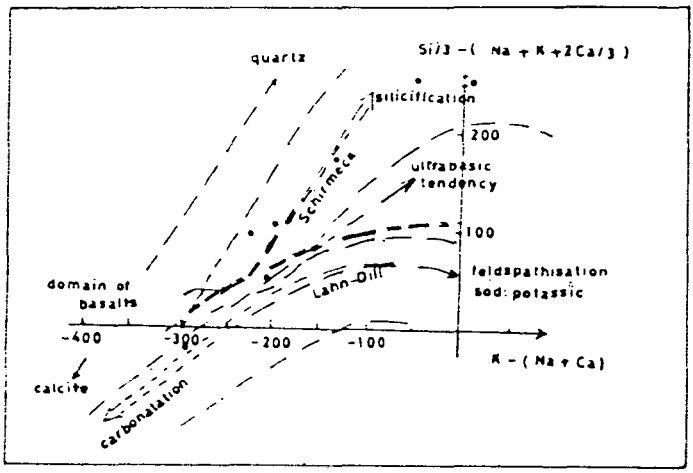


*Fig. 17.* Si—K—Na—Ca variation diagram showing evolution trend of volcanogenic-sedimentary iron-bearing formation in Wadi Kareim.

The diagram indicates that the investigated association of rocks of the iron-bearing formation in Wadi Kareim had an evolution trend similar to the Schirmeck type of preorogenic Hercynian volcanics and is more inclined towards a tholeiitic tendency, i. e. spilites relatively poor in calcium, and rather siliceous keratophyres.

*The FMA variation diagram*

In the FMA ternary diagram illustrating the tholeiitic and calc-alkali series proposed by NOCKOLDS [1954], the metavolcanic and pyroclastic rocks of the studied area show a trend similar to the tholeiitic series *(Fig. 18)*.

*The Na—K—Ca ternary diagram*

The Na—K—Ca ternary diagram for the metavolcanic and pyroclastic rocks of Wadi Kareim is very comparable to such diagrams published by JUTEAU and ROCCI [op. cit., 1974] for some spilite-keratophyre association of the Lahn-Dill rock series rather than the Schirmeck rock series of the Hercynian orogeny. The same similarity

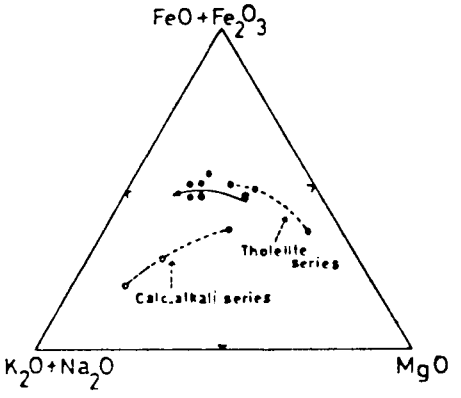


*Fig. 18.* FMA ternary diagram.

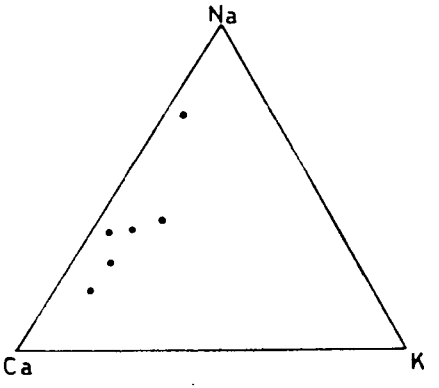


*Fig. 19.* Na—K—Ca ternary diagram.

is again noted from the Na—K—Ca ternary diagram of the amalyzed rocks *(Fig. 19)*, based on the number of calculated atoms.

This discrepancy in the presentation of chemical data of the studied rock association on the Si/3 — (Na+K+2 Ca/3) *versus* K — (Na+Ca) diagram, and the Na—K—Ca ternary diagram is most probably due to he presence of abundant calcite veinlets intersecting most of the studied metavolcanic rocks in Wadi Kareim area.

*Niggli-values*

The Niggli-values for the metavolcanic and pyroclastic rocks of the iron-bearing formation in Wadi Kareim, are calculated according to the method suggested by NIGGLI [1954], and the modifications adopted by BARTH [1959].

From the Niggli values given in Table 2, it is evident that most of the rocks are saturated with respect to silica. The quartz value (qz) is more than −12, with the exception of analysis No. 9, which indicates that olivine is absent. The k-value also is less than 0.36, which points that the studied rocks do not contain potash feldspars,

TABLE 2

*Niggli-values of W. Kareim metavolcanics and pyroclastics*

| Analysis No | 1 | 3 | 5 | 8 | 9 | 10 |
|---|---|---|---|---|---|---|
| si | 138 | 239 | 134 | 215 | 130 | 198 |
| al | 28 | 32 | 27 | 27 | 22 | 34 |
| fm | 40 | 39 | 45 | 30 | 28 | 38 |
| c | 20 | 14 | 19 | 30 | 39 | 9 |
| alk | 12 | 15 | 9 | 13 | 11 | 19 |
| k | 0,18 | 0,23 | 0,13 | 0,26 | 0,29 | 0,04 |
| mg | 0,35 | 0,4 | 0,61 | 0,36 | 0,48 | 0,49 |
| ti | 4,9 | 2,5 | 1,5 | 1,7 | 1,3 | 2,4 |
| p | 0,34 | 0,23 | 0,16 | 0,22 | 0,16 | 0,20 |
| qz | −10 | 79 | −2 | 63 | −14 | 22 |

Analyses numbers as those indicated in Table 1.

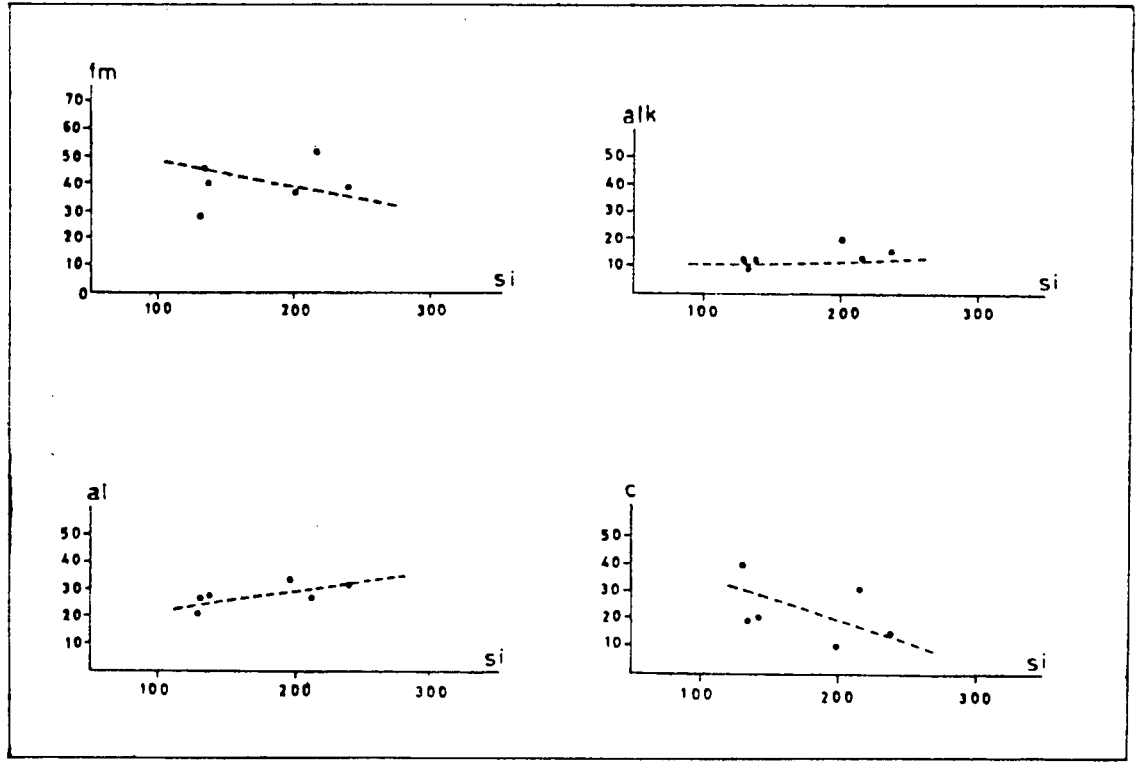


*Fig. 20.* The relation between si and al, fm, c, alk values of Niggli.

and that the sum of potassium should be incorporated in the plagioclase structure [CHETVERIKOV, 1956]. However, uncommon sanidine and perthitic intergrowths are occasionally observed in some rock varieties. The calculated k-values, are also similar to the data reported by FIALA [1967] for spilitic rocks from Bohemia, which k-values vary from 0.1 to 0.31, with the higher values are specific for keratophyres and quartz-keratophyres. Also, silicates with isomorphous replacement of magnesium by iron are more high-temperature, the more they contain magnesium. Therefore, the calculated mg-values for the studied metavolcanic and pyroclastic rocks (more than 0.35) possibly indicate they are high-temperature [CHETVERIKOV, 1956].

*Fig. 20* illustrates the correlation diagrams; si—al, si—fm, si—c, and si—alk for the analysed rock samples. It is obvious that by increasing the values of si those of al and alk increase, while those of fm and c decrease consequently. Such relationships are quite normal for igneous rocks. The relations between si and al and alk are rather linear, which indicate positive correlations between si—al, and si—alk values, i. e. most of $Al_2O_3$, $Na_2O$ and $K_2O$ are combined with $SiO_2$ in the silicate minerals. The relations between si and fm and c, however, deviate from the linear arrangement, that point to presence of iron oxide minerals, and calcite in the investigated rocks beside their sharing in the structure of silicates.

## CONCLUSIONS

From the foregoing discussion it sould be concluded that the Precambrian iron-bearing formation at Wadi Kareim consists of low-grade regionally metamorphosed greywackes, schists, volcanics and tuffs, of the green schists facies.

The greywackes are mainly represented by volcanic greywackes grading to volcanic breccias and infrequent normal greywackes. The described metasediments contain abundant polymictic and mesomictic ill-sorted fragments and grains indicating rapid transportation as was mentioned by KAMEL *et al.* [1977]. The mechanically carried pebbles and particles are relatively fresh fragments and represent many of the associated volcanic rocks. Such polymictic rock fragments and grains point to deposition during the period of intense subsidence of the geosyncline.

The schists are represented by chlorite, chlorite-calcite and actinolite-epidote varieties. Chlorite schist is most probably the regionally metamorphosed product of the geosynclinal pelitic and psammopelitic sediments, whereas the chlorite-calcite schists are either the products of some basic volcanic rocks or calc-pelitic sediments. The actinolite-epidote schists, however, belong to the albite-epidote hornfelses of the contact metamorphic facies. It is suggested that such schists were most probably developed along the sheared parts of the metavolcanic and associated pyroclastic rocks. Near the contact surfaces of granodiorite, the described schists may be facially changed to chlorite-biotite and chlorite-biotite-garnet varieties.

The metavolcanic rocks comprise keratophyre, quartz-keratophyre, spilite, spilitic diabase and diabase, that commonly occur as sheeted dykes and sill-like bodies, concordant with the schists, greywackes, lapilli tuffs (mainly spilitic), and banded lithic and crystal tuffs.

Application of the Al/3—K *versus* Al/3—Na diagrams aids in the petrochemical classification of the investigated rocks, and the designation of their magmatic differentiation or sedimentary degradation. The spilite of Wadi Kareim is similar to the average world spilite reported by VALLANCE [1960]. The keratophyre has an intermediate composition and is comparable to the aphanitic keratophyre of Schirmeck-type [JUTEAU and ROCCI, 1974]. The volcanic graywacke has a composition compa-

rable to the spilitic volcanics. Normal graywacke, however, has an intermediate composition between graywackes and shales. The chlorite schist also has a composition similar to shales. Again, the chlorite-calcite schists have a composition similar to tholeiitic dacites of the calc-alkaline series. Meanwhile, tuff has a different composition from normal volcanic and sedimentary rocks, but rather near to that of spilitic volcanics.

The Si/3—(Na + K + 2 Ca/3) *versus* K—(Na + Ca) diagram of the investigated group of rocks shows an evolution trend similar to the Schirmeck-type of preorogenic Hercynian volcanics denoting a magmatism of "folds" for the preorogenic Precambrian volcanics of Wadi Kareim, Central Eastern Desert, Egypt. Also, the FMA diagram of the studied rocks indicates a variation trend similar to the tholeiitic rock series. However, the Na—K—Ca diagram is rather comparable to the diagrams of the spilite-keratophyre rock association of the Lahn-Dill series, characteristic for a magmatism of "grabens". This discrepancy, may be partly due to the presence of abundant calcite veinlets in the studied group of rocks. However, the present authors feel that more petrochemical data concerning the Precambrian iron-bearing formation in the Eastern Desert are required to confirm the above suggested ideas concerning the paleographic and paleostructural conditions affecting the early geosynclinal volcanism.

## REFERENCES


ABDEL AZIZ, M. GH. [1968]: Geology of Wadi Kareim area, Eastern Desert. Ph. D. Thesis, Cairo Univ.

ABDEL NASSER, S., and AFIA, M. S. [1949]: Report on Wadi Kareim deposit. Unpublished report, Mineral Research Division, Mines Dept., Cairo.

AKAAD, M. K. [1959]: Geology of Wadi Kareim iron ore deposit, Eastern Desert. Bull. Sci and Tech., Assiut Univ.

ANDREW, G. [1939]: The greywackes of the Eastern Desert of Egypt. Bull. Inst. Egypt **71**.

BARTH, T. W. [1959]: Theoretical Petrology. Wiley and Sons, New York.

CHETVERIKOV, S. D. [1956]: Guide to Petrochemical Calculations for Chemical Analyses of Rocks and Determination of their Chemical Types (in Russian). Gosgeoltekhizdat, Moscow.

EL-SHAZLY, E. M. [1957]: Classification of the Egyptian mineral deposits. Egypt. Jour. Geol., **1**, No. 1.

EL-RAMLY, M. F. and AKAAD, M. K. [1960]: The basement complex in the central Eastern Desert of Egypt. Geol. Surv. Egypt. Paper No. **8**.

FIALA, F. [1967]: The chemism of the Algonkian and Eocambrian volcanites in the Železné Hory Mountains. In: "Geochemistry in Czechoslovakia", Transactions of the first Conference on Geochemistry, Ostrava, 1965 p. 15—29.

FRIED KRUPP ROHSTOFFE [1959]: Report on the iron occurrences of Quseir Region.

GINDY, A. R. [1957]: The succession and correlation of the pre-Nubian sandstone rocks around the phosphate mining district of Quseir, Red Sea Province, Egypt. Arab Sci. Congress, p. 529—610.

JUTEAU, TH. and ROCCI, G. [1974]: Vers une meilleure connaissance du problème des spilites a partir, de données nouvelles sur la cortége spilite-keratophyrique hercynotype. In: AMSTUTZ, G. C. (Ed.): Spilites and Spilitic Rocks. Inter. Union of Geol. Sci. Series A, No. **4**, Springer-Verlag Berlin, 253—329.

HILMY, M. E., KAMEL, O. A., and NIAZY, E. A. [1972]: Mineralogy of iron ore deposits of Wadi Kareim, Eastern Desert, A. R. Egypt. Proc. 6th. Arab Sci. Cong., Damascus, **4*B***, 685—716.

KAMEL, O. A., HILMY, M. E., and NIAZY, E. A. [1977]: Origin of Precambrian iron ore deposits from Wadi Kareim, Eastern Desert, Egypt. Bull. NRC, Egypt **2**, 401—413.

LA ROCHE H. DE [1966]: Sur l'usage du concept d'association minérale dan l'étude chimique des roches. C. R. Acad. Sci. (Paris), **262**, series D., 1665—1668.

LA ROCHE, H. DE, ROCCI, G. and JUTEAU, TH. [1974]: Essai de caracterisation chimique des associations spilitique. In: AMSTUTZ, G. G. (Ed.): Spilites and Spilitic Rocks. Inter. Union of Geol. Sci., Series A, No **4**, Springer Verlag, Berlin, p. 39—58.

NAKHLA, F. M. [1954]: Notes on the mineralography of some Egyptian ore minerals. Trans. Min. Petrol. Assoc. Egypt **9**, No. 3.
NIAZY, E. A. [1969]: Mineralogy of the iron ore deposits of Wadi Kareim and some other occurrences in the Eastern Desert, Egypt, U. A. R., M. Sc. Thesis, Ain Shams Univ.
NIGGLI, P. [1954]: Rocks and Mineral Deposits. Freeman, San Francisco.
NOCKOLDS, S. R. [1954]: Average chemical composition of some igneous rocks. Bull. Geol. Soc. America **65**, 1007—1032.
SHUKRI, N. M., EL SHAZLY, E. M., and SABET, A. H. [1959]: The iron ore deposit of Umm Ghamis El-Zarqa, Eastern Desert. Egypt. Jour. Geol., **III**, No. 2, 123—146.
SIGAEV, N. A. [1959]: Report on Wadi Kareim iron deposit. Unpublished report, Geol. Survey, Egypt.
TURNER, F. J. [1958]: Mineral assemblages of individual metamorphic facies, Mem. Geol. Soc. Amer.
TURNER, F. J. and VERHOOGEN, J. [1960]: Igneous and Metamorphic Petrology. Mc. Graw-Hill Book Company, New York.
VALLANCE, T. G. [1960]: Concerning spilites. Proc. Linnean Soc. N. S. Wales **IXXXV**, Part I. 8—52.
VALLANCE, T. G. [1965]: On the chemistry of pillow lavas and the origin of spilites. Mineralogical Magazine **34**, No. 268, 471—481.

*Manuscript received, 1 October. 1983*

E. A. NIAZY
National Research Centre, Cairo, Egypt

A. EL BAKRY and KAMEL, O. A.
El-Minia University, El-Minia, Egypt

*Acta Mineralogica-Petrographica, Szeged, XXVI/2, 207—220, 1984*

# PETROCHEMISTRY AND TECTONIC IMPLICATION OF THE UMM GHEIG FORMATION, EASTERN, DESERT, EGYPT

M. F. GHONEIM and M. A. EL-ANWAR


## SUMMARY

The Umm Gheig Formation belongs to the Abu Ziran Group of the Central Eastern Desert of Egypt. Rocks of this formation are originally derived from basalt, andesite and subordinate rhyolite. Although the formation includes two petrographic associations suffering different grades of metamorphism, however, they have close consanguineous magmatic relationship. It is suggested that these associations belonging to tholeiitic magma type which are tectonically emplaced as island arc.


## INTRODUCTION

Detailed geological mapping of the area around Wadi Umm Gheig, Eastern Desert of Egypt, reveal the occurrence of new separate formation pertaining to the Abu Ziran Group [AKAAD and NOWEIR, 1969]. This formation was named for the first time Umm Gheig Formation by EL-ANWAR [1983] after Wadi Umm Gheig where the best exposures of the formation occur around its main course.

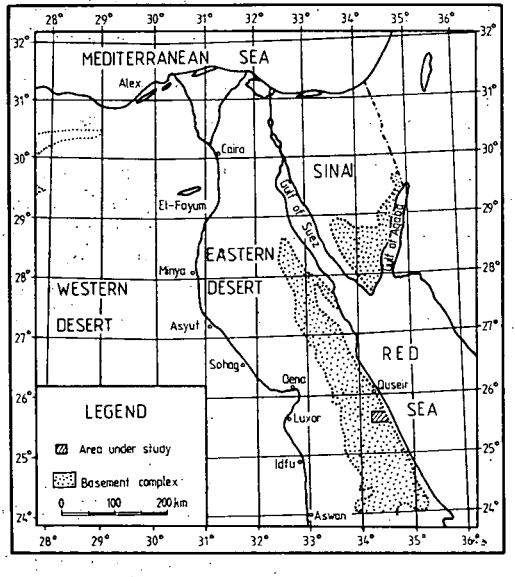


*Fig. 1.* Location map

The Umm Gheig Formation lies between latitudes 25° 35', 25°45' N and longitudes 34°15', 34°30' E *(Fig. 1)*. The dominant rocks of the present formation are volcanic flows and tuffs together with subordinate rocks made of tuffaceous sediments derived therefore. This association have undergone various degree o regional metamorphism including both the greenschist and epidote-amphibolite facies. Comparison of this association with the already established eight formations of the Abu Ziran Group [AKAAD and NOWEIR, 1980] reveal that the present association is different and unique. The detailed field, structure, petrography and metamorphism of this formation will be dealt with in a separate publication.

Few attempts has been carried out to elucidate the petrochemical characteristics of the metavolcanic rocks of Eastern Desert of Egypt e. g. NOWEIR and EL SHARKAWI [1978]. For the present rocks, the main objectives in this work are estimate the various petrochemical parameters and versus, define different petrographic varieties, elucidate the magma type and finally to determine their tectonic implication in light of plate tectonic framework.

## FIELD OCCURRENCE AND PETROGRAPHIC CHARACTERISTIC

The Umm Gheig Formation is separated and named by EL ANWAR [1983] as new formation belonging to Abu Ziran Group. SABET [1961] considers the present rocks as a part of the metasedimentery rock of the Egyptian basement. The formation appears as a part of the Geosynclinal Metasediments in the newly published map of Geological Survey of Egypt scale: 1:2.000,000 [1981].

The Umm Gheig Formation occupies a rather irregular and extensive outcrop, covering about 185 km$^2$ and trending NW—SE to NNW—SSE. The best outcrops is exposed around Wadi Umm Gheig after which the formation was named.

The extreme NE part of the belt is tectonically emplaced by serpentinites and intruded by metagabbros. The northern, northwestern, south western and southern parts of the Umm Gheig Formation are later intruded by members of the Younger Granites.

The present formation is unconformably overlain by the Igla Formation in the mid-eastern side and by Micoene-Pliocene-Quaternary Red Sea coastal strip from the east.

Petrographically the Umm Gheig Formation consists of an interbedded sequence of regionally metamorphosed volcanics and their equivalent tuffs together with subordinate tuffaceous sediments. This heterogeneous sequence can be classified into two distinct associations depending on the distribution of the different rock types and the degree of metamorphism. These associations are the Wizr greenschist association and the Kab Ahmed epidote — amphibolite association.

## PETROCHEMISTRY

Fifteen representative samples were selected from the belt of the Umm Gheig Formation for chemical analysis of major elements. The result are presented in Table 1.

Regarding the chemical composition of the present rocks, the cation mesonorm [WEDEPOHL, 1969] and the colour index were calculated and plotted on QAP diagram

TABLE 1

*Chemical analyses (wt%) for rocks of the Umm Gheig Formation, Eastern Desert, Egypt*

| | Greenschist Association | | | | | | | Epidote-Amphibolite Association | | | | | | | |
|---|---|---|---|---|---|---|---|---|---|---|---|---|---|---|---|
| | Metavolcanics | | | | | Metatuffs | | Schists & sub-schists | Amphibolite | | | | Metarhyolite | | |
| Sample no. | 1 | 4 | 213 | 701 | 750 | 443 | 7 | 18 | 284 | 90 | 226 | 253 | 17 | 719 | 741 |
| Petrographic name | Meta-andesite | Qz-H.B.-meta-andesite | Qz-biotite porphyritic meta-andesite | Metadolerite | Metabasalt with pyroxene relics | Coarse crystal metatuffs (andesitic) | Coarse crystal metatuffs (basaltic) | H.B. Qz subschist | Amphibolitic meta-andesite | Amphibolitic-metabasalt | | | Metarhyolite | | |
| $SiO_2$ | 58.89 | 55.07 | 60.00 | 46.43 | 48.11 | 59.70 | 50.46 | 57.66 | 61.23 | 45.11 | 58.07 | 47.11 | 67.75 | 66.50 | 66.53 |
| $TiO_2$ | 1.20 | 1.44 | 0.90 | 1.68 | 1.08 | 0.52 | 0.72 | 0.58 | 0.50 | 1.28 | 0.64 | 0.84 | 0.26 | 0.18 | 0.24 |
| $Al_2O_3$ | 16.15 | 15.83 | 15.99 | 17.19 | 16.77 | 15.73 | 15.89 | 16.51 | 17.29 | 16.87 | 15.89 | 17.08 | 15.37 | 14.59 | 14.48 |
| $Fe_2O_3$ | 3.13 | 4.29 | 3.07 | 2.43 | 1.23 | 4.04 | 4.67 | 1.58 | 3.23 | 5.16 | 3.87 | 3.61 | 1.18 | 1.16 | 0.91 |
| FeO | 4.86 | 5.03 | 5.16 | 9.28 | 10.68 | 3.78 | 7.78 | 3.65 | 3.57 | 8.62 | 6.00 | 7.14 | 2.47 | 4.35 | 6.27 |
| MnO | 0.14 | 0.15 | 0.12 | 0.20 | 0.22 | 0.08 | 0.24 | 0.14 | 0.12 | 0.24 | 0.16 | 0.19 | 0.07 | 0.06 | 0.06 |
| MgO | 2.76 | 4.18 | 2.18 | 7.49 | 7.14 | 2.44 | 3.31 | 5.44 | 2.68 | 7.70 | 2.18 | 7.75 | 1.51 | 1.41 | 1.54 |
| CaO | 5.57 | 5.86 | 5.21 | 10.30 | 10.06 | 4.79 | 8.27 | 7.03 | 5.86 | 10.67 | 5.45 | 9.38 | 4.69 | 3.53 | 3.47 |
| $Na_2O$ | 3.37 | 3.57 | 3.71 | — | 1.35 | 5.39 | 3.10 | 5.05 | 3.67 | 2.09 | 3.57 | 2.56 | 3.84 | 2.70 | 2.70 |
| $K_2O$ | 1.38 | 1.56 | 1.81 | 2.41 | 1.81 | — | 0.12 | 0.24 | 1.20 | 0.36 | 1.08 | 1.38 | 1.20 | 2.11 | 2.11 |
| $H_2O^+$ | 2.10 | 2.44 | 1.36 | 2.48 | 1.01 | 2.93 | 3.46 | 0.87 | 0.54 | 1.44 | 1.46 | 2.47 | 0.98 | 1.39 | 0.83 |
| $H_2O^-$ | 0.19 | 0.20 | 0.21 | 0.16 | 0.27 | 0.11 | 0.16 | 0.12 | 0.06 | 0.12 | 0.13 | 0.15 | 0.10 | 0.16 | 0.18 |
| $P_2O_5$ | 0.285 | 0.122 | — | — | — | — | 0.045 | 0.102 | 0.089 | 0.004 | 0.126 | 0.078 | 0.054 | — | — |
| Total | 100.02 | 99.77 | 99.72 | 100.05 | 99.73 | 99.51 | 98.23 | 98.97 | 100.04 | 99.66 | 98.63 | 99.74 | 99.51 | 98.14 | 99.32 |

TABLE 2

*Mesonorm and geochemical parameters for rocks of the Umm Gheig Formation, Eastern Desert, Egypt*

| | | | | | | | | | | | | | | | |
|---|---|---|---|---|---|---|---|---|---|---|---|---|---|---|---|
| Q | 21.13 | 14.36 | 14.82 | 11.87 | 9.95 | 15.39 | 13.46 | 11.54 | 20.89 | 4.99 | 19.03 | 6.77 | 26.56 | 29.3 | 27.27 |
| Ab | 31.4 | 33.25 | 34.35 | — | 12.45 | 50.1 | 30.05 | 45.35 | 33.35 | 19.3 | 33.6 | 23.55 | 35.3 | 25.6 | 25.2 |
| An | 22.4 | 22.55 | 21.2 | 35.75 | 23.0 | 16.0 | 21.45 | 11.05 | 26.85 | 23.1 | 25.2 | 19.35 | 20.75 | 17.85 | 17.1 |
| Or | — | — | 11.0 | — | — | — | — | — | — | — | — | — | 7.25 | 13.2 | 13.0 |
| Bi | 13.52 | 15.36 | — | 23.92 | 17.9 | — | 1.2 | 2.32 | 11.52 | 3.52 | 10.72 | 13.44 | — | — | — |
| HO | — | 2.04 | 2.7 | 14.1 | 29.34 | 8.16 | 23.82 | 25.5 | — | 32.04 | — | 29.94 | 2.16 | — | — |
| Hyp | 3.58 | 4.42 | 10.68 | 8.04 | 4.04 | 4.86 | 3.02 | 1.18 | 2.42 | 8.48 | 5.48 | 1.12 | 6.04 | 10.48 | 13.98 |
| Di | — | — | — | — | — | — | — | — | — | — | — | — | — | — | — |
| Ap | 0.62 | 0.25 | — | — | — | — | 0.11 | 0.21 | 0.24 | 0.008 | 0.27 | 0.16 | 0.11 | | |
| Sph | 2.61 | 3.12 | 1.95 | 3.66 | 2.31 | 1.11 | 1.62 | 1.2 | 1.05 | 2.76 | 1.41 | 1.8 | 0.57 | 0.39 | 0.51 |
| Mt | 3.39 | 4.65 | 3.3 | 2.66 | 1.32 | 4.37 | 5.27 | 1.65 | 3.42 | 5.65 | 4.23 | 3.87 | 1.26 | 1.28 | 0.99 |
| Cor | 1.35 | — | — | — | — | — | — | — | 0.26 | — | 0.05 | — | — | 1.9 | 1.96 |
| Hem | — | — | — | — | — | — | — | — | — | — | — | — | — | — | — |
| C.I. | 25.07 | 29.84 | 18.65 | 52.38 | 54.61 | 18.5 | 35.04 | 32.04 | 18.91 | 52.35 | 22.1 | 50.33 | 10.14 | 14.05 | 17.44 |
| Total | 100.00 | 100.00 | 100.00 | 100.00 | 100.01 | 99.99 | 100.00 | 100.00 | 100.00 | 99.95 | 100.00 | 100.00 | 100.00 | 100.00 | 100.00 |
| si | 194.58 | 162.70 | 201.96 | 100.88 | 109.78 | 202.31 | 138.48 | 165.74 | 202.17 | 97.67 | 189.34 | 107.31 | 284.46 | 289.31 | 271.95 |
| al | 31.39 | 27.51 | 31.66 | 23.17 | 22.51 | 31.36 | 25.65 | 27.92 | 33.58 | 21.49 | 30.51 | 22.89 | 37.96 | 37.34 | 34.82 |
| fm | 35.21 | 40.79 | 33.57 | 48.02 | 47.28 | 33.57 | 41.59 | 35.94 | 31.43 | 49.38 | 36.91 | 46.57 | 22.12 | 28.98 | 33.80 |
| c | 19.72 | 18.55 | 18.79 | 25.28 | 24.60 | 17.39 | 24.32 | 21.65 | 20.73 | 24.75 | 19.06 | 22.89 | 21.10 | 16.46 | 15.20 |
| alk | 13.69 | 13.15 | 15.98 | 3.52 | 5.62 | 17.68 | 8.44 | 14.49 | 10.26 | 4.38 | 13.53 | 7.65 | 18.82 | 17.23 | 16.19 |
| k | 0.21 | 0.22 | 0.24 | 1 | 0.47 | — | 0.02 | 0.03 | 0.18 | 0.11 | 0.17 | 0.26 | 0.17 | 0.34 | 0.34 |
| mg | 0.39 | 0.45 | 0.33 | 0.54 | 0.52 | 0.37 | 0.33 | 0.65 | 0.42 | 0.51 | 0.29 | 0.57 | 0.43 | 0.32 | 0.28 |
| qz | 39.82 | 10.1 | 38.04 | −13.2 | −12.7 | 31.59 | 4.72 | 7.78 | 45.13 | −19.85 | 35.22 | −23.29 | 109.18 | 120.39 | 107.19 |
| ti | 2.97 | 3.19 | 2.27 | 2.89 | 1.85 | 1.32 | 1.48 | 1.25 | 1.24 | 2.08 | 1.57 | 1.44 | 0.82 | 0.59 | 0.74 |
| p | 0.40 | 0.15 | — | — | — | — | 0.05 | 0.12 | 0.12 | 0.003 | 0.17 | 0.08 | 0.095 | | |
| Rittmann's Suite I. | 1.42 | 2.18 | 1.79 | 1.69 | 1.95 | 1.74 | 1.39 | 1.91 | 1.30 | 2.84 | 1.43 | 3.78 | 1.03 | 0.98 | 0.98 |
| W. Alkalinity Ratio | 1.90 | 1.98 | 2.08 | 1.19 | 1.27 | 3.21 | 1.69 | 2.50 | 1.93 | 1.20 | 2.01 | 1.35 | 2.24 | 1.85 | 1.86 |
| Larsen's D.I. | 10.86 | 7.51 | 12.86 | −3.61 | −2.99 | 10.67 | 3.15 | 3.56 | 10.94 | −7.17 | 11.31 | −4 | 15.97 | 18.57 | 18.8 |
| Thornton & Tuttle's D. I. | 52.53 | 47.61 | 60.17 | 11.87 | 22.4 | 65.49 | 43.51 | 56.89 | 54.24 | 24.29 | 52.63 | 30.32 | 69.11 | 68.1 | 65,47 |
| FeO/MgO | 2.78 | 2.13 | 3.63 | 1.53 | 1.65 | 3.04 | 3.62 | 0.39 | 2.42 | 1.72 | 4.35 | 1.34 | 2.34 | 3.82 | 4.60 |
| $F_2$ | −1.32 | −1.319 | −1.292 | −1.24 | −1.36 | −1.47 | −1.39 | −1.555 | −1.367 | −1.47 | −1.323 | −1.39 | −1.357 | −1.207 | −1.23 |
| $F_3$ | −2.422 | −2.406 | −2.43 | −2.297 | −2.336 | −2.442 | −2.268 | −2.56 | −2.492 | −2.319 | −2.348 | −2.373 | −2.499 | −2.369 | −2.375 |

of STRECKEISEN [1967] *(Fig. 2)*. The plots reveal that the rocks of the Umm Gheig Formation compositionaly have three main petrographic equivalents:

*a)* Basalt and andesite (Field 10)
*b)* Qz-andesite (Field 5)
*c)* Rhyolite (Field 3a).

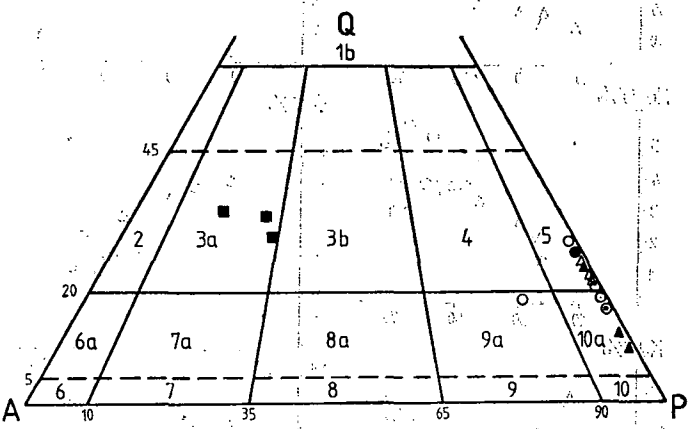


*Fig. 2.* Distribution of the rocks of Umm Gheig Formation in the QAP diagram [STRECKEISEN, 1967].

| *Wizr Greenschist Association* | | *Kab Ahmed Amphibolite Association* | |
|---|---|---|---|
| Metadolerit and metabasalt | Δ | Amphibolite (basaltic) | ▲ |
| Metaandesite | o | Amphibolite (andesitic) | ● |
| Metatuffs (basaltic) | Δ | Subschist (andesitic) | ⊙ |
| Metatuffs (andesitic) | ⊙ | Metarhyolite | ■ |

For delimination between basalt and andesite, STRECKEISEN (op. cit. p. 182) has suggested a delimitation by colour index at M=40 as limit. BARTH [1931] has given preference to colour index at the limit M=35 (see Table 2).

The characteristics of the distribution of the major oxides in the rocks of the Umm Gheig Formation can be investigated by variation diagrams. On plotting the chemical analysis of the major oxides *versus* Thornton and Tuttle's D.I. *(Fig. 3)* several characteristics can be denoted.

*a)* Plots for $SiO_2$, $Na_2O$, FeO*, CaO and MgO with D.I. shown linear trends *(Fig. 3, a, b, d, e, f)*.

*b)* Plots for $SiO_2$ and $Na_2O$ are well positively correlated with D.I. *(Fig. 3, a, b)*.

*c)* Plots of CaO, MgO and FeO are negatively correlated with D.I. *(Fig. 3, e, f, d)*.

*d)* Plots belong to the amphibolitic samples (amphibolite of basic and intermediate origin, Nos. 90, 253) confirm well to the smooth descending trend *(Fig. 3, a, b, d, e* and *f)*.

*e)* Potash is weakly positively correlated with D.I. *(Fig. 3c)*.

Denotion *a, b* and *c* nicely reveal close consanguineous magmatic relationship for the present rocks. Denotion *d* confirms the ortho-origin of the present amphibolites. Denotion *e* donates partial migration or addition of potash for some samples during processes of alteration and metamorphism.

Larsen's variation diagram of the studied rocks is shown in *Fig. 4*. The percentage frequency of the individual elements are plotted on ordinate *versus* the corresponding

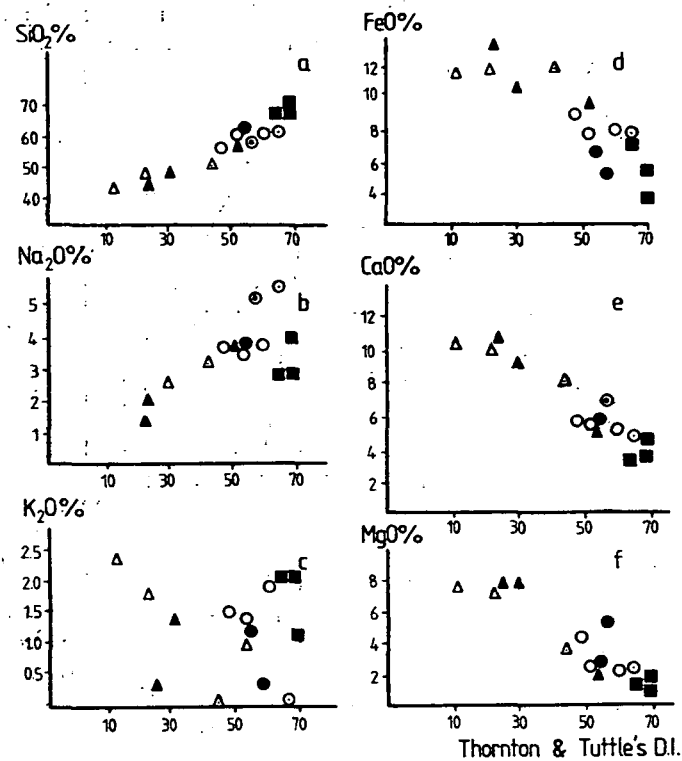


*Fig. 3.* Variation diagrams of major oxides *vs* differentiation index (D.I.) according to THORNTON and TUTTLE [1960] for samples from Umm Gheig Formation. Symbols as in *Fig. 2.*

"differentiation index, D.I." on the abscissa (D.I.$=(\frac{1}{3}$ Si$+$K$)-$(Ca$+$Mg). The figure indicate typical continuous magmatic trend of the present rocks, i. e., with proceeding the magmatic differentiation Si and Na regularly increase whereas Mg and Ca linearly decrease. Out of these regular trends potash is exceptionally varied that is attributed to either later potash metasomatism and/or migration of K during regional metamorphism.

*Fig. 5.* Alkalies — silica variation diagram for rocks of the Umm Gheig Formation. The broken line means the boundary between alkalic and tholeiitic basalts in Hawai [MCDONALD and KATSURU 1964], the solid line gives the boundary between alkalic and non-alkalic volcanic rocks in Japan Kuno, 1966].
1. Oceanic tholeiitic basalt, 2. continental tholeiitic basalt, 3. oceanic alkalic basalt, 4. continental alkalic basalt (1—4 according to LOESCHKE, 1976), 5. island arc tholeiitic basalt, 6. island arc tholeiitic andesite, 7. island arc tholeiitic dacite (5—7 according to JAKES and WHITE, 1972). Symbols as in *Fig. 2.*

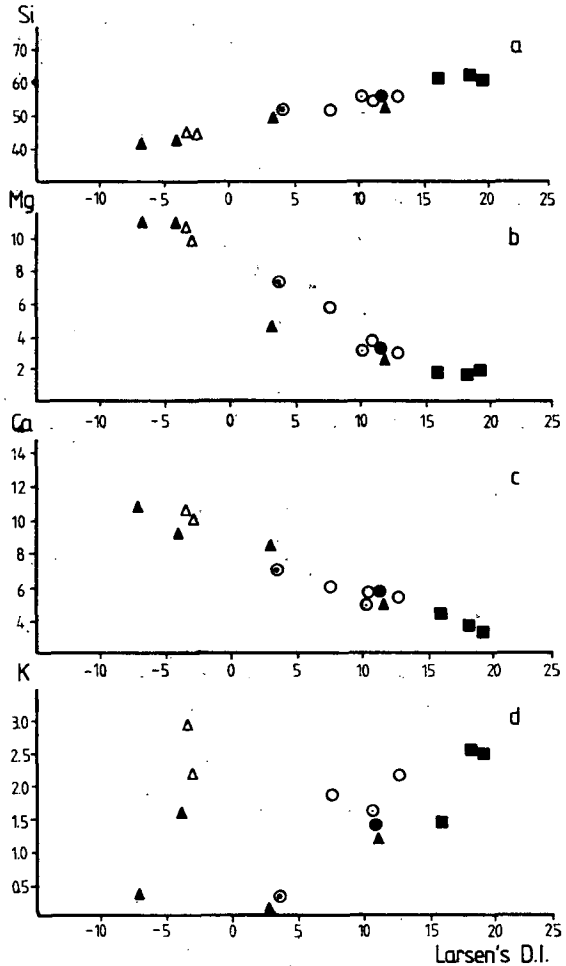


*Fig. 4.* Variation diagrams of Si, Mg, Ca and K per cent *vs* differentiation index (D.I.) according to LARSEN for samples from Umm Gheig Formation indicating co-magmatic differentiation. Symbols as in *Fig. 2.*

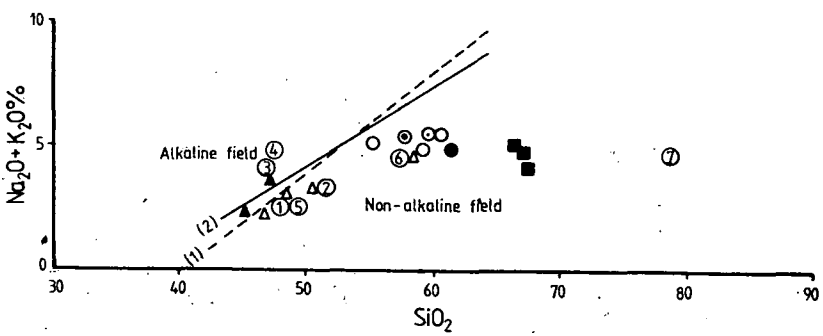

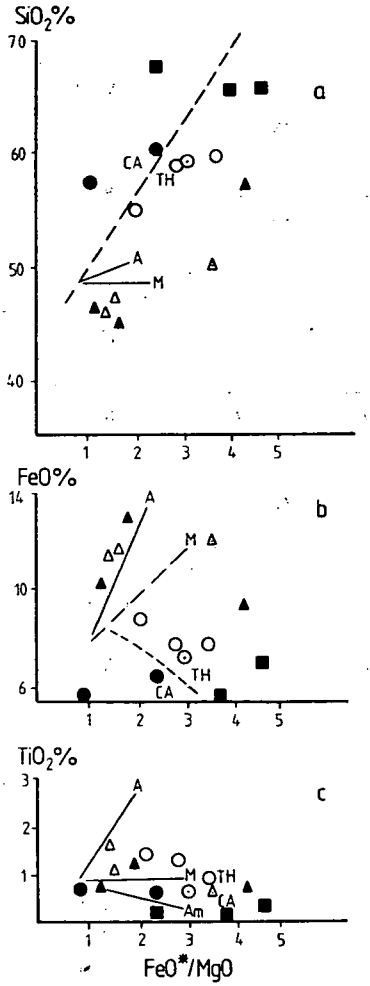


*Fig. 6.* Variation diagrams of $TiO_2$, FeO, $SiO_2$ *vs* FeO*/MgO for rocks of the Umm Gheig Formation. FeO* means the total iron as FeO. The field boundaries separate the tholeiitic (TH) and calc-alkaline (CA), and the trend lines for abyssal tholeiites (A), Macauley Island arc tholeiite series (M) and the Amagi calc-alkaline series (AM) after MIYASHIRO [1975b). Symbols as in *Fig. 2.*

*Non-alkalic volcanic trend of the Umm Gheig Formation:*

Plotting the present analyses on the alkali-silica variation diagram *(Fig. 5)* reveals that all the volcanic rocks under consideration (with one exception) fall within the non-alkalic field (the field of tholeiite according to IRVINE and BARAGER, 1971). The exceptional sample plot just above the dividing line, which is most probably due to the low silica and high potash content of that sample (see *Fig. 3c* and *4d).*

The non-alkalic affinity of the present rocks is simillar to affinites for most of the metavolcanic rocks of the Central Eastern Desert [NOWEIR and EL SHARKAWI, 1978, and TAKLA and SHENOUDA, 1981].

*Predominance of tholeiite magma type in Umm Gheig Formation:*

MIYASHIRO [1975 *a, b)* has classified the volcanic rock series of the Earth into alkalic and non-alkalic groups. The latter may be subdivided into tholeiitic (TH) and calc-alkalic (CA) series. FeO*/MgO *versus* $SiO_2$, FeO*/MgO *versus* FeO* and FeO*/MgO *versus* $TiO_2$ diagrams were proposed by MIYASHIRO [1973] to distinguish between tholeiitic and calc-alkaline volcanic series. The above mentioned diagrams are widely used for fresh as well as metamorphosed volcanic rocks, e.g. GALE, [1975], FURNES *et al.*, [1976].

Plotting the chemical data of the Umm Gheig Formation on Miyashiro's diagram *(Fig. 6)* indicate that almost all plots lie within the tholeiitic field.

IRVINE and BARAGER [1971] have demonstrated the usefulness of triangular diagram with Mg, FeO* and $Na_2O+K_2O$ at the corners (AFM) to discriminate the tholeiitic and calc-alkalic volcanic rocks. The present data are presented on (AFM) diagram *(Fig. 7)*, they firmly indicate that most of rocks of the Umm Gheig Formation were the product of originally tholeiitic volcanic rock.

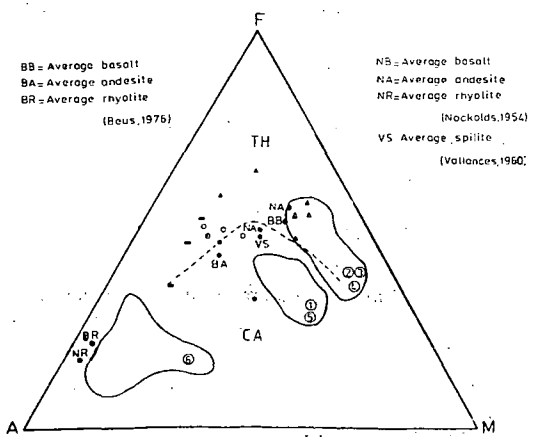


*Fig. 7.* Rocks of the Umm Gheig Formation plotted on AFM variation diagram ($A=Na_2O+K_2O$, F = FeO (total Fe), M = MgO. The field boundary separating the tholeiitic (TH) and calc-alkaline composition is after IRVINE and BARAGAR [1971]. Compositional fields (1—6) are after NOWEIR and EL-SHARKAWI [1978]:

1. Eraddia Formation A
2. Um Seleimat Formation
3. Sukkari Formation
4. Muweilih Formation
5. Eraddia Formation B
6. Atalla Formation

Symbols as in *Fig. 2.*

*Petrochemical correlation with other metavolcanic rocks of North Central Eastern Desert of Egypt:*

By using AFM and FeO—$Fe_2O_3$—$TiO_2$ ternary diagrams constructed by NOWEIR and EL SHARKAWI [1978] for differentiation between the metavolcanic rocks of North Central Eastern Desert of Egypt, the present rocks overlap the fields of the Um Seleimat Formation, the Sukkari Formation the Muweilih Formation and part of the Eraddia Formation field, *(Fig. 7, 8)*.

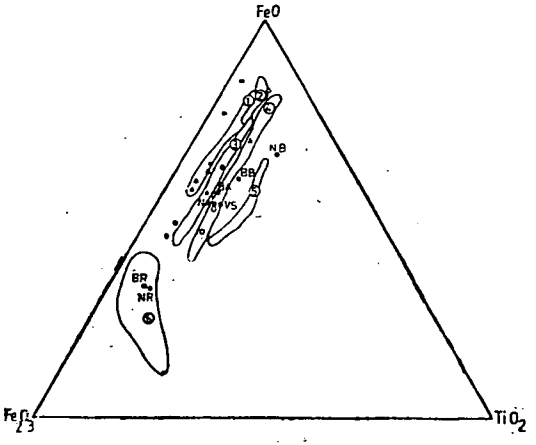


*Fig. 8.* FeO—$Fe_2O_3$—$TiO_2$ ternary diagram showing field of location of the Umm Gheig Formation with respect to published metavolcanic formation of Eastern Desert, Egypt. Symbols as in *Figs. 2* and *7*.

*Tectonic implication of the Umm Gheig Formation:*

It is clear that there is a close relationship between different types of volcanic rocks and their tectonic setting. After the establishment of tholeiitic volcanic trend for the rocks of the Umm Gheig Formation it is neccessary to find out the possible original tectonic environment on the light of plate tectonic theory.

Unfortunately, tholeiitic magma exist in large quantities in island arc sequences, but they also occur in oceanic rift environment (abyssal tholeiities) and as continental floor basalt [JAKES and GILL, 1970 and MIYASHIRO, 1974].

Throughout the literature survey, the geochemical methods are the most effective in discriminating different tectonic setting of volcanic rocks. Applications of these methods for rocks of the Um Gheigh Formation might help in deducing the past-tectonic environment prevailing during their eruption.

The preliminary impression about the tectonic implication of the present rocks is taken from alkali-silica variation diagram *(Fig. 5)*. In this diagram the present rocks appear much more similar to tholeiitic rocks developed in island arcs [JAKES and WHITE 1972] than any other tholeiitic type of different tectonic setting.

FLOYD and WINCHESTER [1978] and other, have demonstrated that $TiO_2$ is one of the immobile elements during post-consolidation alteration processes (e.g. spilitic alteration, metamorphism) that is significantly used in constructed diagrams for the identification of ancient volcanic suite and comparing them with the recent volcanics. MIYASHIRO [1975*a*] indicates that the abyssal tholeiites show a higher rate of increasing of $TiO_2$ with increasing FeO*/MgO than do island arc tholeiitic rocks. *Fig. 9* represents the composition fields of abyssal tholeiites and island arc volcanic rocks constracted by MIYASHIRO (op. cit). This figure confirms the island arc tectonic setting for rocks of the Umm Gheig Formation, since all present plots are completly enclosed within the field of island arc volcanic rocks.

MIYASHIRO [1975*b*], used the $Na_2O/K_2O$ *versus* $Na_2O+K_2O$ diagram for old metamorphosed rocks (e.g. Franciscan terrane) in order to clarify both alkali

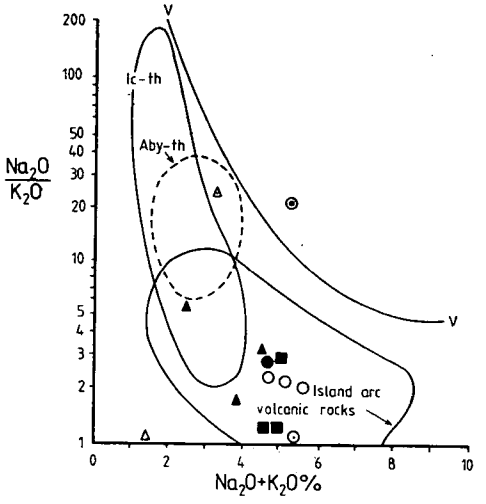


*Fig. 9.* $Na_2O/K_2O$ *vs* $Na_2O+K_2O$ diagram for rocks of Umm Gheig Formation. V——V curve represents the upper limit for all fresh volcanic rocks, Ic-th means the field of Icelandic tholeiites, and Aby-th that of the abyssal tholeiites after MIYASHIRO [1975*b*]. Symbols as in *Fig. 2.*

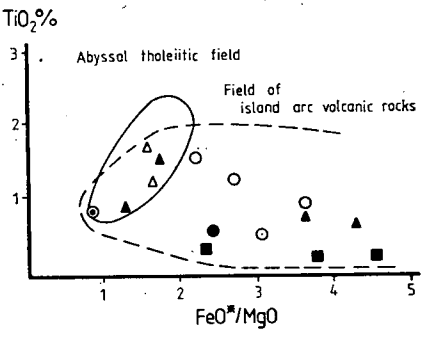


*Fig. 10.* Composition field of abyssal tholeiites and island arc tholeiites in diagram of $TiO_2$ *vs* FeO/MgO after MIYASHIRO [1975*a*]. Symbols as in *Fig. 2.*

migration during metamorphism and past-tectonic environments for these rocks. Using the above diagram *(Fig. 10)* it shows that rocks of the Umm Gheig Formation lies below the V—V indicating little migration of alkalies during metamorphism. It also shows that the present rocks behave similar to the island arc volcanic rocks of the Franciscan terrane.

PEARCE [1976] compiled large number of major element oxides analyses for the basaltic rocks from different tectonic settings. By using discriminant function it was possible to represent visually the separation of six tectonically defined magma, (OFB) ocean-floor basalts, (LKT) island arc tholeiites, (CAB) calc-alkalic basalt, (SHO) shoshonites, (OIB) ocean island basalt, and (CON) continental basalt.

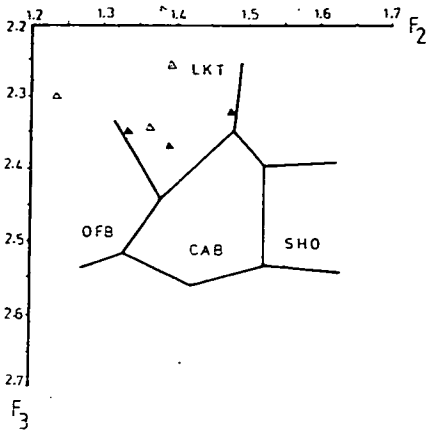


*Fig. 11.* Plot of discrimination functions $F_2$—$F_3$ [PEARCE, 1976] for rock varieties of the Umm Gheig Formation.
LKT = island arc tholeiites
OFB = ocean-floor basalt
CAB = calc-alkaline basalt
SHO = shoshonites.
Symbols as in *Fig. 2.*

Application of the Pearce's numerical method to lavas of unknown tectonic setting of the Archean metabasalts gives the mostly geological consistant results.

The chemical analysis for rocks of the Umm Gheig Formation are treated on the basis of Pearce's discrimination method where $F_2$ and $F_3$ were calculated (Table 2). Rock varieties have basaltic and quartz-basalt original composition are plotted well inside island arc tholeiitic field (LKT) *(Fig. 11)*.

Generally, the mechanism of continental growth [HAMILTON, 1970], has contributed the addition of primary, but relatively highly fractional sialic material in the form of andesite basalt volcanism in island arcs.

Finally, on the basis of major element pattern, it is here highly suggested that the present tholeiitic volcanic rocks of the Umm Gheig Formation was formed in island arc environment.

## CONCLUSIONS

The Umm Gheig Formation was formerly described as a new and unique metavolcanic formation belonging to the Abu Ziran Group of the Central Eastern Desert of Egypt [EL-ANWAR, 1983]. It constitutes a heterogeneous sequence of volcanic flows and tuffs together with subordinate amounts of tuffaceous sediments.

Based on the petrography, structure setting and regional metamorphism, the Umm Gheig Formation was subdivided into two distinct associations namely the Wizr greenschist association and the Kab Ahmed epidote-amphibolite association.

Interpretation of chemical data of different rock types included in both associations of the Umm Gheig Formation revealed the following conclusions:

1) Rocks of the Umm Gheig Formation were originally derived from basalt, andesite, quartz andesite with subordinate rhyolite (the latter is restricted to the Kab Ahmed epidote-amphibolite association).

2) Variation diagrams between major oxides and differentiation indices indicate a close consanguineous magmatic relationship of both associations of the Umm Gheig Formation including the amphibolite rock varieties.

3) Variation diagrams of alkali-silica, $FeO^*/MgO+FeO^*$ *versus* $FeO^*$, $SiO_2$ and $TiO_2$ as well as AFM diagram indicate that these rocks are likely to be originated as a product of tholeiitic magma type.

4) Rocks of the Umm Gheig Formation are clustered within the field composition belonging to the Umm Seleimat Formation, the Sukkari Formation, the Muweilih Formation and part of the Eraddi Formation on AFM and $FeO$—$Fe_2O_3$—$TiO_2$ diagrams which were used for separation different metavolcanic rocks of the Central Eastern Desert of Egypt.

5) Plotting the data with the newly published diagrams discriminating different tectonic settings, particularly volcanic rocks occur in orogenic belt similar to the present rocks, it is highly favoured that the Umm Gheig Formation implicated in island arc past tectonic environment.


## ACKNOWLEDGEMENT

The authors thanks PROF. M. K. AKAAD and PROF. A. M. NOWEIR, Tanta University for assistance in the revision of the manuscript and valuable discussions.


## REFERENCES


AKAAD, M. K. and NOWEIR, A. M. [1969]: Lithostratigraphy of the Hammamat-Umm Seleimat District, Eastern Desert, Egypt. Nature **223**, No. 5203, 284—285.

AKAAD, M. K. and NOWEIR, A. M. [1980]: Geology and Lithostratigraphy of the Arabian Desert Orogenic Belt between Latitudes 25°35' and 26°30'. Symp. on "Evolution and mineralization of Arabian-Nubian shield" Inst. Appl. Geol. (Jeddah). Bull., **3**, 4, 127—135.

BARTH, T. F. W. [1931]: Mineralogical petrography of Pacific lavas. Amer. J. Sci., **21**, 377—305 and 491—530.

BEUS, A. A. [1976]: Geochemistry of the Lithosphere. Mir Publishing Hous. Moscov.

EL-ANWAR, M. A. [1983]: Geology of the area around Wadi Umm Gheig, Eastern Desert, Egypt. M. Sc. Thesis. Tanta University. Under preparation.

FLYOD, P. A. and WINCHESTER, J. A. [1978]: Identification and discrimination of altered and metamorphosed volcanic rocks using immobile elements. Chem. Geol., **21**, 291—306.

FURNES, H., SKJERLIE, F. J. and TYSSELAND, M. [1978]: Plate tectonic model based on greenstone geochemistry in the late Precambrian — Lower Palaeozoic sequence in the Solund-Slavfjorden area, west Norway. Norsk Geol. Tidsskrift **56**, 161—186.

GALE, G. H. [1975]: Ocean floor-type basalts from the Grimeli Formation. Stavenes Group Sunnfjord. Norges. Geol. Unders., **319**, 47—58.

GEOLOGICAL SURVEY OF EGYPT [1981]: Geological map of Egypt. Scale 1:2.000.000.

HAMILTON, W. [1970]: Mesozoic California and the underflow of Pacific mantle. Geol. Soc. America Bull., **80**, 2409—2430.

IRVINE, T. N. and BARAGAR, W. R. A. [1971]: A guide to the chemical classification of the common volcanic rocks. Can. J. Earth Sci., **8**, 523—548.

JAKES, P. and GILL, J. [1970]: Rare earth elements and the island arc tholeiitic series. Earth Planet. Sci. Letters **9**, 17—28.

JAKES, P. and WHITE, A. J. R. [1972]: Major and trace element abundance in volcanic rocks of orogenic areas. Geol. Soc. Amer. Bull., **83**, 29—40.

KUNO, H. [1966]: Lateral variation of basalt magma type across continental margins and island arcs. Bull. Volcanol., **29**, 195—222.

LOESCHKE, J. [1976]: Petrochemistry of eugeosynclinal magmatic rocks of the area around Trondheim (Central Norwegian Caledonides), N. Jb. Miner. Abh., **128**, 41—74.

MACDONALD, G. and KATSURU, T. [1964]: Chemical composition of Hawaiian lavas. J. Petrol., **5**, 82—113.

MIYASHIRO, A. [1973]: The Troodos ophiolitic complex was probably formed in an island arc Earth Planet. Sci. Lett., **19**, 218—224.

MIYASHIRO, A. [1974]: Volcanic rock series in island arcs and active continental margins. Am. J. Sci. **274**, 321—355.
MIYASHIRO, A. [1975a]: Volcanic rock series and tectonic setting. Annual Rev. Earth Planet. Sci., **3**, 251—269.
MIYASHIRO, A. [1975b]: Classification, characteristics and origin of ophiolites. J. Geol., **83**, 249—281.
NOCKOLDS, S. R. [1954]: Average chemical composition of some igneous rocks. Geol Soc. Amer. Bull., **65**, 1007—1032.
NOWEIR, A. M. and EL-SHARKAWI, M. A. [1978]: Geochemical characteristics of the metavolcanic formations of the North Central Eastern Desert, Egypt. Bull. Fac. Sci. Cairo. Univ. (accepted for publication).
PEARCE, J. A. [1976]: Statistical analysis of major elements patterns in basalts. J. Petrology **17**, Part 1, 15—83.
SABET, A. H. [1961]: Geology and mineral deposits of Gabel El-Sibai area. Red Sea Hills, Egypt. Ph. D. Thesis, Leiden State University, The Netherlands
STRECKEISEN, A. L. [1967]: Classification and nomenclature of igneous rocks. N. Jb. Min. Abh., **107**, 144—214.
TAKA, M. A. and SHENOUDA, H. H. [1981]: Determination of magma type for some Egyptian ortho-amphibolite. Egyptian Acad. Sciences (under publication).
THORNTON, C. P. and TUTTLE, O. F. [1960]: Chemistry of igneous rocks I. Differentiation index. Amer. J. Sci., **258**, 664—684.
VALLANCES, T. G. [1960]: Concerning spilites. Proc. Linn. Soc. N. S. Wales **LXXXV**, 8—52.
WEDEPOHL, K. H. [1969]: Handbook of geochemistry. Vol. 1, Springer-Verlag, New York, 442 p.

*Manuscript received, 1 July, 1983*

M. F. GHONEIM and M. A. EL-ANWAR
Dept. of Geology, Faculty of Science
Tanta University

*Acta Mineralogica-Petrographica, Szeged, XXVI/2, 221—233, 1984*

# LATE PRECAMBRIAN VOLCANISM IN GABAL ABU HAD, EASTERN DESERT — EGYPT: EVIDENCE FOR AN ISLAND—ARC ENVIRONMENT

MOHAMED A. HEIKAL and ABDEL-AAL M. AHMED

ABSTRACT

Gabal Abu Had represents one of the widely distributed localities of the Late Precambrian Dokhan Volcanics in Egypt. The Abu Had volcanics are characterized by predominance of pyroclastics similar in that character to modern volcanic arcs. Chemically, they belong to the calc-alkaline series which characterize volcanism in island-arcs and continental margins. An island-arc environment is suggested for the Dokhan volcanics of Gebel Abu Had based on major and immobile trace elements.

## INTRODUCTION

The basement complex of Egypt covers an area of about 100.000 square kilometres among which the Dokhan volcanics occupy limited areas attaining about 10% of the basement outcrop [STERN, 1979]. The Dokhan Volcanics are best developed north of Latitude 26° in the Eastern Desert, particularly at Gabal Dokhan, from which they acquired their name *(Fig. 1)*. The Dokhan Volcanics represent the oldest unmetamorphosed volcanics in Egypt and are considered of Late Precambrian in age [EL SHAZLY *et al.*, 1973; STERN, 1979].

Gabal Abu Had represents one of the widely distributed localities of the Dokhan Volcanics in the Eastern Desert of Egypt where they form a greyish-black belt that extends in a NE—SW direction *(Fig. 1)*. The Abu Had volcanics frequently occurs in the form of successive sheets, mainly represented by lavas and pyroclastics with the latter as the most dominant varieties. The bulk composition of the lavas is mainly andesitic comprising augite — and quartz-bearing varieties. Rhyodacites are uncommonly observed. The pyroclastics are made up of dacitic and andesitic ashfall tuffs of relatively thick units. Ignimbritic rhyolites are recorded among the Abu Had rock association.

In the present study, field and geochemical features are used in an attempt to identify the tectonic environment in which Abu Had volcanics were formed. Field criteria are largerly based on those given by GARCIA [1978]. Chemical discrimination parameters proposed by recent workers are also applied, using major elements as well as immobile trace elements (Table 1) of the studied volcanics. *Fig. 2* shows the chemical identification of Abu Had volcanics according to their silica and alkali contents [MIDDLEMOST, 1980].

## FIELD EVIDENCES

Continental and island arc volcanoes, particularly those in orogenic belts, are normally much more explosive than oceanic volcanoes [RITTMANN, 1962; RITTMANN and RITTMANN, 1976]. According to WILLIAMS and MCBIRNEY [1979] the continental

TABLE 1

*Chemical analyses of Abu Had Volcanics*

| % | 1* | 2 | 3 | 4 | 5 | 6 | 7 | 8 | 9 | 10 | 11 | 12 | 13 | 14 | 15 | 16 | 17 | 18 | 19 |
|---|---|---|---|---|---|---|---|---|---|---|---|---|---|---|---|---|---|---|---|
| $SiO_2$ | 69.54 | 63.82 | 63.03 | 58.78 | 58.40 | 58.19 | 57.91 | 57.73 | 57.61 | 57.60 | 57.58 | 72.24 | 66.43 | 64.84 | 63.15 | 62.38 | 61.98 | 60.79 | 59.21 |
| $TiO_2$ | 0.30 | 0.52 | 0.34 | 0.33 | 0.92 | 0.64 | 0.68 | 0.62 | 0.32 | 0.52 | 0.60 | 0.27 | 0.60 | 0.26 | 0.52 | 0.26 | 0.20 | 0.80 | 0.26 |
| $Al_2O_3$ | 14.38 | 14.42 | 14.61 | 16.33 | 16.33 | 15.82 | 16.33 | 16.93 | 16.28 | 16.42 | 16.98 | 13.31 | 15.31 | 14.88 | 14.19 | 15.63 | 16.09 | 15.49 | 15.73 |
| $Fe_2O_3$ | 0.59 | 4.05 | 3.29 | 3.86 | 5.07 | 3.33 | 3.34 | 3.02 | 3.73 | 3.56 | 3.98 | 0.61 | 0.64 | 2.67 | 2.91 | 1.93 | 2.91 | 4.34 | 3.24 |
| FeO | 3.36 | 1.39 | 2.17 | 2.69 | 2.26 | 3.71 | 3.91 | 3.85 | 3.53 | 3.80 | 3.42 | 1.59 | 2.72 | 1.96 | 2.32 | 1.74 | 2.11 | 2.78 | 3.97 |
| MnO | 0.16 | 0.11 | 0.12 | 0.13 | 0.12 | 0.19 | 0.13 | 0.15 | 0.14 | 0.15 | 0.13 | 0.06 | 0.07 | 0.14 | 0.12 | 0.10 | 0.09 | 0.12 | 0.13 |
| MgO | 0.84 | 1.84 | 2.23 | 2.89 | 2.64 | 3.26 | 2.97 | 2.68 | 3.05 | 3.26 | 3.01 | 0.38 | 1.38 | 2.38 | 2.51 | 1.76 | 2.10 | 2.51 | 2.38 |
| CaO | 2.33 | 4.37 | 4.37 | 6.12 | 5.99 | 3.77 | 6.10 | 6.06 | 6.29 | 6.01 | 5.48 | 1.45 | 3.73 | 4.84 | 4.25 | 4.78 | 4.66 | 5.59 | 7.05 |
| $Na_2O$ | 4.19 | 3.98 | 4.12 | 2.96 | 3.37 | 3.61 | 3.40 | 4.41 | 2.61 | 3.26 | 3.46 | 3.69 | 3.69 | 3.83 | 3.11 | 4.41 | 3.40 | 3.11 | 2.61 |
| $K_2O$ | 3.69 | 3.94 | 2.23 | 3.21 | 1.96 | 2.69 | 1.80 | 0.97 | 2.30 | 1.93 | 1.85 | 4.82 | 3.28 | 2.83 | 4.59 | 2.16 | 3.83 | 2.82 | 2.37 |
| $P_2O_5$ | 0.10 | 0.13 | 0.13 | 0.17 | 0.17 | 0.19 | 0.21 | 0.18 | 0.19 | 0.22 | 0.20 | 0.05 | 0.19 | 0.15 | 0.15 | 0.14 | 0.20 | 0.16 | 0.18 |
| Loss on ignition | 0.57 | 0.54 | 0.85 | 2.29 | 1.25 | 1.45 | 1.19 | 2.21 | 2.08 | 1.71 | 1.53 | 1.28 | 0.91 | 0.71 | 1.33 | 3.51 | 1.08 | 1.02 | 1.52 |
| $H_2O$ | 0.12 | 0.93 | 0.98 | 0.26 | 0.18 | 0.18 | 0.11 | 0.15 | 0.06 | 0.18 | 0.18 | 0.17 | 0.08 | 0.15 | 0.17 | 0.20 | 0.37 | 0.12 | 0.37 |
| Total | 100.17 | 100.04 | 98.47 | 100.02 | 98.66 | 99.03 | 98.08 | 98.96 | 98.19 | 98.62 | 98.40 | 99.92 | 99.03 | 99.64 | 99.22 | 99.00 | 99.02 | 99.65 | 99.04 |
| Trace elements (ppm) | | | | | | | | | | | | | | | | | | | |
| Sr | 100 | 500 | 500 | 200 | 100 | 150 | 100 | 300 | 150 | 100 | 100 | n. d. | 300 | 300 | 150 | 400 | 200 | 150 | 50 |
| Ba | 200 | 500 | 500 | 300 | 150 | 300 | 150 | 200 | 300 | 200 | 200 | 150 | 400 | 400 | 300 | 500 | 400 | 300 | 150 |
| Zr | 50 | 60 | 60 | 40 | 30 | 40 | 10 | 80 | 50 | 20 | 20 | 30 | 50 | 50 | 50 | 60 | 50 | 30 | 30 |
| Nb | 5 | 5 | 5 | 5 | 5 | 5 | 5 | 5 | 5 | 5 | 5 | 5 | 5 | 5 | 5 | 5 | 5 | 5 | 5 |
| V | 20 | 50 | 100 | 80 | 100 | 60 | 60 | 100 | 80 | 60 | 60 | 10 | 30 | 40 | 60 | 40 | 60 | 60 | 60 |
| Cr | 80 | 300 | 200 | 60 | 100 | 300 | 100 | 50 | 150 | 80 | 80 | 80 | 80 | 200 | 150 | 100 | 100 | 60 | 60 |
| Co | 3 | 10 | 20 | 20 | 20 | 10 | 20 | 3 | 5 | 10 | 10 | n. d.** | 3 | 6 | 10 | 3 | 6 | 10 | 20 |
| Ni | n. d | 40 | 50 | 5 | 30 | 10 | 20 | 5 | 5 | 20 | 20 | 3 | 10 | 20 | 40 | 20 | 30 | 20 | 10 |
| Cu | 10 | 20 | 30 | 20 | 20 | 30 | 50 | 10 | 10 | 40 | 30 | 5 | 20 | 20 | 30 | 20 | 80 | 50 | 30 |

* 1 Rhyodacite, 2—3 Quartz-andesites (Imperial Porphyry), 4—11 Andesites, 12 Ignimbritic rhyolite, 13—17 Dacite tuffs and 18—19 Andesitic tuffs.

** n. d. Not detected.

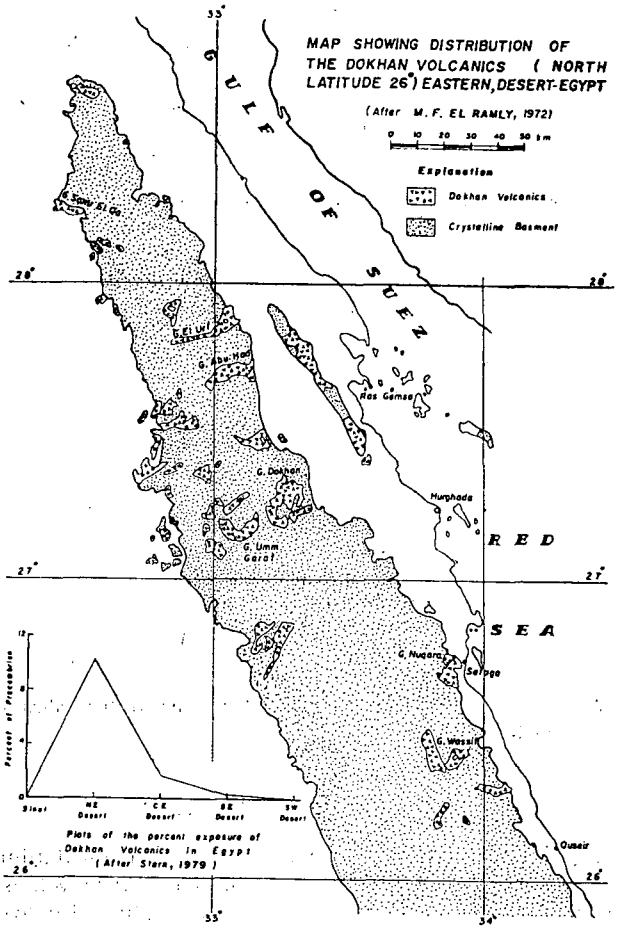


*Fig. 1.* Sketch of the northern part of the Eastern Desert of Egypt showing distribution of the Dokhan Volcanics and location of the investigated area.

and island arc volcanics have contributed 95% or more of all the pyroclastic deposits laid down during historic times. The important controlling factor for the predominance of pyroclastics within a volcanic sequence, is their tectonic setting without regard of magma type [GARCIA, 1978].

In Abu Had volcanics, pyroclastics (dacitic and andesitic tuffs) are predominant similar in that character to modern volcanic arcs. In general, the Egyptian Dokhan volcanics are characterised by abundance of explosive products [e. g. FRANCIS, 1972]. In addition, the upper part of Abu Had succession is interbedded with sediments of the Hammamat Group. The basal part of the Hammamat Group is mainly derived from the Dokhan volcanics [AKAAD and NOWEIR, 1980, p. 132]. GARCIA [1978] has reported that pyroclastic rocks in island arcs are interbedded with volcanoclastic sedimentary rocks derived from such arcs.

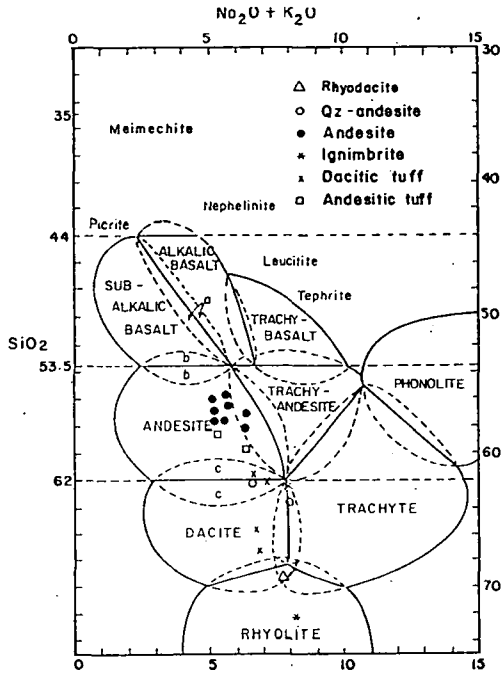


*Fig. 2.* Chemical classification of Abu Had volcanics according to their silica and alkali contents [MIDDLEMOST, 1980].

## GEOCHEMICAL EVIDENCES

The following discussion and diagrams outline the chemical affinity of Abu Had volcanics and assess the possibility of using major elements as well as immobile trace elements in identifying the tectonic environment of the studied volcanics.

MIYASHIRO [1974] has concluded that volcanic rocks of island arcs and active continental margins consist of three main rock series: calc-alkalic, tholeiitic, and alkalic. The alkalic series form only a very small part of these rocks. Such artificial distinction has the merit of permitting comparison with published data on modern examples where the temporal and spatial variation in island arcs and continental margins is defined mainly in terms of the calc-alkalic and tholeiitic series [JAKES and GILL, 1970; JAKES and WHITE, 1972; MIYASHIRO, 1974; STILLMAN and WILLIAMS, 1978]. MIYASHIRO [1974] suggested that tholeiitic series could be defined by a slower rate of increase of $SiO_2$ content and higher enrichment of FeO* (total iron as FeO) and titanium with advancing fractional crystallization than the calc-alkaline series. The advance in fractional crystallization is measured by increase in FeO*/MgO ratio. *Fig. 3* shows that the main trend of evolution of Abu Had volcanics is calc-alkalic with slight tendency towards the tholeiitic trend.

The Abu Had volcanics show a $K_2O$ to $SiO_2$ trend *(Fig. 4)* similar to that of the calc-alkaline rocks of the Cascades and Central Andes island arcs [MIYASHIRO, 1974]. The Halaban Group of Saudi Arabia (which is considered equivalent to the Egyptian Dokhan Volcanics) shows the same trend of Abu Had volcanics [GREENWOOD *et al.*, 1980, p. 16].

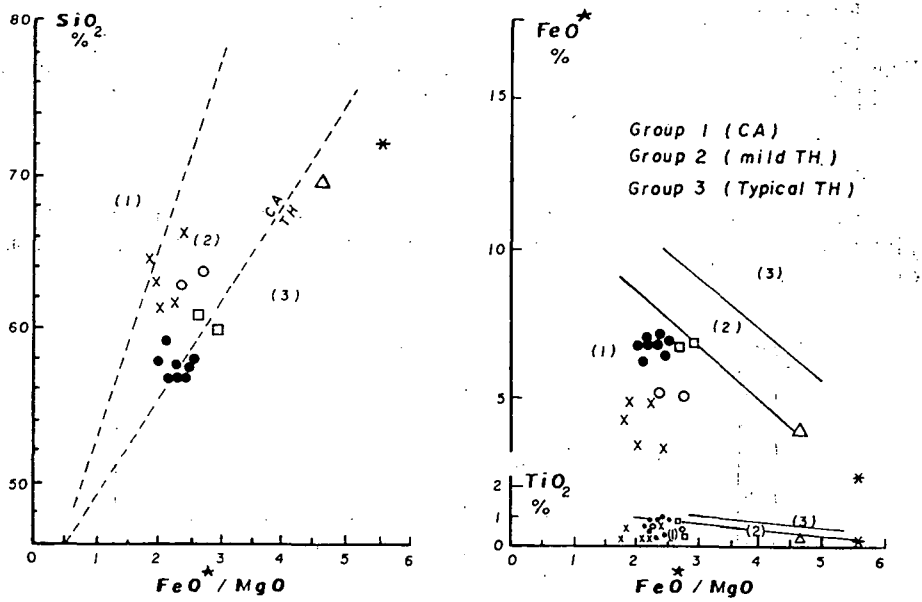


*Fig. 3.* Changes of $SiO_2$, FeO* and $TiO_2$ contents with FeO*/MgO ratio in Abu Had volcanics. Dividing lines are from MIYASHIRO [1973].
FeO*: total iron as FeO. Key for *Fig. 3* to *Fig. 8* as for *Fig. 2*.

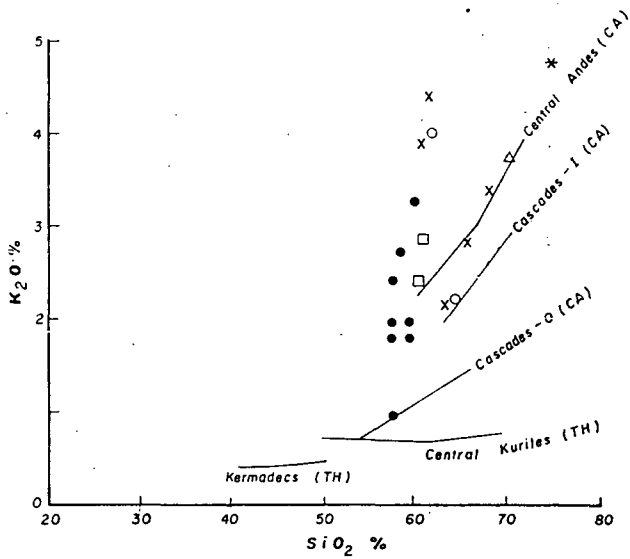


*Fig. 4.* Plot of $K_2O$ against $SiO_2$ for Abu Had volcanics. Trend lines with names show average values for volcanic rocks in those volcanic arcs [MIYASHIRO, 1974].
Th: tholeiitic rocks, CA: calc-alkaline rocks, O: outer volcanic arcs, I: Inner volcanic arcs.

RITTMANN [1973], pointed out that lavas of all active volcanics can be divided into two well separated groups which reflect the tectonic situation of the volcanoes. This appears clearly in a diagram the coordinates of which are the value $\tau$ [GOTTINI, 1968] and the value $\sigma$ (serial index of RITTMANN, 1957) being:

$\tau = Al_2O_3 - Na_2O/TiO_2$ (weight %)
$\sigma = (K_2O + Na_2O)^2/SiO_2 - 43$ (weight %).

*Fig. 5* shows GOTTINI—RITTMANN diagram on which the Abu Had volcanics plot exclusively in field B, designated by RITTMANN [1973] for volcanic rocks in orogenic belts and island arcs.

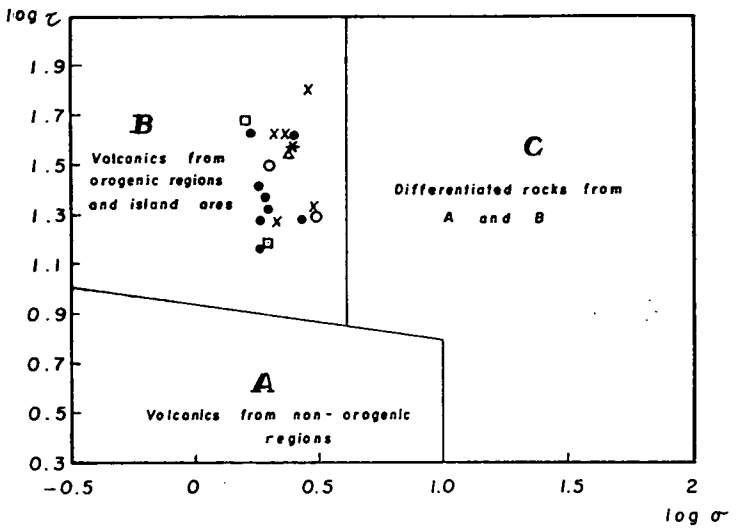


*Fig. 5.* Abu Had volcanics plotted in GOTTINI—RITTMANN diagram [RITTMANN, 1973]. Field A: Tholeiites, plateau basalts, alkali basalts, hawaiites. Field B: High-Al basalts, andesites, dacites, rhyodacites. Field C: Nephelinites, tephrites, trachytes, leucitites.

To determine the relation betwen the tectonic evironment and trace element contents, MIYASHIRO and SHIDO [1975] have constructed various diagrams using the trace element data for rocks in typical tectonic setting. *Fig. 6* shows a log V—log Cr diagram and $SiO_2$—log Cr diagram to discriminate between tholeiitic and calc-alkaline volcanic rock series. The Abu Had volcanics plot in the calc-alkaline field. *Fig. 7* shows the variation of chromium and nickel with increasing FeO*/MgO ratio in tholeiitic and calc-alkaline series of various tectonic setting. The studied volcanics fall in the field defined by MIYASHIRO and SHIDO for the volcanics of island arcs and active continental margins. The trace element data again reveal the calc-alkaline affinity of Abu Had volcanics.

According to MIYASHIRO [1973, p. 220] "the calc-alkalic trend, or at least the abundance of calc-alkalic rocks is characteristic of the volcanism in island arcs and continental margins, that is, in the covergent margins of plates". GARCIA [1978, p. 153] stated that the identification of a thick sequence of calc-alkaline volcanic rocks in the rock record strongly suggests the presence of a former volcanic arc.

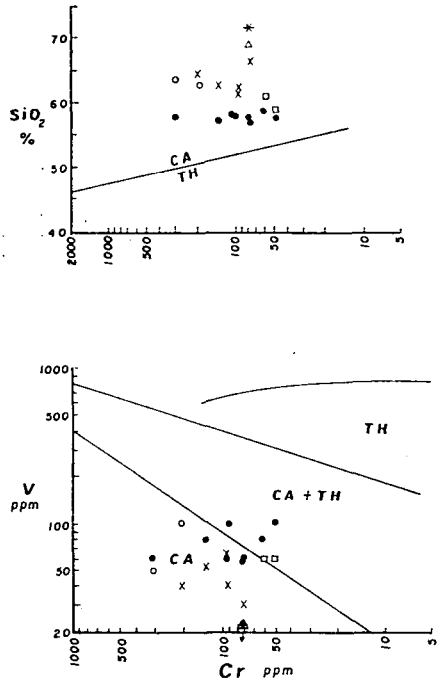


*Fig. 6.* Log V-log Cr and $SiO_2$—log Cr to discriminate between tholeiitic and calc-alkaline volcanic rocks of Abu Had [MIYASHIRO and SHIDO, 1975].

Accordingly, the calc-alkalic trend of Abu Had volcanics may indicate their evolution in the island arc or continental margin environments.

Recently, EWART [1979, 1981] has reviewed the lava analyses from various modern geotectonic settings and gave average abundances of 30 minor and trace elements from the main volcanic environments. RAMSAY *et al.*,[1981] used such data to plot the most important of these elements against $SiO_2$ for the following geotectonic settings:

1. Active continental margins (Western USA and Andean South America).
2. Anorogenic environments (Iceland, S. E. Queensland, and the Western Scotland-Northern Ireland province).
3. Oceanic islands (Galapagos, Hawaii, Canaries, and the Zephyr Shoal).
4. Primitive ensimatic island-arcs (Tonga-Kermadec and Lesser Antilles).

*Fig. 8* shows that plots of Abu Had volcanics (except those of Cu) fall mainly in the field defined by RAMSAY *et al.* [1981] after EWART [1979, 1981] for immature island arcs. Whilst a few individual analyses may be incorrecrly allocated, the bulk of population lie in the island arcs field. RAMSAY *et al.*, stated that the defined fields "are the fields of average values for defined $SiO_2$ ranges, and therefore indicate only typical concentrations of the relevant elements. The actual fields of individual points are, of course, larger".

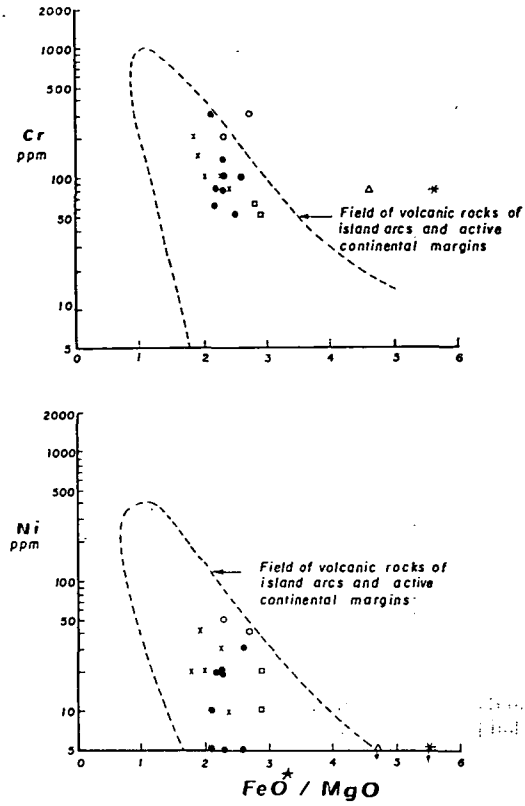


*Fig. 7.* Variation of Cr and Ni with FeO*/MgO for Abu Had volcanics [MIYASHIRO and SHIDO, 1975].

Table 2 compares some chemical features of Abu Had volcanics and those of rocks of different tectonic settings. Chemistry of the Dokhan volcanics, at the type locality, Gabal Dokhan — Egypt as well as that of the Helaban Group of Saudi Arabia are also given. The chemical data of Abu Had volcanics generally resemble data for the island arc calc-alkaline series. The same tectonic setting had been suggested for volcanics of Gabal Dokhan [BASTA *et al.*, 1980], as well as for the Halaban Group of Saudi Arabia which is considered to be equivalent for the Egyptian Dokhan volcanics [GREENWOOD *et al.*, 1980].

## DISCUSSION

The crystalline rocks of the Eastern Desert of Egypt (including the Dokhan Volcanics) form a part of the Arabian Nubian Shield which includes the crystalline basement of western Saudi Arabia, the Egyptian Eastern Desert and the northeastern Sudan. In turn, the Arabian-Nubian Shield forms a part of a widespread, U-shaped non-cratonic belt of rocks covering a significant portion of Africa *(Fig. 9)*. This belt is considered to be developed during the Pan-African orogeny [KENNEDY, 1964]

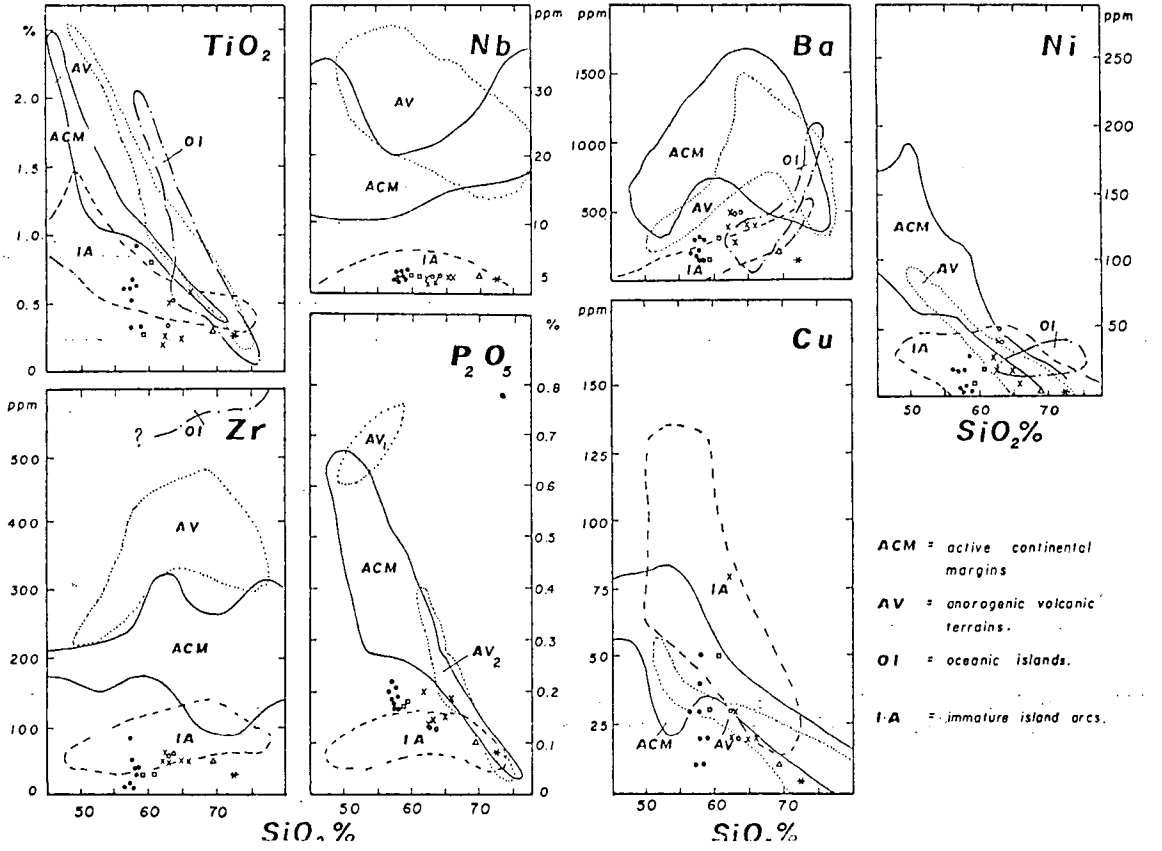


*Fig. 8.* Abundances of $TiO_2$, Zr, Nb, $P_2O_5$, Ba, Ni and Cu in Abu Had volcanics, compared with average fields of magmas from various modern geotectonic environments. [defined by RAMSAY *et. al.*, 1981 after EWART, 1979 and 1981].

TABLE 2

*Comparison of major element chemistry of continental tholeiite, abyssal tholeiite behind the arc tholeiite, island-arc tholeiite, and Island-arc calc-alkaline volcanic rocks with Halaban Group of Saudi Arabia, Dokhan Volcanics (G. Dokhan-Egypt) and Abu Had Volcanics*

| | Continental tholeiite[1] | Abyssal tholeiite[1] | Behind the arc tholeiilite[1] | Island-arc tholeiite[1] series | Island-arc calc-alkaline series[1] | Halaban Group Saudi Arabia[2] | | G. Dokhan Volcanics (Egypt)[3] | | Abu Had Volcanics | |
|---|---|---|---|---|---|---|---|---|---|---|---|
| | | | | | | Range | Median | Range | Avg. | Range | Avg. |
| $SiO_2$ | 51.5 | 47—62 | 48—50 | 45—70 | 50—66 | 57—76 | 68 | 54—70 | 61 | 57.6—72.2 | 61.6 |
| $TiO_2$ | 1.2 | 1—2 | 1—2 | 0.5—1 | 0.2—1 | 0.3—1.4 | 0.5 | 0.3—1.5 | 1.0 | 0.2—0.9 | 0.5 |
| $Al_2O_3$ | 16.3 | 14—15 | 14—17 | 14—17.5 | 16—18 | 12—18 | 14 | 13—17 | 15 | 13.3—17.0 | 15.6 |
| $Na_2O$ | 2.5 | 2.5—3 | 1—3.5 | 2—3 | 2.9—5 | 1.0—5.4 | 4.3 | 1.6—5.7 | 3.7 | 2.6—4.4 | 3.5 |
| $K_2O$ | 0.86 | 0.1—0.2 | 0.2—0.6 | 0.5 | 1—2.7 | 1.0—5.6 | 3.2 | 1—5 | 1.7 | 1.8—4.8 | 2.8 |
| $Na_2O/K_2O$ | 3 | 10—15 | 6—10 | 4—6 | 1.3 | 0.2—5.6 | 1.6 | 0.7—4.4 | 1.6 | 0.7—4.6 | 1.5 |

1. Compiled by GREENWOOD *et al.*, [1980] after COATS [1968], MANSON [1968], JAKES and WHITE [1972], ANHAEUSSER [1973] and ROGERS *et al.*, [1974]
2. GREENWOOD *et al.*, [1980]
3. BASTA *et al.*, [198—]

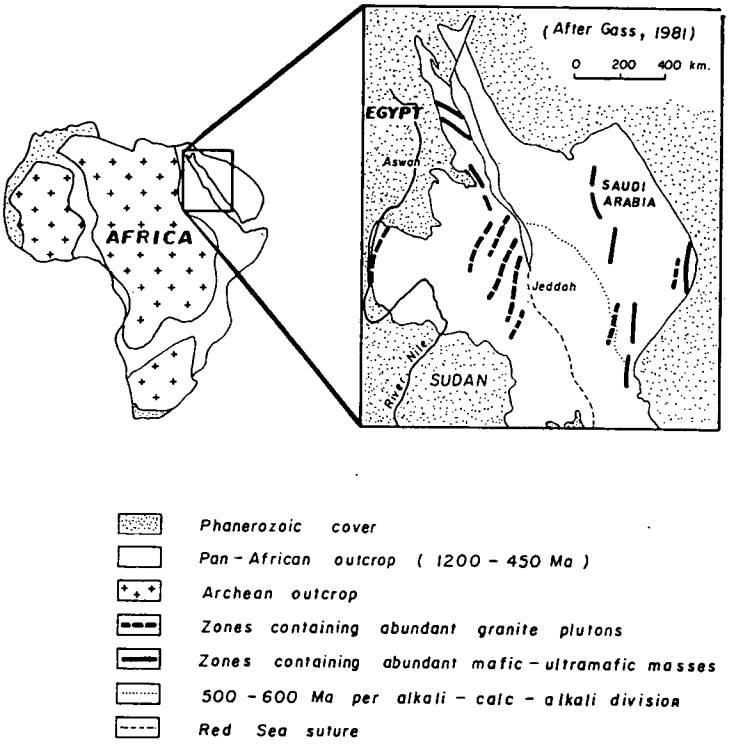


*Fig. 9.* Regional sketch map of the Arabian—Nubian Shield showing the disposition of mafic-ultramafic complexes (marking the approximate position of arc sutures) and linear granitic zones (possible arc axes). The Red Sea has been closed to a pre-Miocene position. The map of Africa shows outcrop areas of dominantly Pan-African age rocks whichs tend to encircle older cratonic rocks of Africa.

which has an age ranges of 1200—450 Ma [GASS, 1977, 1981; KRÖNER, 1979; International Geological Correlation Program (IGCP) Project 164, Saudi Arabia, 1979].

The origin of the Pan-African orogeny of the Arabian-Nubian Shield is controversial. Some authors suggest that this part of the Pan-African represents an Archean crust that was remobilized during the Pan-African orogeny (1200—450 Ma). This hypothesis requires the presence of continental (sialic) material older than the Pan-African orogeny [HUME, 1934; CLIFFORD, 1968; AKAAD and NOWEIR, 1980].

On the other hand, some authors suggest a plate-tectonic model suggesting that the continental crust of the Arabian-Nubian shield evolved in an oceanic environment within the Upper Proterozoic. According to GASS [1981], subduction occurred some 1200 Ma ago between converging plates of oceanic lithosphere. During this process oceanic crust of back-arc basins or marginal seas may have been consumed along predominantly westerly-inclined Benioff zones [GARSON and SHALABY, 1976] and obducted fragments of this crust are now found as well preserved or partly dismembered ophiolite complexes in western Arabian and from northern Ethiopia to Egypt *(Fig. 9)* [BAKOR *et al.*, 1976; GARSON and SHALABY, 1976; NEARY *et al.*, 1976; GASS, 1977; FRISCH and AL-SHANTI, 1977; EL SHAZLY and ENGEL, 1978; EL SHARKAWY and EL BAYOUMI, 1979; SHANTI and ROOBOL, 1979]. Finally, when

subduction ceased, about 500 Ma ago, the whole region had developed a continental character [GASS, 1981]. The final stages of cratonization are marked by change from calc-alkaline to peralkaline magmatism, occurred earlier in some areas than in others. The line drawn on *Fig. 9* is that of STOESSER and ELLIOT [1979], and separates 500—600 Ma Arabian peralkaline (to the east) from calc-alkaline products (to the west).

In conclusion, the geological and geochemical features of Abu Had volcanics correlated with other features mentioned in this study strongly suggest the island-arc environment in which the studied volcanics were formed. Worthy of remark, such ensimatic island-arc cratonization model is faced by some difficulties. HASHAD and HASSAN [1979] stated that "It may perhaps be more reasonable to see the shield development in terms of an Andean type setting". The same tectonic setting was proposed by KRÖNER [1979]. Further geological, geochemical and geophysical studies of the Egyptian basement complex may reveal its proper tectonic setting.

## REFERENCES


AKAAD, M. K. and NOWEIR, A. M. [1980]: Geology and lithostratigraphy of the Arabian Desert Orogenic belt of Egypt between latitudes 25°35′ and 26°30′ N. In: Evolution and Mineralization of the Arabian Nubian Shield. Inst. Applied Geol., King Abdulaziz Univ., Jeddah, Bull. **3** 4 (ed. COORAY, P. G. and TAHOUN, S. A.), Pergamon Press, Oxford, 127—135.

ANHAEUSSER, C. R. [1973]: The evolution of the early Precambrian crust of southern Africa. Royal Soc. London Philos. Trans., **A 272**, 359—388.

BAKOR, A. R., GASS, I. G. and NEARY, C. R. [1976]: Jabal Al Wask: An Eocambrian, back-arc ophiolite in NW Saudi Arabia. Earth Planet. Sci. Lett., **30**, 1—9.

BASTA, E. Z., KOTB, H. and AWADALLAH, M. F. [1980]: Petrochemical and geochemical characteristics of the Dokhan Formation at the type locality, Jabal Dokhan, Eastern Desert, Egypt. In: Evolution and Mineralization of the Arabian-Nubian Shield. Inst. Applied. Geol., King Abdulaziz Univ., Jeddah, Bull. **3**, 4, (ed. AL-SHANTI, A.), Pergamon Press, Oxford, 122—140.

CLIFFORD, T. N. [1968]: Radiometric dating and the pre-Silurian geology of Africa, In: Radiometric Dating for geologists (eds. HAMILTON, E. I. and FARQUAHAR, R. M.), J. Wiley — Interscience, 299—416.

COAST, R. R. [1968]: Basaltic andesites, in: Basalts, Vol. II, (eds. HESS, H. H. and POLDERVAART, A.), John Wiley and Sons, New York, 689—736.

EL RAMLY, M. F. [1972]: A new geological map for the basement rocks in the Eastern and Southwestern Deserts of Egypt. Annal. Geol. Surv. Egypt, II. 1—18.

EL SHARKAWY, M. A. and EL BAYOUMI [1979]: The ophiolites of Wadi Ghadir Area Eastern Desert, Egypt. Annal. Geol. Surv. Egypt **IX**, 125—135.

EL SHAZLY, E. M. and ENGEL, A. E. J. [1978]: Proterozoic rifting and refractionation of northeast Africa (Abstr.) Precambrian Res., **6**, A20.

EL SHAZLY, E. M., HASHAD, A. H., SAYYAH, T. A. and BASSYUNI, F. A. [1973]: Geochronology of Abu Swayel area, South Eastern Desert. Egypt. J. Geol., **17**, 1—18.

EWART, A. [1979]: A review of the mineralogy and chemistry of the Tertiary-Recent dacitic, latitic, rhyolitic and related salic volcanic rocks. In: Trondhjemites dacites and related rocks (ed. BARKER, F.) Elsevier, Amsterdam, 13—121.

EWART, A. [1981]: The mineralogy and petrology of Tertiary-Recent orogenic volcanic rocks: with special reference to the andesitic-basaltic compositional range. In: Andesites (ed. THORPE, J.), Elsevier, Amsterdam.

FRANCIS, M. [1972]: Geology of the basement complex in the north Eastern Desert between latitudes 27°30′ and 28°00′ N. Annal. Geol. Surv. Egypt **II**, 161—180.

FRISCH, W. and AL-SHANTI, A. [1977]: Ophiolite belts and the collision of island arcs in the Arabian Shield. Tectonophysics **43**, 293—306.

GARCIA, M. O. [1978]: Criteria for the identification of ancient volcanic arcs. Earth Sci. Rev., **14**, 147—165.

GARSON, M. S. and SHALABY, I. M. [1976]: Precambrian-Lower Paleozoic plate tectonics and metallogenesis in the Red Sea region. Geol. Assoc. Canada Spec. paper **14**, 573—596.

GASS, I. G. [1977]: The evolution of the Pan-African crystalline basement in NE Africa and Arabia. J. Geol. Soc. London **134**, 129—138.

GASS, I. G. [1981]: Pan-African (Upper Proterozoic) plate tectonics of the Arabian-Nubian Shield. In: Precambrian plate tectonics, (ed. KRÖNER, A.) Elsevier, Amsterdam, 387—405.
GOTTINI, V. [1968]: The $TiO_2$ frequency in volcanic rocks. Geol. Rundsch., **57**, 930—935.
GREENWOOD, W. R., ANDERSON, R. E., FLECK, R. J. and ROBERTS, R. J. [1980]: Precambrian geologic history and plate tectonic evolution of the Arabian Shield. Saudi Arabian Dir. Gen. Miner. Resour., Bull. **24**, 35.
HASHAD, A. H. and HASSAN, M. A. [1979]: On the validity of an ensimatic island-arc cratonization model to the evolution of the Egyptian Shield. Annal Geol. Surv. Egypt **IX**, 70—80.
HUME, W. F. [1934]: Geology of Egypt, Vol. II. The fundamental pre-Cambrian rocks of Egypt and the Sudan. Part I The Metamorphic rocks. Egypt, Surv. Dept., Cairo.
JAKES, P. and GILL, J. [1970]: Rare earth elements and the island arc tholeiitic series. Earth. Planet. Sci. Lett., **9**, 17—28.
JAKES, P. and WHITE, A. J. R. [1972]: Major and trace element abundances in volcanic rocks of orvgenic areas. Geol. Soc. Am., Bull., **83**, 29—40.
KENNEDY, W. Q. [1964]: The structural differentiation of Africa in the Pan-African ($\pm 500$ m. y.) tectonic episode. Univ. Leeds. Res Inst. Afr. Geol., Dept. Earth Sci., Annu. Rep. Sci. Results **8**, 48—49.
KRÖNER, A. [1979]: Pan African plate tectonics and its repercussions on the crust of northeast Africa. Geol. Rund., **68**, 2, 565—583.
MANSON, V. [1968]: Geochemistry of basaltic rocks: Major elements, In: Basalts, V. I., (eds. HESS, H. H. and POLDERVAART, A.), John Wiley and Sons, New York, 215—269.
MIDDLEMOST, E. A. K. [1980]: A contribution to the nomenclature and classification of volcanic rocks. Geol. Mag., **117**, 51—57.
MIYASHIRO, A. [1973]: The Troodos ophiolitic complex was probably formed in an island arc. Earth Planet. Sci. Lett., **19**, 218—224.
MIYASHIRO, A. [1974]: Volcanic rock series in island arcs and active continental margins. Am. J. Sci., **274**, 321—355.
MIYASHIRO, A. and SHIDO, F. [1975]: Tholeiitic and calc-alkalic series in relation to the behaviours of titanium, vanadium, chromium and nickel. Am. J. Sci., **275**, 265—277.
NEARY, C. R., GASS, I. G. and CAVANACH, B. J. [1976]: Granitic association of north-eastern Sudan. Geol. Soc. Am. Bull., **87**, 1501—1513.
RAMSAY, C. R., BASAHEL, A. N. and JACKSON, N. J. [1981]: Petrography, geochemistry and origin of the volcano-sedimentary succession between Jabal Ibrahim and Al-Aqiq, Saudi Arabia. Fac. Earth Sci., King Abdulaziz Univ., Bull., **4**, 1—24.
RITTMANN, A. [1957]: On the serial character of igneous rocks. Egyptian J. Geol., **1**, pp. 23—48.
RITTMANN, A. [1962]: Volcanoes and their activity. John Wiley and Sons, New York, 305 pp.
RITTMANN, A. [1973]: Stable mineral assemblages of igneous rocks. Spinger-Verlag, Berlin.
RITTMANN, A. and RITTMAN, L. [1976]: Volcanoes. G. P. Putnam's Sons, New York, N. Y., 97 pp.
ROGERS, J. J. W., BURCHFIEL, B. C., ABBOTT, E. W., ANEPOHL, J. K., EWING, A. H., KOEHNKEN, P. J., NOVITSKY-EVANS, M. and TALUKDAR, S. C. [1974]: Paleozoic and lower Mesozoic volcanism and continental growth in the western United States: Geol. Soc. America Bull., **85**, 1913—1924.
SHANTI, M. and ROOBOL, M. J. [1979]: A late Proterozoic ophiolite complex at Jabal Ess in northern Saudi Arabia. Nature **279**, 488—491.
STERN, R. J. [1979]: Late Precambrian ensimatic volcanism in the Central Eastern Desert of Egypt. Unpub. Ph. D. Thesis, California Univ., San Diego.
STILLMAN, C. J. and WILLIAMS, C. T. [1978]: Geochemistry and tectonic setting of some Upper Ordovician volcanic rocks in east and southeast Ireland. Earth Planet. Sci. Lett., **41**, 288—310.
STOESSER, D. B. and ELLIOT, J. E. [1979]: Post-orogenic peralkaline and calc-alkaline granites and associated mineralization of the Arabian Shield, Kingdom of Saudi Arabia. USGS Saudi Arabia Project Rep. SA (IR) **265**, 1—42.
WILLIAMS, H. and MCBIRNEY, A. R. [1979]: Volcanology, Freeman, Cooper and Co., San Francisco

*Manuscript received, 12. October, 1983*

MOHAMED A. HEIKAL
Geology Department,
Al-Azhar University,
Cairo, Egypt.
ABDEL-AAL M. AHMED
Geological Survey of
Egypt, Cairo.

*Acta Mineralogica-Petrographica, Szeged, XXVI/2, 235—245, 1984*

# ROUNDNESS AND SPHERICITY OF THE DELTA COASTAL SANDS

N. M. EL FISHAWI


## ABSTRACT

The roundness and sphericity of the Nile Delta coastal sands were studied. Definite correlations between the size and the roundness and sphericity were established. The roundness and sphericity were observed to be complex functions of each other, rather than to be in a linear relationship. A difference in roundness and sphericity was found normal to the shoreline, so that a distance of a few hundred metres makes a complete change in their values. The principal difference comes from the sorting processes of the hydrodynamic forces affecting the coast. It is possible that these studies can be used to differentiate sediments of the Nile Delta coast. The lateral variation of roundness and sphericity was found to be improved and can be applied to the tudy of the sediment movement.


## INTRODUCTION

Early studies of roundness and sphericity of the sand grains were made by many authors [WADELL, 1935; MACCARTHY and HUDDLE, 1938; RUSSELL and TAYLOR, 1937; PETTIJOHN and LUNDAHL, 1943]. More recent works have been published by MATTOX [1955], BEAL and SHEPARD [1956], WASKOM [1958], SHEPARD and YOUNG [1961] and MISDORP [1967]. Few comprehensive studies have been carried out on the relation between size and roundness and sphericity. Whether or not sand grains show a progressive increase in roundness and sphericity with distance of transport is an unsettled problem. Many investigators have questioned the authenticity of any actual difference in roundness and sphericity normal to the shoreline.

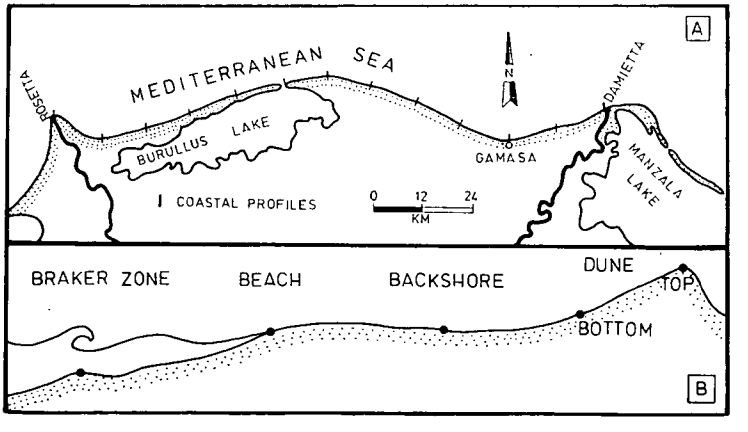


*Fig. 1.* Location map *(A)* and sampling sites *(B)* for the recent environments of the Nile Delta coast.

The studied area located between Rosetta and Damietta and extends for about 144 km along the coast *(Fig. 1)*. Theoretically, samples collected along profiles normal to the shoreline indicate the importance of waves and winds as selectors of round and spherical grains. Therefore, samples were collected along profiles perpendicular to the shoreline: in total 13 profiles being chosen *(Fig. 1A)*. Each profile contains a breaker zone, beach, backshore and dune sample where possible *(Fig. 1B)*. In this way, it may be possible to obtain appreciable differences between adjacent environments and to detect if there is a definite change over a distance of some hundred metres.

The aim of the present study is to correlate the roundness and sphericity with the grain size, depositional environments and distance of transport along the Nile Delta coast.

## METHODS OF STUDY

BOGGS [1967] describes the use of grain photographs and the Zeiss electronic particle size analyzer (Zeiss TGZ 3) in the analysis of grain roundness and sphericity. This technique is used in the present study, where the photographic print is mounted on the analyzer and the radius measurements are rapidly and automatically tabulated for each grain image. The study was made on grain sizes of 2000—1000 $\mu$m, 1000—500 $\mu$m, 500—250 $\mu$m, 250—125 $\mu$m, 125—63 $\mu$m. Sieve fractions were put through a microsplitter to obtain a few hundred representative grains. Loose grains to be photographed are placed on a slide and tapped gently so that they come to rest with long and intermediate axes in projection view. 50—100 grains are photographed and a suitably enlarged photomicrograph is prepared on thin photographic paper.

Of the several formulae proposed for measuring roundness in detrital particles, Wadell's may be regarded as the most indicative measure [FLEMMING, 1965; SWAN, 1974]. This measure was applied in the present study:

WADELL [1933] roundness $= \sum D_c / N D_i$

where: $D_c$ is the diameter of the curvature of a corner; N is the number of corners; and $D_i$ is the diameter of the largest inscribed circle.

Because of the difficulty of making three-dimensional measurements of sand grains, the sphericity method of RILEY [1941] was applied in this study. He proposed an expression of sphericity based on two intercept dimensions. His projection sphericity is defined as the square root of the ratio of the inscribed and circumscribed circles, as indicated by the formula:

Projection sphericity $= \sqrt{D_i / D}$

where $D_i$ refers to the diameter of the inscribed circle; and D to the diameter of the circumscribed circle.

### *Roundness and size*

All roundness values for each environment were plotted against size, as shown in *Fig. 2*. A line connecting the mean roundness of each size is presented; the comparison generally shows a marked decrease in roundness with decreasing size. This is in agreement with RUSSELL and TAYLOR [1937], PETTIJOHN and LUNDAHL [1943], INMAN [1953], INMAN *et al.*, [1966], RAMEZ and MOSALAMY [1969], KHOLIEF *et al.* [1969], BALAZS and KLEIN [1972] and MISDORP [1976]. The mean roundness line for each environment shows similar behaviour. It is observed that there is a sharp decrease in roundness with decrease in size between 500—125 $\mu$m; little difference was found with grain sizes smaller than 125 $\mu$m. It may be true that the coarser sands show a better tendency to selective wear than the finer sands.

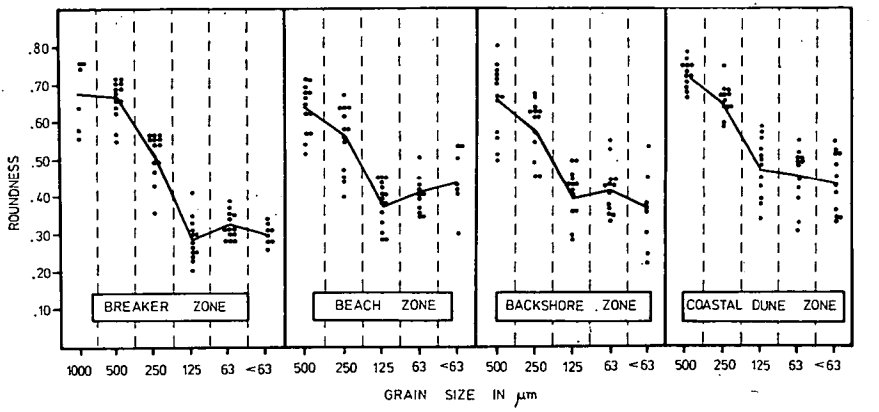


*Fig. 2.* Relationship between roundness and grain size of the coastal sands.

*Sphericity and size*

The most striking result comes from testing the sphericity of various grain sizes, as indicated in *Fig. 3*. The coastal sands are characterized by a steep decrease in sphericity, associated with a decrease in grain size. This marked correlation between sphericity and size has been investigated by MACCARTHY [1935], WADELL [1935], RUSSELL and TAYLOR [1937], PETTIJOHN and LUNDAHL [1943] and MATTOX [1955]. The mean sphericity line for each environment shows similar behaviour.

The lines connecting the mean roundness and sphericity values for each size of various coastal sands were overlapped *(Fig. 4)* to correlate between them. A significant difference in roundness values was found between the different coastal sands

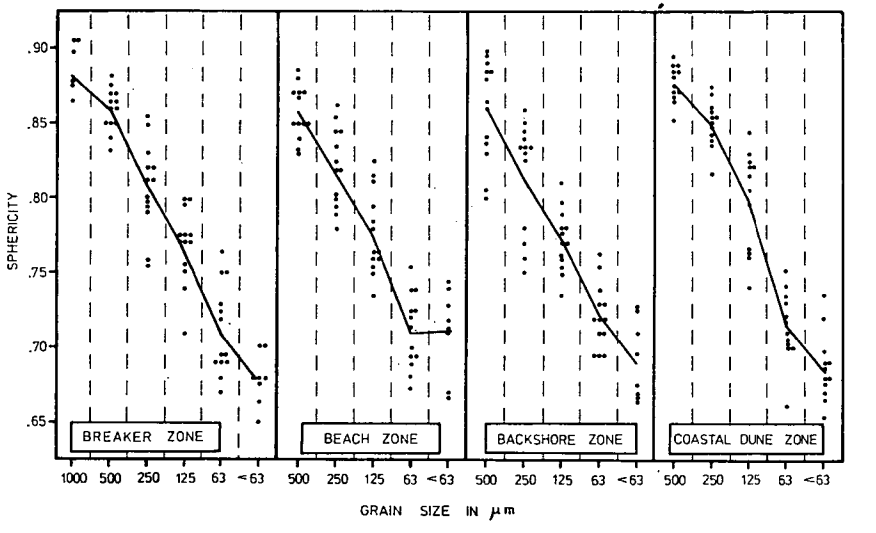


*Fig. 3.* Relationship between sphericity and grain size of the coastal sands.

*(Fig. 4A)*. As regards sphericity, it is generally possible to distinguish the dune sands, because little sphericity difference exists between breaker zone, beach and backshore sands.

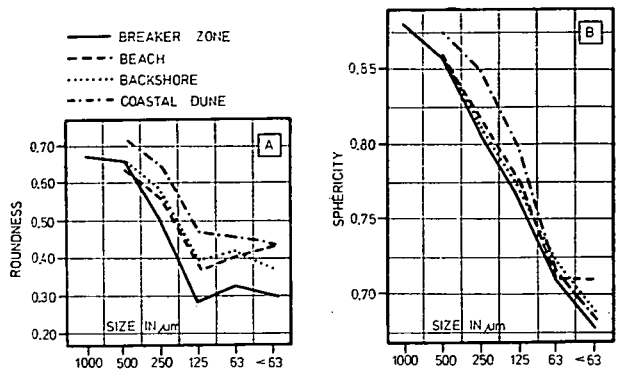


*Fig. 4.* An overlap of the mean roundness *(A)* and mean sphericity *(B)* for the coastal sands.

*Relationship between roundness and sphericity*

Early studies mentioned that the roundness and sphericity are functions of each other, and the roundness seems to bear a linear relation to the sphericity [WADELL, 1935; RUSSELL and TAYLOR, 1937; PETTIJOHN and LUNDAHL, 1943]. These studies depended upon few samples, which gives the impression that the data were insufficient. Moreover, it is observed that the slope of their curves is probably a little too steep. ROSENFELD and GRIFFITHS [1953] feel that this sympathetic relationship arises from pshychological bias on the part of the operator.

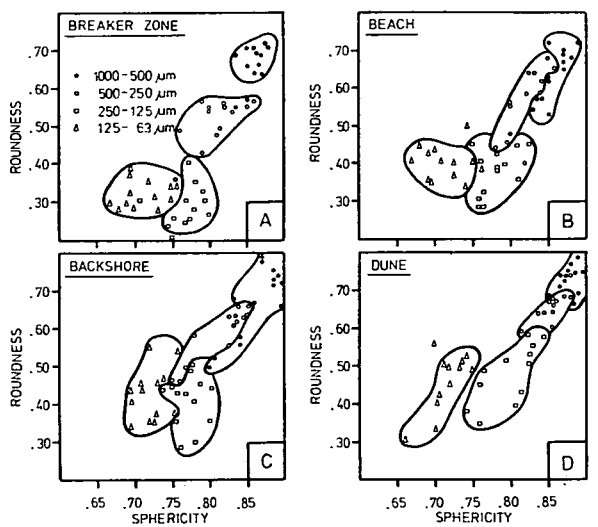


*Fig. 5.* Relationship between roundness and sphericity.

In fact, the roundness and sphericity are functions of the grain size, and the better rounded grains are the more spherical. The two parameters, however, were found to be complex functions of each other. *Figure 5* shows the relationship between them for each coastal sand. Roundness and sphericity data are based on measurements on four size grades; at least 12 pairs of roundness and sphericity vallues are drawn for each size grade. *Fig. 5* deals with the following observations:

1. The field of each size grade was found to be separated from the other size grade fields. The separation may be complete, as in the breaker zone, and may involve some overlaps, as in the backshore.

2. The increase of the roundness and sphericity with increasing grain size found to be a general trend. The coarse sizes (1000—250 μm), however, display a better roundness-sphericity relation than do the finer sizes (250—63 μm).

3. The best correlation between the size grade fields was demonstrated for the coastal dune sands. The size grades are gradually arranged according to size, roundness and sphericity. This arrangement may be related to the wind action.

4. Mathematically, it is very difficult to consider that the roundness bears a linear relation to the sphericity, in spite of the positive correlation between them. It is better for such relationships to be expressed as fields of data than as regression equations.

*Roundness and sphericity in relation to depositional environments*

For many years sedimentary petrographers have attempted to determine the relationship between the depositional environment and the form of sand grains. To detect this relationship in this study, the mean roundness and sphericity values for each size grade were plotted against the coastal environments *(Fig. 6)*; the values are summarized in Table 1.

TABLE 1

*Mean roundness (R) and sphericity (S) values for the Nile Delta coastal sands*

| Size | 1000—500 μm | | 500—250 μm | | 250—125 μm | | 125—63 μm | | Mean | |
|---|---|---|---|---|---|---|---|---|---|---|
| Environ | R | S | R | S | R | S | R | S | R | S |
| Breaker zone | .664 | .860 | .516 | .808 | .289 | .767 | .327 | .712 | .449 | .787 |
| Beach zone | .638 | .858 | .560 | .822 | .378 | .777 | .408 | .712 | .496 | .792 |
| Backshore | .664 | .859 | .589 | .816 | .413 | .772 | .423 | .721 | .522 | .790 |
| Dune bottom | .748 | .876 | .671 | .856 | .479 | .802 | .471 | .718 | .592 | .813 |
| Dune top | .706 | .877 | .647 | .842 | .490 | .794 | .443 | .710 | .572 | .806 |

a) Roundness and depositional environments

At first sight, it will be seen that a difference in roundness was found between the Nile Delta coastal sands, so that a distance of a few hundred metres makes a complete change in the roundness values *(Fig. 6A)*. All size classes show a definite improvement in roundness normal to the shoreline. In moving from the breaker zone through the beach and backshore, and up to the dune, the mean roundness increases from 0.449 to 0.592. The sands of the dune top are relatively less rounded than those of the bottom, but are still more rounded than the other types of sands.

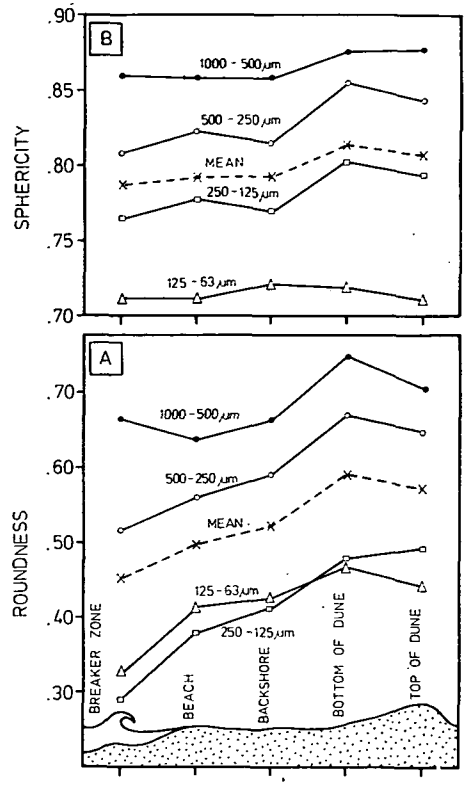


*Fig. 6.* Variations of mean roundness *(A)* and mean sphericity *(B)* normal to the shoreline.

Roundness has been referred to by a number of authors as being greater in dune sands than in the adjacent beach from which the dune was derived [MACCARTHY, 1935; RUSSELL, 1939; BEAL and SHEPARD, 1956; PETTIJOHN, 1957; SHEPARD and YOUNG, 1961]. In contrast, WASKOM [1958] found that the beach ridge sand grain roundness is greater than that of sands in other environments. Other sedimentologists have questioned the authenticity of any actual difference in roundness between beach and dune sands [MATTOX, 1955; MASON and FOLK, 1958]. Many textbooks and articles contain statements to the effect that sand grains found in aeolian deposits generally possess a higher degree of roundness than do grains found in other environments. There is no reason to believe that the grains are rounded appreciably by the wind in transit to the dunes, but very little rounding may occur in transporting sand from the beach to the adjacent dunes.

The principle difference in roundness between the adjacent coastal environments comes from the sorting action of the hydrodynamic forces affecting the coast. The possible explanation for the greater roundness in the beach than in the breaker zone is that the waves carrying the sand up onto the beach may select the rounder grains. The increase in roundness landwards may be related to the sorting action of the wind in picking up more rounded grains from the beach. It is evident that well rounded grains can roll and be blown more easily than grains with angular corners. Therefore, the wind can select the more rounded grains from the beach to be rolled, the relatively

less rounded grains may be added to the backshore zone, while the more rounded ones can easily continue to be transported and finally to be added to the dune. In some areas, where beaches and dunes are most difficult to distinguish, it is thought that the dune sands are blown back onto the beaches, causing intermixture. In some cases, the dunes are derived from sources other than the adjecent beach [BEAL and SHEPARD, 1956].

b) Sphericity and depositional environments

*Figure 6B* shows that the sphericity values of the coastal dune sands are consistently larger than those of the other environments. The sphericity values of the breaker zone and backshore zone sands are generally lower than for all other sands. The dune top sands are slightly less spherical than the bottom ones. It is noted that the sphericity of the 125—63 μm size grade behaves separately.

The increase in the sphericity of the dune sands can best be explained by the hypothesis that a more spherical grain will roll more easily than a less spherical one. BAGNOLD [1937], however, has shown that most aeolian transportation occurs by saltation. Therefore, another idea must be suggested to explain this condition. On the basis of a series of experiments, MACCARTHY and HUDDLE [1938] concluded that aeolian transportation favours sand grains with high sphericity values, because such grains tend to bounce higher than grains with lower sphericity values. A critical examination of this conclusion leads to disagreement along the lines suggested by MATTOX [1955]. He stated that a grain with a lower sphericity value will have a greater tendency to move, because of the larger surface area exposed to the wind, and thus the dune sands are less spherical than the beach sands.

During the present study on the Nile Delta coast, it is observed that most of the sand transportation takes place during normal conditions, when the wind velocity is enough only to initiate sand movement. During the course of transportation, a considerable amount of sand was observed in motion by rolling. If two grains of different sphericity values, but of equal mass, are subjected to the action of wind which is strong enough to initiate the movement, the grain with the higher sphericity value will have the greater tendency to start rolling. Therefore, because they roll more easily, grains with higher sphericity values, are transported greater distances by traction than grains with lower sphericity values.

To sum up, where the dunes are formed close to the adjacent beach, the few hundred metres distance of transportation is enough to allow the development of sphericity. The wing picks up from the beaches more grains with higher sphericity values than those with lower values. As a result, the grains of the dune sands become relatively more spherical than those of the beach sands. In fact, during storm periods sands movement takes place regardless of shape. On the other hand, the possible reason for the relatively higher sphericity in the beach than in the breaker zone may be related to the effect of waves in selecting spherical grains to be added to the beach sediments.

*Lateral variations of roundness and sphericity*

In all experimental and field work, the roundness and sphericity of beach sands increased with distance [KRUMBEIN, 1941; PETTIJOHN, 1957]. The studies of beach and river sands by MACCARTHY [1935], RUSSELL and TAYLOR [1937] and PETTIJOHN and LUNDAHL [1943] show a small, though unequivocal decline in sphericity during movement. They attribute their findings to progressive fracturing or sorting action.

Variations of roundness and sphericity for each size grade of the breaker zone, beach, backshore and dune sands along the coast are shown in *Figs. 7* and *8*. Sands grains apparently become better rounded and more spherical as a result of abrasion during the course of transport. Abrasive action in the absence of coarse materials is exceedingly slow [PETTIJOHN, 1957], which may explain the decline in roundness and sphericity of the fine sands of the Damietta beaches. Although roundness and sphericity are geometrically distinct, they react in a dynamically similar manner to abrasion along the coast. It is observed that a small increase in sphericity is accompanied by a large increase in roundness.

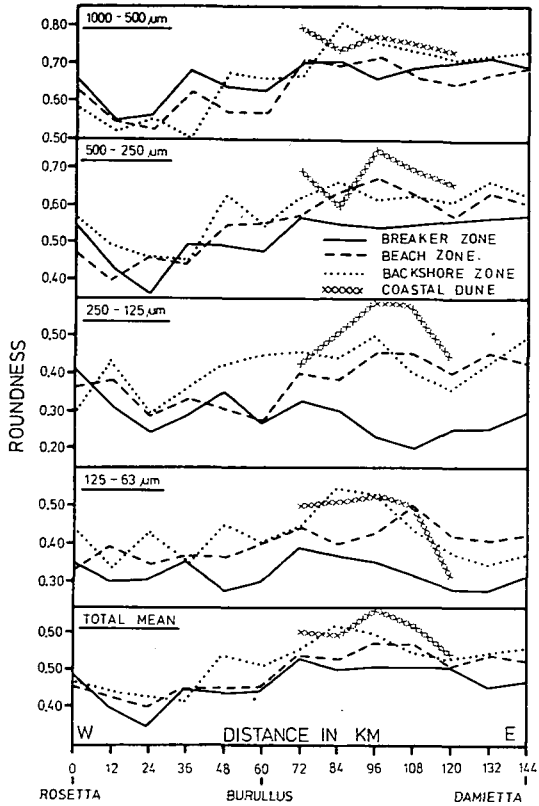


*Fig. 7.* Relation of roundness of coastal sands to distance of transport along the Nile Delta coast.

The relation of grain roundness to distance of transport *(Fig. 7)* involves the following concepts:

1. The mean roundness of the coastal sand grains generally exhibits a definite though fluctuating increase with distance of transport eastward. In the early stages of transport (0—24 km), the roundness of the coastal sands shows a relative decrease, and then progressively increases to the maximum value near the location 96 km. It tends to decrease relatively eastwards.

2. In all the cases, it seems that the change in roundness may quite abrupt at first, but subsequently it becomes rather smooth. This suggests that the process of

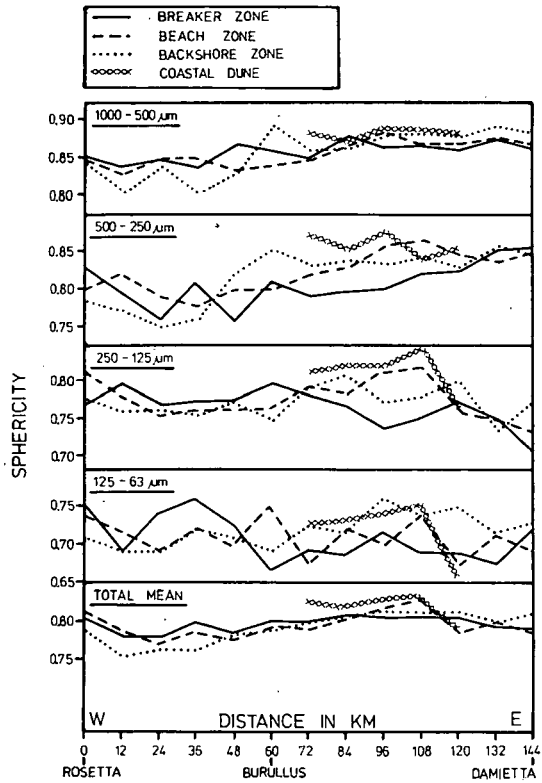


*Fig. 8.* Relation of sphericity of coastal sands to distance of transport along the Nile Delta coast.

rounding is more rapid when the grain is angular and that it slows down as it becomes more rounded.

3. The roundness of the coarser sands increases more rapidly than that of the finer sands. The coarse sands are most readily rounded because they may wear most rapidly.

4. The difference in roundness between the sands of the different environments in greater in the finer grades than in the coarser ones.

5. No significant difference in the lateral variation of roundness of breaker zone sands for 250—125 µm and 125—63 µm size grades could be correlated with transport.

Lateral variations of sphericity are shown in *Fig. 8*. The following were observed:

1. The mean sphericity values of the coastal sands reveal that the grains become more spherical with transport. Little, but definite sphericity change is found.

2. The lateral variation of the coarser grades (1000—250 µm) is more pronounced than that of the finer ones (250—63 µm). It seems evident that the coarser grains moved undergo a modification.

3. The sphericity changes for the 1000—500 µm size grade are slow, which may be related to the limited effect of abrasion. These changes become quicker for the 500—250 µm size grade.

4. For the 250—125 μm size grade, the wear plays little role from Rosetta to the location 84 km. These sediments attain higher sphericity values between 84 and 120 km and then tend to decrease sharply.

5. No significant change in sphericity for the 125—63 μm size grade could be correlated with distance.

6. A rapid increase in sphericity takes place in the early stages of transport for the backshore sands; the other coastal sands do not display such a feature.

## CONCLUSIONS

1. A definite correlation between the size of the coastal sands and both the roundness and sphericity is established. The sands are characterized by a steep decrease in roundness and sphericity, associated with a decrease in size. The coarse sands may be abraded more easily than the finer sands. It was found that the better rounded grains are the most spherical.

2. The roundness and sphericity were observed to be complex functions of each other, rather than to be in a linear relationship, in spite of the positive correlation between them.

3. A difference in roundness and sphericity was observed normal to the shoreline, so that a distance of a few hundred metres makes a complete change in their values. All size classes of the sand become more rounded and spherical in moving from the breaker zone through the beach and backshore and up to the dune. The principal difference comes from the sorting processes of the hydrodynamic forces affecting the coast. A possible explanation for the greater roundness and sphericity values in the beach than in the breaker zone is that the waves carying the sand up onto the beach may select the rounder and more spherical grains. The increase in these values landward may be related to the sorting action of the wind in picking up more rounded and spherical grains from the beach. It is evident that well-rounded and spherical grains which can roll and can be blown more easily than grains with angular corners and flat surfaces, are to be added to the dune sands. Therefore, the roundness and sphericity of sands can be used as indicators of depositional environments.

4. The roundness and sphericity of the sands show a definite, though fluctuating increase with the distance of transport along the coast. This change may be quite abrupt at first, but subsequently becomes smoother. It may be suggested that rounding is more rapid when the grain is angular, and it slows down as it becomes more rounded. The change in the coarser sands is more pronounced than in the fine sands, and therefore the coarser sands seem to undergo a modification.

## REFERENCES


BAGNOLD, R. A. [1937]: The transport of sand by wind action. Geog. Jour., **89**, 411—436.

BALAZS, R. J. and KLEIN, G. D. [1972]: Roundness — mineralogical relations of some intertidal sands. Jour. Sed. Petr. **42**, 425—433.

BEAL, M. A. and SHEPARD, F. P. [1956]: A use of roundness to determine depositional environments. Jour. Sed. Petr. **26**, 49—60.

BOGGS, S. [1967]: Measurement of roundness and sphericity parameters using an electronic particle size analyzer. Jour. Sed. Petr., **37**, 908—913.

FLEMMING, N. C. [1965]: Form and function of sedimentary particles. Jour. Sed. Petr., **35**, 381—390.

INMAN, D. L. [1953]: Areal and seasonal variations in beach and nearshore sediments at LaJolla, California. U. S. Army Corps of Eng., B. E. B., Tech. Memo., **39**. 134.

INMAN, D. L., EWING, G. C. and CARLISS, J. B. [1966]: Coastal sans dunes of Guerrero Negro, Baja, California, Geol. Soc. Am. Bull., **22**, 787—802.

KHOLIEF, M. M., HILMY, E. and SHAHAT, A. [1969]: Geological and mineralogical studies of some sand deposits in the Nile Delta, U. A. R., Jour. Sed. Petr., **39**, 1520—1529.
KRUMBEIN, W. C. [1941]: The effects of abrasion on the size, shape and roundness of rock fragments. Jour. Geol., **49**, 482—520.
MACCARTHY, G. R. [1935]: Eolian sands, a comparison. Am. Jour. Sci., **30**, 81—95.
MACCARTHY, G. R. and HUDDLE, J.W. [1938]: Shape sorting of sand grains by wind action. Am. Jour. Sci., **35**, 64—73.
MASON, C. C. and FOLK, R. L. [1958]: Differentiation of beach, dune and aeolian flat environments by size analysis, Mustang Island, Texas. Jour. Sed. Petr., **28**, 211—226.
MATTOX, R. B. [1955]: Eolian shape-sorting. Jour. Sed. Petr., **25**, 111—114.
MISDORP, R. [1976]: Application of grain roundness analysis to sands of the Nile Delta. In: Proc. Sem. on Nile Delta Sed., Oct. 1975, Alexandria, 59—78.
PETTIJOHN, F. J. [1957]: Sedimentary rocks. 2nd ed., Harper and Brothers, New York.
PETTIJOHN, F. J. and LUNDAHL, A. C. [1943]: Shape and roundness of Lake Erie beach sands. Jour. Sed. Petr., **13**, 69—78.
RAMEZ, M. R. and MOSALAMY, F. H. [1969]: The deformed nature of various size fractions in some clastic sands. Jour. Sed. Petr., **39**, 1182—1187.
RILEY, N. A. [1941]: Projection sphericity. Jour. Sed. Petr., **11**, 94—97.
ROSENFELD, M. A. and GRIFFITHS, J. C. [1953]: An experimental test of visual comparison technique in estimating two dimensional sphericity and roundness of quartz grains. Am. Jour. Sci., **251**, 553—585.
RUSSELL, R. D. [1939]: Effects of transportation on sedimentary particles. In: TRASK, P. D. (ed.), Recent marine sediments. Am. Assoc. Petr. Geol., Tulsa, 32—47.
RUSSELL, R. D. and TAYLOR, R. E. [1937]: Roundness and shape of Mississippi River sands. Jour. Geol., **45**, 225—267.
SHEPARD, F. P. and YOUNG, R. [1961]: Distinguishing between beach and dune sands. Jour. Sed. Petr. **31**, 196—214.
SWAN, B. [1974]: Measures of particle roundness: a note. Jour. Sed. Petr., **44**. 572—577.
WADELL, H. [1933]: Sphericity and roundness of rock particles. Jour. Geol., **41**, 310—331.
WADELL, H. [1935]: Volume, shape and roundness of quartz particles. Jour. Geol., **43**, 250—280.
WASKOM, J. D. [1958]: Roundness as an indicator of environment along the coast of Panhandle Florida. Jour. Sed. Petr., **28**, 351—360.

*Manuscript received, 29 November, 1983*

NABIL M. EL FISHAWI
Institute of Coastal Research
Alexandria, Egypt.

*Acta Mineralogica-Petrographica, Szeged, XXVI/2, 247—259, 1984*

# DISTINCTION OF THE NILE DELTA COASTAL ENVIRONMENTS BY SCANNING ELECTRON MICROSCOPY: A STATISTICAL EVALUATION

N. M. EL FISHAWI and B. MOLNÁR

ABSTRACT

Sand grain surface textures were examined from modern Nile Delta coastal deposits of known origin that had been subjected to mechanical and chemical processes during erosion, transportation and deposition. Samples representing breaker zone, beach, backshore, dune and River Nile sands were selected to establish characteristic grain surface textures. There are no simple diagnostic features for any particular environmental history because different mechanical processes produce similar surface features on sand grains. Only by quantitative analysis of sand grain surface feature abundances can accurate evaluation be made.

## INTRODUCTION

DAVID KRINSLEY and his associates pioneered the field of electron microscopy as used on quartz grains [KRINSLEY and TAKAHASHI, 1962; KRINSLEY and DONAHUE, 1968; KRINSLEY and MARGOLIS, 1969; 1971; KRINSLEY and DOORNKAMP, 1973; MARGOLIS, 1968; MARGOLIS and KENNETT, 1971]. With the development of the SEM, however, examination of a sand grain at magnifications up to 10.000 power is accomplished quickly and easily by anyone having access to a machine. The advent of the SEM has made this type of analysis a relatively simple procedure and consequently a viable approach to the solution of appropriate sedimentological problems. As a result, numerous papers have been published during the last decade, dealing with the specialized use of the SEM and suggesting the use of various surface textures on sand grains as environmental indicators [BLACKWELDER and PILKEY, 1972; KRINSLEY *et al.*, 1973; INGERSOLL, 1974; BAKER, 1976; FRIEDMAN *et al.*, 1976; MANKER and PONDER, 1978; HIGGS, 1979; BULL, 1981; CULVER *et al.*, 1983].

The goal of the study of grain surfaces has been the identification of surface markings on sand grains that are uniquely produced by a specific transport process. Thus far, satisfactory results have been obtained predominately from the examination of unconsolidated sediments and from artificially abraded crushed quartz. A summary with photomicrographs of the criteria useful in surface texture texture interpretation has been provided by KRINSLEY and MARGOLIS [1971] and KRINSLEY and DOORNKAMP [1973]. To date, these methods require treatment or simple non-parametric statistical analysis.

Sand grain surface textures were examined along the Nile Delta coast. Samples were collected from the breaker zone, beach, backshore, coastal dune and River Nile *(Fig. 1)*. The aims of the present study are:

1. To examine the sand grain surface textures of the Nile Delta coastal environments. In fact, the distinction between breaker zone and beach sands, and that between backshore and dune sands, do not attract the attention of many authors.

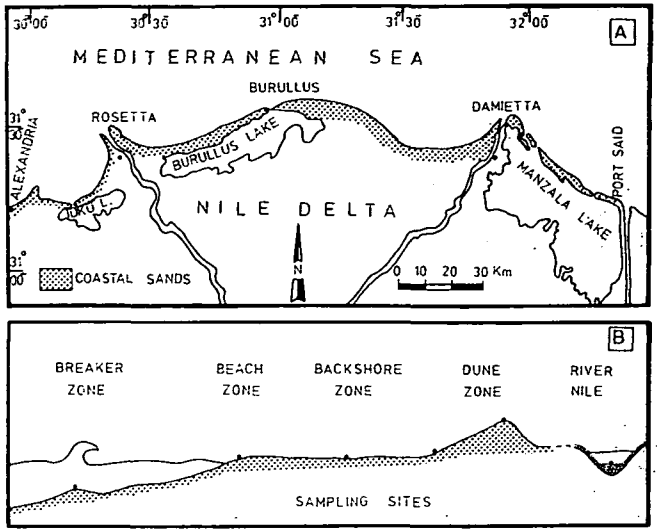


*Fig. 1.* Location map showing the studied area *(A)*, and sampling sites *(B)*.

2. To evaluate quantitatively whether the surface textures can be relied upon to distinguish accurately between various environments, and whether this should be done on the basis of single or groups of feature.

## GRAIN SIZE STUDIED

All investigators seem to agree that sands finer than 250 μm show a relative predominance of chemical features, while coarser sands do that of mechanical features. In the present study, the average grain size in all samples was about 700 μm in diameter, and ranged from 250 μm to 2000 μm. No relationship was observed between grain size and surface texture. About 60 grains of each environmental deposit were examined at approximately 4000× to determine what features might be present. Photomicrographs were made for the grains examined and the most interesting ones are produced in this study.

## RESULTS

Grain surface features for breaker zone, beach, backshore, coastal dune and River Nile sands are shown in Plates I—V, respectively. The various surface features recognized in coastal sands are enumerated below.

*Littoral environments*

These include grains obtained from breaker zone, beach and River Nile sands (Plates I, II, V). The grains affected by littoral action are characterized by V-shaped patterns, straight and curved scratches and grooves with steep and irregular sides, conchoidal fractures and irregular breakage blocks. These features are generally found on the edges of the grains, but may be observed on other grain surface. Numerous grain collision micro-textures and small impact pits were observed. Semi-parallel steps which characterize glacial origin were seen on a few grains from breaker

TABLE 1

*Widths, depths and diameters for some surface features*

| Feature | | Breaker zone | Beach | River Nile |
|---|---|---|---|---|
| V-shaped pits | width: | 2— 20 μm | 2.0—33 μm | 2—10 μm |
| | depth: | 1— 15 μm | 0.2— 6 μm | 1— 3 μm |
| Scratches | width: | 16—100 μm | 12.0—50 μm | 5—70 μm |
| | depth: | 2— 10 μm | 1.0— 5 μm | 1— 5 μm |
| Breakage blocks | diam: | 20— 50 μm | 15.0—50 μm | 3—30 μm |

zone and beach sands. On some grain surfaces, the littoral solution attacked collision grooves, grain edges and breakage corners, and produced solution precipitation surfaces and small deep surface etching.

It is possible to distinguish between high and low wave energy environments on the basis of surface texture. The photomicrographs show sharp scratches and grooves with aligned breakage blocks and deep V-shaped pits, which may be considered as the diagnostic features of high-energy environments (breaker zone, Plate I). These features are easily recognized on most grains; they often coincide with the edges of conchoidal breakage patterns of V-shaped pits. Table 1 summarizes the widths and depths for some surface features of the littoral environmental sands.

KRINSLEY and MARGOLIS [1971] reported that the V-shaped patterns have an average depth of 0.1 μm and there is an average density of two V's per square micron. In the samples of the present study, there was much a wide variation in size and depth of this pattern that no such generalizations seem warranted. V-shaped pits, scratches and grooves of breaker zone sands, however, are relatively deeper, wider and longer than those of beach and river sands. INGERSOLL [1974] stated that the depth and width of the V-shaped pits are probably due to crystalline structure, grain size and mechanical versus chemical effects.

*Aeolian environments*

SEM examination showed that mechanical abrasion features are commonly considered to be characteristic of aeolian sands with surface features dominated by chemical precipitation. Plates III and IV show the diagnostic features for backshore and dune sand grains. Meandering ridges, mechanically upturned plates, dish-shaped concavities, graded arcs and polygonal cracks are characteristics of aeolian action. Scratches and grooves, mechanical pits, cleavage planes and solution precipitation surfaces also occur.

The conchoidal pattern and blocky breakage of aqueous origin may be rapidly abraded and merge into meandering ridges under the wind action. The upturned plates of various sizes, but no larger than 3 μm high, may extend unbroken for 60 μm or more, or may be broken and discontinuous. Additionally, they may be gyreatl subdued or rounded off by solution and precipitation. Rounded, dish-shaped concavities are observed on some grain surfaces. Flat cleavage plates and plate ends are frequently lightly covered by a smooth precipitated layer.

A comparison between backshore and coastal dune sand grains leads to some diagnostic features. In backshore sands, some of the examined grains are characterized by V-shaped patterns and breakage blocks, which indicate their beach origin

(Plate III). On the other hand, there are sand grains derived from coastal dunes as testified by the polygonal cracks and deep surface etching (Plate IV). The backshore zone may be considered as a transitional zone between the beach and the coastal dune.

*Statistical evaluation*

Attempts to estimate the percentage occurrence of the grain surface covered by each feature proved to be highly subjective and very time-consuming. A simple presence or absence (binary data) was tabulated for each feature, to yield the percentage occurrence in this study. Questionable occurrences were tabulated as absent. Twenty textural features were selected for evaluation of their sensitivity in differentiating the Nile Delta coastal environmental sands (Table 2). These features were catalogued by KRINSLEY and DOORNKAMP [1973]. The polygonal cracks were originally identified on desert grains from Libya by LUCCI [1971] and supported by BAKER [1976].

A comparison of percentages occurrence of surface features for breaker zone, beach, backshore, dune and River Nile sands revealed significant difference, as shown in Table 2 and *Fig. 2*. On the grand scale of comparing aqueous features with aeolian ones, only 5 features proved to be distinctive. The V-shaped pattern, conchoidal fractures, breakage blocks, straight scratches and grooves, and stepped cleavage surfaces almost invariably occur together and may be considered as a single class of abrasional

TABLE 2

*Percentage occurrences of surface features for coastal sands*

| Surface features | River Nile | Breaker zone | Beach zone | Backshore zone | Dune zone |
|---|---|---|---|---|---|
| *Chemical* | | | | | |
| Smooth precipitation surface | 7.69 | 19.30 | 12.82 | 5.41 | 47,16 |
| Irregular precipitation surface | 23.08 | 5.26 | 2.56 | 5.41 | 13.21 |
| Precipitated upturned plates | 0.00 | 5.26 | 0.00 | 5.41 | 5.66 |
| Precipitation in grooves | 19.23 | 7.02 | 30.77 | 10.81 | 24.53 |
| Adhering particles | 11.54 | 14.03 | 23.07 | 24.32 | 9.43 |
| Deep surface etching | 7.69 | 5.26 | 7.96 | 0.00 | 9.43 |
| Oriented V-shapes patterns | 7.69 | 3.51 | 0.00 | 0.00 | 0.00 |
| *Mechanical* | | | | | |
| Conchoidal fractures | 3.85 | 35.09 | 25.64 | 0.00 | 0.00 |
| Breakage blocks | 19.23 | 29.82 | 28.21 | 8.11 | 0.00 |
| Straight scratches and grooves | 50.00 | 47.37 | 35.90 | 21.62 | 26.42 |
| Curved scratches and grooves | 73.08 | 73.68 | 66.67 | 54.05 | 35.85 |
| Mechanical pits | 50.00 | 42.10 | 28.21 | 29.73 | 49.06 |
| Cleavage planes | 11.54 | 21.05 | 33.33 | 27.03 | 13.21 |
| Stepped cleavage surface | 0.00 | 7.02 | 12.82 | 0.00 | 0.00 |
| Mechanical V-shaped patterns | 38.46 | 78.95 | 58.97 | 16.21 | 3.77 |
| Mechanically upturned plates | 7.69 | 3.51 | 2.56 | 24.32 | 24.53 |
| Meandering ridges | 0.00 | 0.00 | 0.00 | 27.03 | 50.94 |
| Dish-shaped concavities | 0.00 | 1.75 | 2.56 | 10.81 | 11.32 |
| Polygonal cracks | 0.00 | 0.00 | 0.00 | 0.00 | 7.55 |
| Graded arcs | 0.00 | 0.00 | 0.00 | 8.11 | 11.32 |

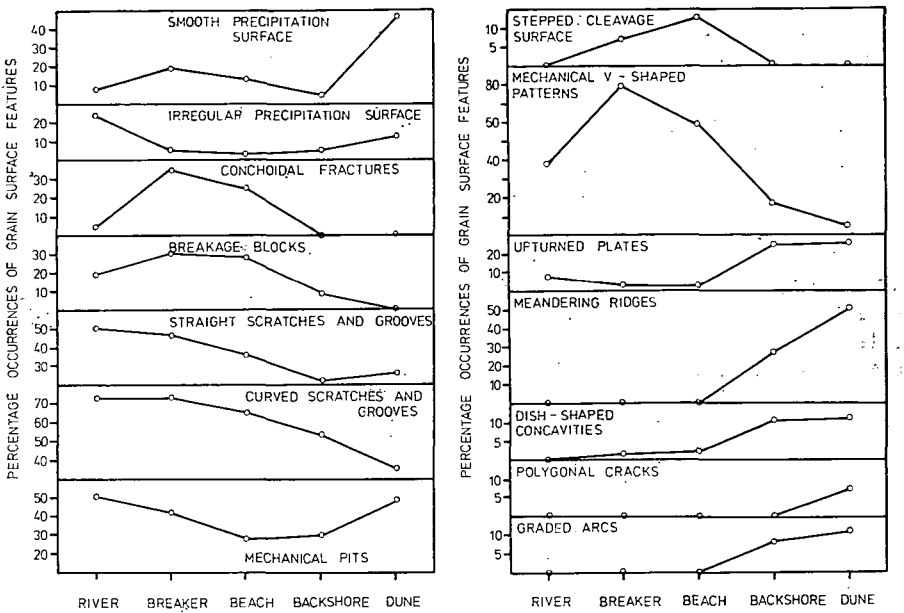


*Fig. 2.* Percentage occurrences of grain surface features for coastal sands.

features. These features occur on between 30% and 80% of the grains throughout the littoral sands, but on fewer than 20% of the grains from the aeolian sands. They also occur on fewer than 40% of the River Nile sands; MARGOLIS and KENNETT [1971] mentioned that they occur on fewer than 50% of the grains taken from river sands. The presence of these features on aeolian sands is not considered diagnostic of non-marine origins, because they do not occur in abundance. Remembering the shoreline history of the backshore flat and coastal dune sands, it seems probable that these features present in the aeolian sands are inherited and their preservation is possible. Besides this preservation, new features are created due to the wind action, which leads to an abundance of upturned plates, meandering ridges, dish-shaped concavities, graded arcs and polygonal cracks on aeolian sand grains.

Although progress has been made in relating quartz grain surface features to specific transport (depositional environments), little attention is given to the features produced by fluvial systems. In the present study, some significant variations were found between littoral sands (breaker zone and beach) and river sands. Littoral sands are characterized by an abundance of V-shaped pits, conchoidal fractures and stepped cleavage surfaces, while the river sands show an abundance of irregular precipitation surfaces and mechanical pits and a higher percentage of oriented V-shaped pits. On the other hand, the breaker zone sands are characterized by more V-shaped pits, conchoidal fractures, scratches and grooves than on the beach sands. As regards the aeolian sands, smooth precipitation surfaces, mechanical pits, meandering ridge sand polygonal cracks occur in higher percentages on the coastal dune sands than on the backshore ones.

The results of this study are consistent with the origins of the micro-textures postulated by KRINSLEY and his students. Those features thought to be most diagnostic of a littoral setting, such as mechanical V-shaped pits, conchoidal fractures

breakage blocks, scratches and grooves and stepped cleavage surfaces, markedly decrease in abundance in a landward direction (from breaker zone through beach and backshore and up to the dune). In contrast, those features thought to be diagnostic of aeolian processes, such as upturned plates, meandering ridges, dish-shaped concavities and graded arcs, increase in a sharp manner. The inland decrease in abundance of the high-energy impact features is logical in that the breaker zone and surf zone are certainly the most persistent high-energy zones along the coast.

It is likely that different mechanical processes produce similar surface features on sand grains *(Fig. 2,* Table 2). Only by quantitative analysis of sand grain surface feature abundances, in addition to other sedimentary information, can accurate evaluation be made. Although it may be true that certain features act as more important environmental indicators, whilst others serve as cosmetic detail, it is not necessarily true that the same textures are the pre-eminent discriminators in every case. Thus, there are no simple diagnostic features for any particular environmental history. This result supports the methodology of MARGOLIS and KENNETT [1971], WHALLEY and KRINSLEY [1974] and CURVER *et al.,* [1983].

## CONCLUSIONS

1. Scanning electron microscopy examination of the grain surface texture was performed on the Nile Delta coastal deposits. It is possible to distinguish between river, breaker zone, beach, backshore and coastal dune sands in the basis of surface textures. The grain surface features may be applied to the study of ancient deposits.

2. V-shaped pits, conchoidal fractures, breakage blocks, scratches, grooves and stepped cleavage surfaces appear to be good indicators of subaqueous environments. Upturned plates, meandering ridges, dish-shaped concavities, graded arcs and polygonal cracks may be used tentatively as indications of proximity to aeolian environments.

3. Attempts to estimate the percentage occurrence of the grain surface covered by each feature proved to be highly subjective and revealed significant differences between environments. The subaqueous features occur on between 30% and 80% of the grains throughout the breaker zone and beach sands, but on fewer than 40% of the grains from the river sands. The presence of these features on fewer than 20% of the aeolian grains is not considered diagnostic of non-marine origins. Remembering the shoreline history of the backshore and coastal dune sands, it seems probable that these features present in the aeolian sands are inherited and their preservation is possible. Besides this preservation, the aeolian features are created due to wind action.

4. The subaqueous features markedly decrease in abundance, while the aeolian features increase sharply in the landward direction (from the breaker zone across the beach and backshore and up to the dune). It is likely that different mechanical processes produce similar surface features, and only by quantitative analysis of surface feature abundances can accurate evaluation be made.

## REFERENCES

BAKER, H. W. [1976]: Environmental sensitivity of submicroscopic surface textures on quartz sand grains: a statistical evaluation. Jour. Sed. Petr., **46**, 871—880.

BLACKWELDER, P. L. and PILKEY, O. H. [1972]: Electron microscopy of quartz grain surface textures: The U. S. Eastern Atlantic continental margin. Jour. Sed. Petr., **42**, 520—526.

BULL, P. A. [1981]: Environmental reconstruction by electron microscopy. Prog. Phys. Geog., **5**, 368—397.

CULVER, S. J., BULL, P. A., CAMPBELL, S., SHAKESBY, R. and WHALLEY, W. B. [1983]: Environmental discrimination based on quartz grain surface textures: a statistical investigation. Sedimentology **30**, 129—136.
FRIEDMAN, G. M., ALI, S. A. and KRINSLEY, D. H. [1976]: Dissolution of quartz accompanying carbonate precipitation and cementation in reefs: example from the Red Sea. Jour. Sed. Petr. **46**, 970—973.
HIGGS, R. [1979]: Quartz grain surface features of Mesozoic-Cenozoic sands from the Labrador and western Greenland Continental margins. Jour. Sed. Petr., **49**, 599—610.
INGERSOLL, R. V. [1974]: Surface textures of first cycle quartz sand grains. Jour. Sed. Petr., **44**, 151—157.
KRINSLEY, D. H. and DONAHUE, J. [1968]: Environmental interpretation of sand grain surface textures by electron microscopy. Geol. Soc. Am. Bull., **79**, 743—748.
KRINSLEY, D. H. and DOORNKAMP, J. C. [1973]: Atlas of quartz sand surface texture. Cambridge Univ. Press. London.
KRINSLEY, D. H. and MARGOLIS, S. [1969]: A study of quartz sand grain surface textures with the scanning electron microscope. New York Acad. Sci. Trans., **31**, 457—477.
KRINSLEY, D. H. and MARGOLIS, S. [1971]: Grain surface texture. In: CARVER, R. E., ed., Procedures in sedimentary petrology. Wiley — Interscience, New York, 151—180.
KRINSLEY, D. H. and TAKAHASHI, T. [1962]: The surface textures of sand grains, an application of electron microscopy. Science **138**, 923—925.
KRINSLEY, D. H., BISCAYE, P. E. and TUREKIAN, K. [1973]: Argentine basin sediment sources as indicated by quartz surface textures. Jour. Sed. Petr., **43**, 251—257.
LUCCI, F. R. [1971]: Shrinkage cracks on frosted surface of desert sand grains. JEOL News, **9**, 18—20.
MANKER, J. P. and PONDER, R. D. [1978]: Quartz grain surface features from fluvial environments of northern Georgia. Jour. Sed. Petr., **48**, 1227—1232.
MARGOLIS, S. V. [1968]: Electron microscopy of chemical solution and mechanical abrasion features on quartz sand grains. Sed. Geol., **7**, 243—256.
MARGOLIS, S. V. and KENNETT, J. P. [1971]: Cenozoic paleoglacial history of Antarctica recorded in Subantarctic deep sea cores. Am. Jour. Sci., **221**, 1—36.
WHALLEY, W. B. and KRINSLEY, D. H. [1974]: A scanning electron microscope study of quartz grains from glacial environments. Sedimentology, **21**, 87—105.

*Manuscript received, 29 November, 1983*

NABIL M. EL FISHAWI
Institute of Coastal Research
Alexandria, Egypt.
B. MOLNÁR
József Attila University
Department of Geology
and Palaeontology
6722 Szeged, Egyetem u. 2.
Hungary

PLATE I

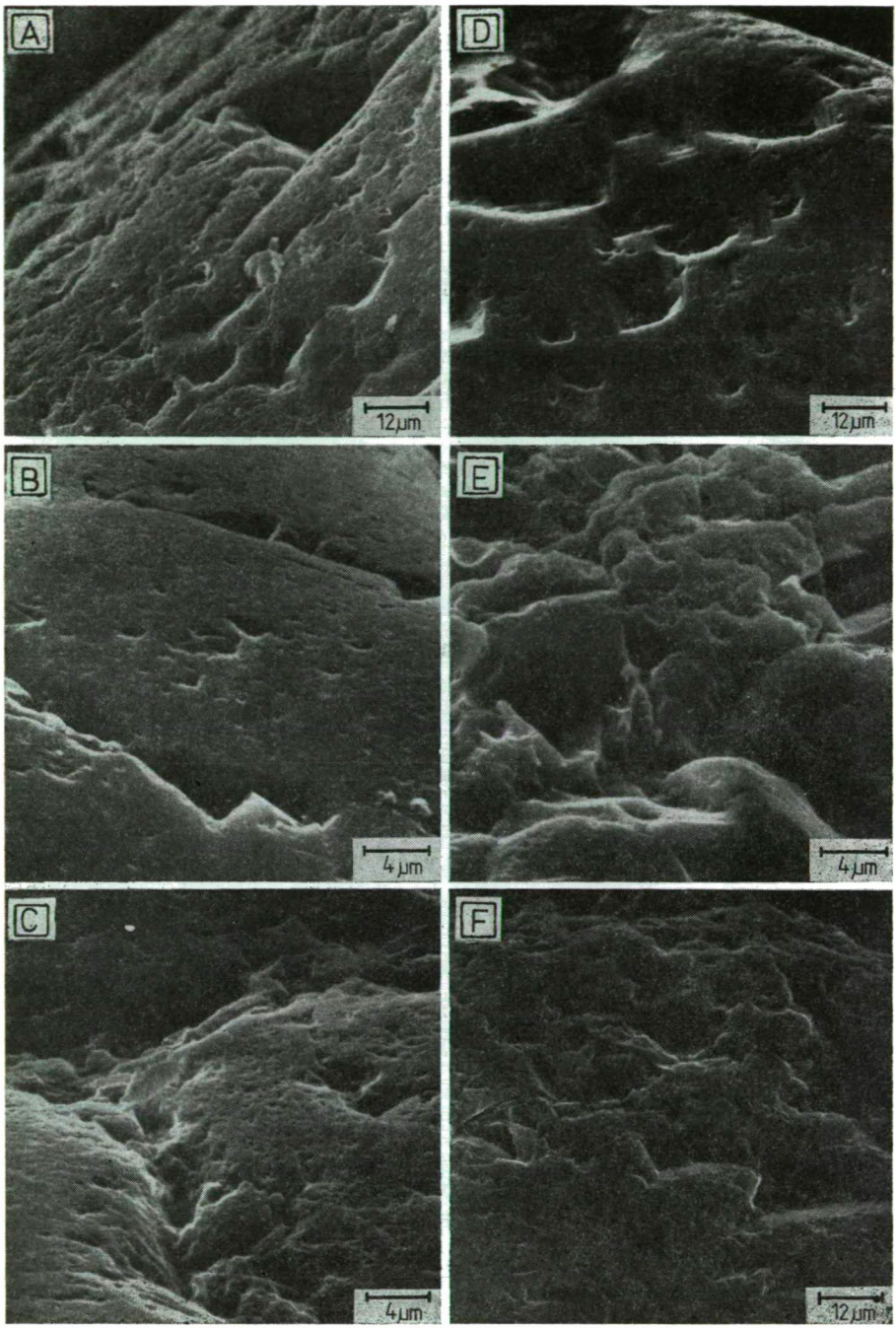

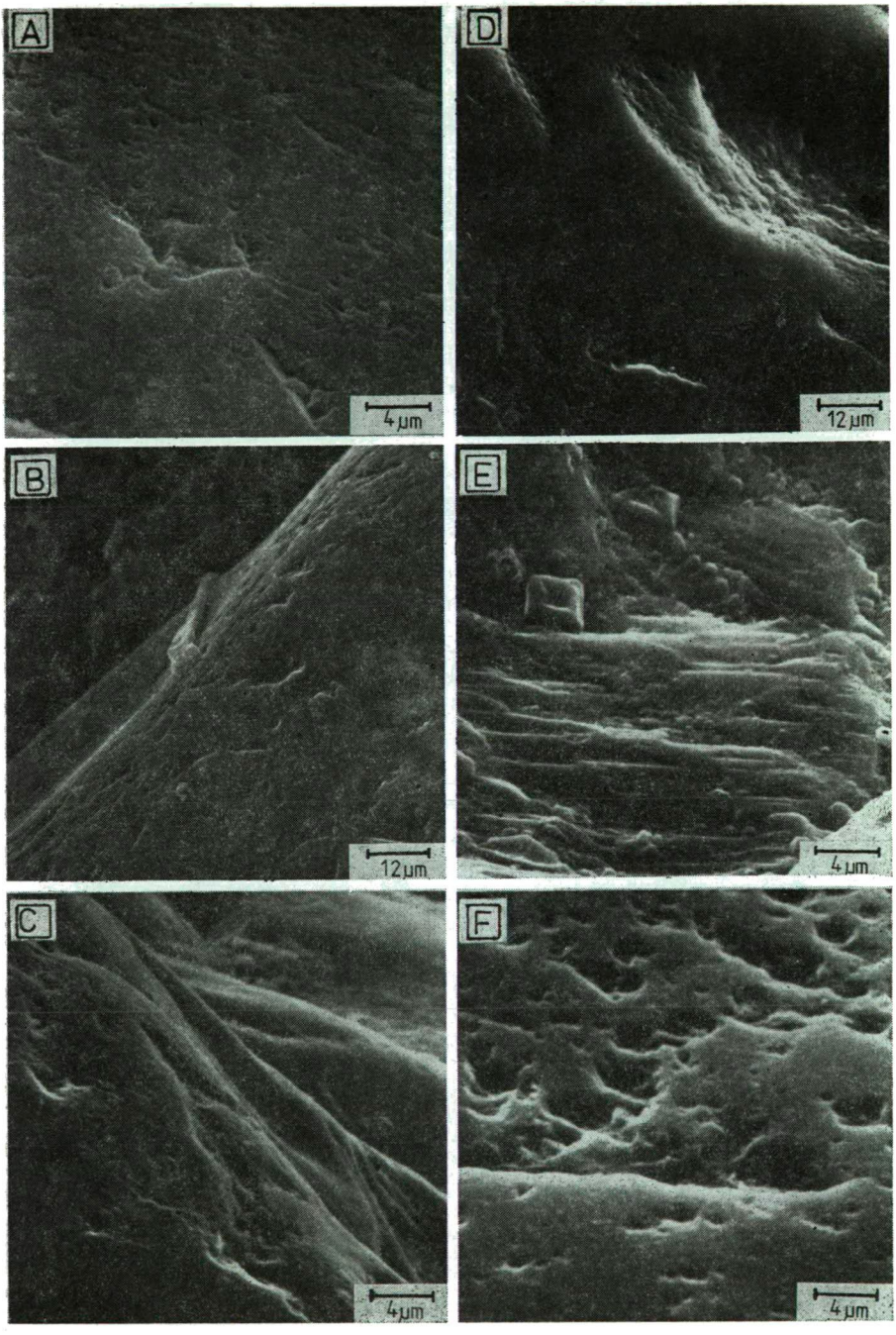
A
4 µm
D
12 µm
B
12 µm
E
4 µm
C
4 µm
F
4 µm

PLATE III

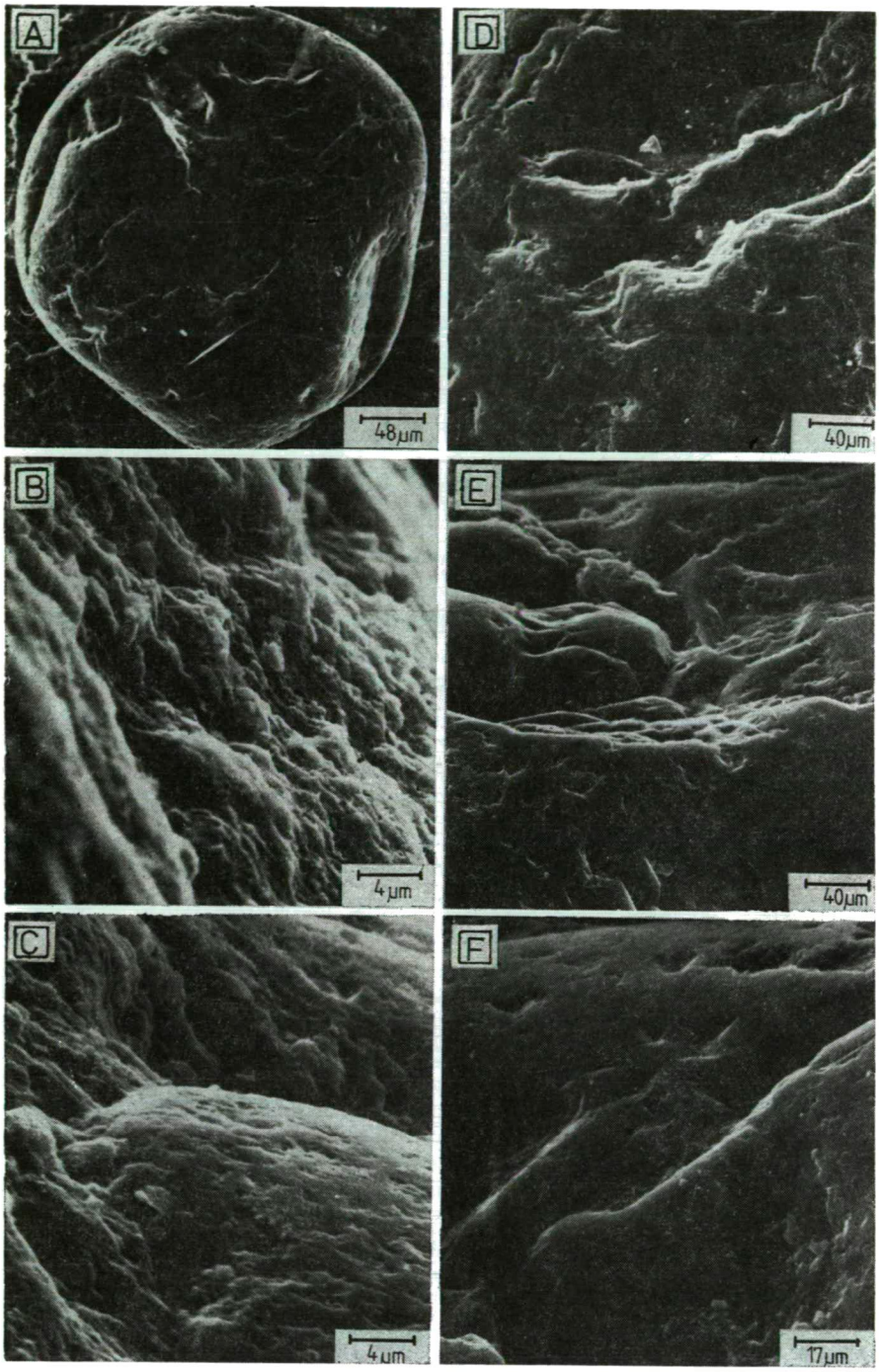

PLATE V

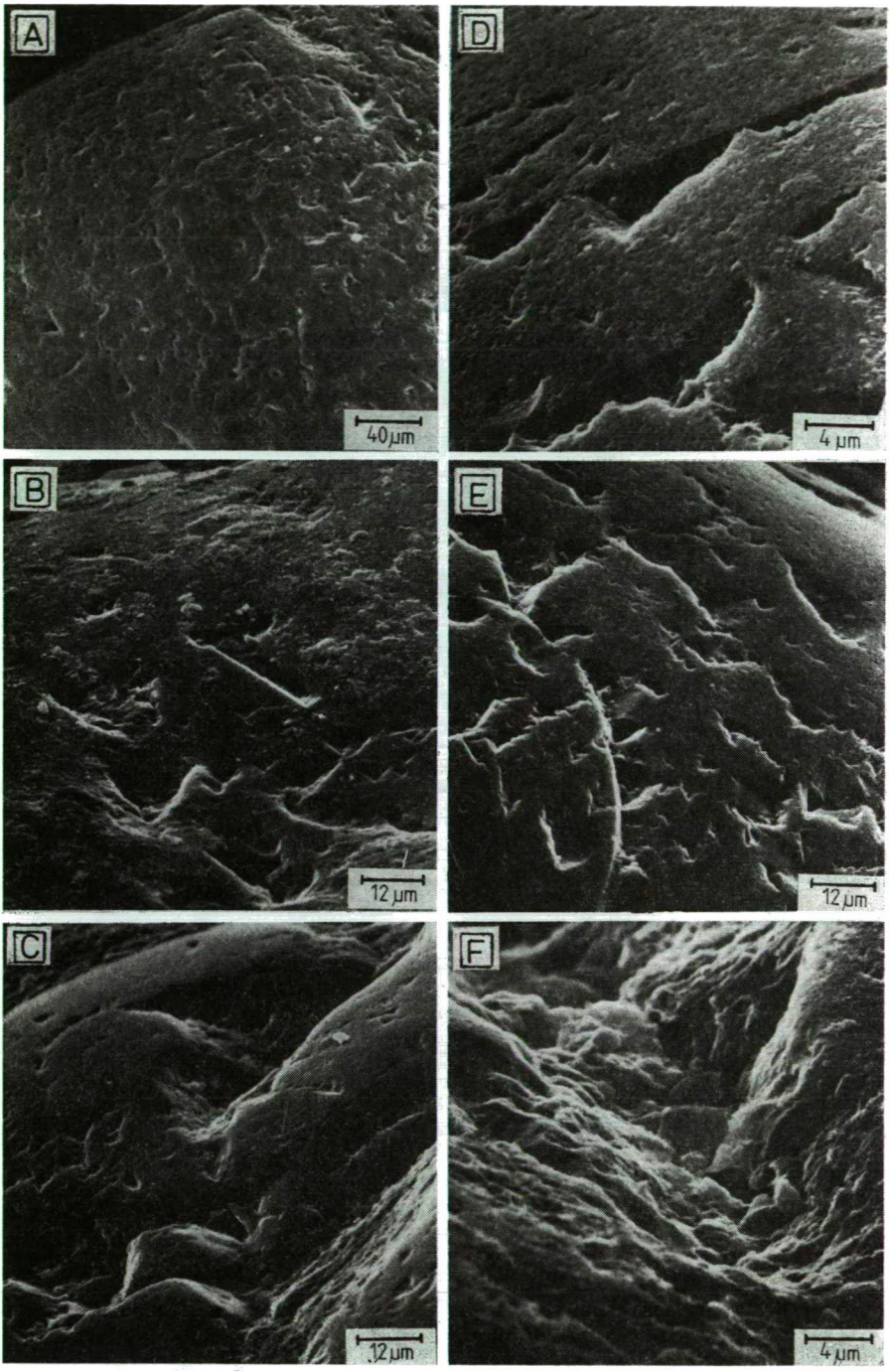

## EXPLANATION OF PLATES I-V

PLATE I: Scanning electron micrographs of breaker zone sand grains. A: V-shaped patterns and pits. B: V-shaped patterns and straight groove. C: Curved grooves. D: V-shaped and straight scratches. E: Blocky conchoidal breakage pattern. F: Stepped cleavage.

PLATE II: Scanning electron micrographs of beach sand grains. A: V-shaped patterns and straight scratches. B: Pits and curved scratches. C: Blocky conchoidal breakage patterns. D: Curved scratches and grooves. E: Chemical precipitation. F: Etching surface.

PLATE III: Scanning electron micrographs of backshore sand grains. A: Dish-shaped concavities. B: Upturned plates. C: Precipitation surface. D: Cleavage planes and grooves. E: Breakage blocks, pits and scratches, F: V-shaped pattern indicating subaqueous origin.

PLATE IV: Scanning electron micrographs of coastal dune sand grains. A: Dish-shaped concavities, V-shaped patterns and pits. B: Meandering ridges. C: Upturned plates and precipitation surface. D: Polygonal cracks. E: Graded arcs and precipitation. F: Straight scratches and precipitation.

PLATE V: Scanning electron micrographs of River Nile sand grains. A: Pits scratches and grooves. B: Oriented V-shaped patterns and chemical precipitation. C: V-shaped patterns and grooves. D: V-shaped patterns and scratches. E: Breakage blocks and scratches. F: Precipitation in grooves.

Felelős kiadó: Grasselly Gyula

Készült: monószedéssel, íves magasnyomással, 11,8 A/5 ív terjedelemben,
az MSZ 5601—59 és 5602—55 szabvány szerint
84-1111 — Szegedi Nyomda — Felelős vezető: Dobó József igazgató

**Illustrations**

Figures should be used only where they are essential to elucidate the text.

The illustrations should be numbered according to their sequence in the text, and in the text references should be made to each figure.

All illustrations should be given separately, not stuck on sheets and not folded. The number of figure and the authors name should be noted on the reverse side of the photograph and on the frontside of drawings, indicating at the same time the top of the figure where it is necessary.

Captions for all figures should be given typewritten on a separate list at the end of the manuscript. Drawn text in the figures should be kept to a minimum.

Drawings should be made on tracing paper by Indian ink. The thickness of the lines and the size of the lettering should be big enough to allow a necessary reduction.

Photographs of good contrast and intensity on glossy paper are only acceptable. Colour photographs or drawings cannot be accepted.

Use bar scale on all illustrations instead of numerical scales that must be changed if reduction is necessary.

**References**

All references to publications made in the text should be made by quoting the author's name (without initials) and year of publication in parenthesis.

The list of references at the end of the manuscript should be arranged alphabetically by author's names and chronologically per author.

If the referred publications are written by more than two authors, in the text only the name of the first author should be indicated, the other co-authors are denoted by "et al.", however, in the list of references the names of authors and all co-authors should be mentioned.

In the list of references all references should be written, e.g. Balogh, K., A. Barabás [1972]: The Carboniferous and Permian of Hungary. Acta Miner. Petr., Szeged, XX/2, 191—207.

At references to books beside the author's name, year of publication, title and the publishing house should also be mentioned.

In the case of references for symposium volumes, special issues or multi-authors books, the following system should be used: Roser, B. P., C. W. Childs, and G. P. Glasby [1980] : Manganese in New Zealand. In: I. M. Varentsov and Gy. Grasselly (Editors): Geology and Geochemistry of Manganese, Vol. II. Akadémiai Kiadó, Budapest, 199—211.

Manuscripts that are not adequately prepared will be returned to the author(s).